UNIVERSIDADE DE LISBOA

FACULDADE DE CIÊNCIAS

DEPARTAMENTO DE FÍSICA

Monte Carlo LINAC Simulations using PRIMO for IMRT Treatment Verification

Mestrado Integrado em Engenharia Biomédica e Biofísica

Perfil de Radiações em Diagnóstico e Terapia

Vanessa Cristina Inácio Pita

Dissertação orientada por:

Professor Doutor João Miranda Santos

Professor Doutor Luís Filipe Peralta

2016

Acknowledgments

The realization of this project was an achievement to my professional life as much as it was an experience for my personal life. I would like to express my sincere gratitude to all of those who made it possible and helped me to overcome all the adversities.

Dr. João Santos, I would like to thank you for the opportunity to join me in Medical Physics, Radiobiology and Radiation Protection Group, in Porto IPO Research Center (CI-IPO); and also for guiding me in this project, being always available and motivating me with your enthusiasm for this subject.

Dr. Anabela Dias, thank you for the supervision provided in partnership with Dr. João and for all the help given.

Alessandro, the huge knowledge in Monte Carlo and your ideas were an asset for this work. Thank you so much for sharing them with me and for always making things look simpler than I figured.

Bruno, Fábio, Filipa, Filipe, Rafael, Rita, Susana, e Vera, ex- interns of the service and frequent presence in laboratory 2, a big thank you to everyone. Without you my adaptation process to IPO would have not been so easy. Thank you for the affection, for the concern and for the friendship and all the good moments we shared, I will never forget each of you.

Dra Joana, Diana, Sofia and all the Medical Physics Department of Porto IPO, with no exception, you were incredible to me. Thank you for your friendliness, for always being very helpful to me, and for welcoming me so openly.

Professor Luis Peralta, I am thankful to you for being my internal supervisor and also for your availability and concern.

Sofia, Sílvia, Raquel and Débora, my dear friends, thank you very much for your regular presence in my life in Porto and for always being with me.

My dear Fábio, your strength and unconditional support in the final phase of this project was crucial to me. Therefore, an enormous “thank you” for always believed in me.

Irene, Paulo, João and my whole family, I have no words to express my gratitude to you, for all you have done for me. Without your support, none of this would have been possible.

Resumo

As simulações de Monte Carlo são consideradas o método mais eficiente para executar cálculos de dose absorvida em radioterapia externa, porque fornecem uma descrição muito detalhada e completa dos campos de radiação e do transporte de partículas nos tecidos. Existem atualmente vários códigos de Monte Carlo neste contexto, mas este trabalho focar-se-á no PRIMO. O principal objetivo com o desenvolvimento deste projeto é mostrar que o PRIMO é uma ferramenta com enorme potencial para simular tratamentos de IMRT, e que por esta razão pode ser muito útil na verificação clínica destes tratamentos.

A radioterapia de intensidade modulada (IMRT, do inglês *Intensity-Modulated Radiation Therapy*), resulta da evolução da técnica de radioterapia conformacional tridimensional (3D-CRT, do inglês *Three-Dimensional Conformal Radiotherapy*). Esta veio acrescentar à conformação geométrica do feixe de radiação, a capacidade de modulação da intensidade do mesmo. Por ser extremamente precisa a aplicação de um feixe de radiação nesta técnica, é possível aplicarem-se elevadas doses de radiação ao tumor, preservando ao máximo os tecidos saudáveis. Contudo, esta técnica requer um planeamento mais complexo e um maior número de profissionais envolvidos desde o planeamento até à execução do tratamento.

Antes de ser efetuado um tratamento de IMRT é necessário fazer uma verificação precisa da dose que será administrada ao paciente, recorrendo a ferramentas de garantia do controlo da qualidade. Com estas, são comparadas as distribuições de dose adquiridas com um fantôma com as simuladas no sistema de planeamento do tratamento. Para que o tratamento seja aplicado a um paciente, é necessário que a compatibilidade seja superior a 95%, utilizando um índice gama a 3% e 3mm, o que não ocorre sempre. Quando este nível de concordância não é atingido é necessário analisar o que influenciou esse resultado, e por vezes refazer o plano de tratamento, sem que grandes conclusões acerca desta não concordância sejam apontadas. Uma vez que, para realizar estes testes, é utilizada uma matriz com várias câmaras de ionização separadas entre si, neste caso em concreto, uma matriz com 729 câmaras de ionização separadas por 1 cm, é associado a esta medição um dado erro. Este erro poderá estar, por vezes, na origem da não concordância entre o planeamento efetuado e a sua irradiação num fantoma. Por esta razão, nestas situações, seria interessante a existência de um método alternativo de teste para contrapor estes resultados, como por exemplo aqueles que têm por base os cálculos de Monte Carlo, tal como é o caso do PRIMO.

O PRIMO é um programa de simulações de Monte Carlo, que tem por base o código PENELOPE. Este permite que sejam calculadas distribuições de dose em fantômas ou num

paciente, com a precisão característica dos métodos de Monte Carlo. Contudo, contrariamente ao que acontece com a maioria dos programas de Monte Carlo, o PRIMO apresenta a particularidade de ter uma interface gráfica muito apelativa ao utilizador, sendo muito intuitivo, e por isso de fácil utilização. Este programa permite escolher o acelerador linear a utilizar, recorrendo a uma base de dados disponibilizada pela IAEA, e definir muitos outros fatores (energia nominal, SSD, tamanho do campo, etc.), tal como ocorre aquando de uma aquisição de distribuições de dose num fantôma. É por este motivo, que se acredita que este programa poderá ser um ótimo complemento à verificação e aprovação de tratamentos de IMRT, tendo sido esta razão pela qual o programa foi escolhido para realizar este trabalho.

Tratando-se de um programa bastante recente, a primeira etapa deste trabalho consistiu na validação do mesmo para os aceleradores utilizados. Este processo consistiu na comparação das curvas de dosimetria básica: o perfil que mostra a percentagem de dose em profundidade (PDD, do inglês *Percentage Depth Dose*), e ainda os perfis transversais X e Y.

Na prática, estas curvas são medidas diretamente num LINAC, utilizando um tanque de água para a sua aquisição e os seus resultados foram usados para a comparação com os dados simulados. Esta medição é efetuada a cada 6 meses (ou sempre que haja intervenções no acelerador que as justifiquem), no sentido de verificar se as curvas medidas se encontram dentro dos parâmetros aceitáveis, por comparação às curvas obtidas aquando da instalação do LINAC e sua consequente aceitação (processo designado comummente por *commissioning*). Para escolher as curvas a usar na validação do programa, foi realizado um estudo sobre a sua evolução ao longo do tempo, que resultou na escolha do PDD e perfis laterais obtidos na aceitação do aparelho.

No PRIMO, estas curvas foram simuladas, para o mesmo aparelho utilizado nas medições práticas, num fantoma equivalente ao tanque de água, já existente no programa. O LINAC escolhido para este estudo foi um CLINAC 2300 da Varian, por ser um aparelho existente no serviço de Radioterapia do IPO do Porto e também no PRIMO. A validação foi um processo efetuado por tentativa e erro. A cada simulação se alterava um dado parâmetro (energia inicial, focal spot, técnica de redução da variância, etc.). Quando terminava a simulação, o PDD e perfis laterais eram comparados com as curvas já selecionadas. Se os resultados não apresentassem um grau de concordância de 95% ou mais, segundo o índice gama a 2% e 2mm, alterava-se um parâmetro e refazia-se a simulação. Quando os resultados simulados apresentaram boa concordância, o programa foi validado e o trabalho prosseguiu, rumo ao seu objetivo final. Relativamente a este método de comparação, é pertinente referir que este índice gama é o critério de comparação também utilizado na prática clínica, embora nesse contexto se use o índice gama para 3% e 3 mm.

A comparação das curvas de dosimetria básica simuladas e medidas foi realizada diretamente no PRIMO, nesta etapa inicial. Contudo, para se poder progredir neste trabalho seria necessário comparar imagens e não curvas, isto é comparar distribuições de dose 2D/3D em vez de 1D, o que não é possível usando o PRIMO. Por esta razão, os resultados obtidos nas simulações com o PRIMO tiveram de ser exportados e transformados em imagens DICOM, com o auxílio de funções criadas utilizando o Matlab, para que se pudesse realizar as comparações utilizando outro programa. O programa mais usado neste contexto foi o Verisoft, que é o programa utilizado nas comparações efetuadas aquando da verificação dos tratamentos de IMRT.

A segunda etapa consistiu na adição do MLC aos campos simulados e, na sua consequente, validação. Para isso, foi simulado um campo 10x10 cm^2 com um MLC estático tendo uma dada conformação. Esse campo simulado pelo PRIMO foi comparado com o mesmo campo simulado pelo TPS, e também com o mesmo campo irradiado no LINAC. No final, as três modalidades foram comparadas entre si e todas tinham de ser compatíveis, segundo os mesmos critérios de comparação do índice gama. Quando essa compatibilidade foi encontrada, considerou-se o MLC validado e passou-se à fase seguinte.

O último passo neste projeto foi a simulação de um campo 10x10 cm^2 com MLC dinâmico. Este passo é equivalente a fazer a simulação de um campo de IMRT na técnica que utiliza o MLC por segmentos. Nesta fase foi preciso compilar 89 campos que, no final, perfizeram um campo de IMRT. Esse campo simulado foi, à semelhança do ocorrido anteriormente, comparado também com a sua simulação pelo TPS e irradiação no LINAC. Uma vez verificada uma compatibilidade de 96% entre o campo simulado e medido, para um índice gama a 2% e 2mm, ficou demonstrada a potencialidade do programa para simular tratamentos de IMRT usando simulações de Monte Carlo.

Este projeto foi um estudo preliminar à simulação de tratamentos de IMRT usando o PRIMO, no qual, no final, se conseguiu simular um plano de IMRT com sucesso, pois este apresentou uma concordância aceitável com os resultados experimentais. Apesar de este trabalho ter muito por onde ser continuado, pois estudos mais aprofundados sobre os tratamentos mais complexos são necessários, os resultados corroboram a tese de o PRIMO ser uma ferramenta muito promissora para a simulação de tratamentos de IMRT em ambiente clínico, em especial na garantia de qualidade dos mesmos.

Palavras-chave: Radioterapia; IMRT; Simulações de Monte Carlo; PRIMO; Teste do índice gama.

Abstract

Monte Carlo (MC) approach is considered the gold standard method to perform absorbed dose calculations in external radiotherapy because it provides the most detailed and complete description of radiation fields and particle transport in tissues. Several codes are available and recently a new MC Penelope based code and graphic platform named PRIMO was developed. PRIMO has a user-friendly approach, a suitable and competitive characteristic for clinical activity. Nevertheless, advanced features such as Intensity Modulated Radiotherapy (IMRT) are not introduced yet. The aim of this work is to have a preliminary result on the feasibility of MC simulation of IMRT procedures, making use of the PRIMO software, showing that it can be an useful tool in clinical verification of IMRT treatments.

The first stage of this work was PRIMO validation for a Varian Clinac 2300, the same LINAC model used in practical acquisitions. This process consisted in comparing basic dosimetry curves acquired on LINAC using water tank with PRIMO simulations of them. Once *Percentage Depth Dose* (PDD) and lateral profiles X and Y simulated and acquired in practice showed compatibility higher than 95%, using the gamma index criteria with 2% and 2mm, the program is validated.

After validation, Multileaf Collimator (MLC) was added and validated. To achieve this goal, a 10x10 cm^2 field with a static MLC with a given conformation was simulated. This field simulated by PRIMO was compared to the same field simulated by the TPS, and also with the same field irradiated on LINAC. In the end, the three methods were compared and all had to be compatible, according to the same gamma index comparison criteria. When this compatibility was found, MLC was validated and the work could proceed to the next stage.

The last step in this project was the simulation of a 10x10 cm^2 field with dynamic MLC. At this stage it was necessary to build 89 fields that in the end, their sum make one IMRT field. As it had happened before, this simulated field was also compared with its simulation by TPS and its irradiation on LINAC. The compatibility between them was checked using the gamma index criteria of 2% and 2mm and it was found that 96% of the points were coincident. This fact demonstrated PRIMO capability to simulate IMRT treatments and consequently, IMRT treatments verification.

Key words: Radiotherapy; IMRT; Monte Carlo Simulations; PRIMO; Gamma Index test.

List of Communications

Resulting from the work presented in this thesis a communication was presented in one of the most important conferences in radiotherapy around the world, organized by the European Society for Radiotherapy & Oncology (ESTRO), the ESTRO 35. Bellow is the communication bibliographic reference:

- V. Pita, A. Esposito, A.G.Dias, J. Lencart, J.A.M. Santos, “PRIMO software as a tool for Monte Carlo treatment quality control in IMRT: a preliminary study”, poster presentation in ESTRO 35, Turin, Italy, April 2016.

Acronyms

AAA	Anisotropic Analytical Algorithm
CT	Computed Tomography
CTV	Clinical Tumor Volume
DCS	Differential cross sections
DICOM	Digital Imaging and Communications in Medicine
DVH	Dose volume histogram
EPID	Electronic Portal Imaging Device
FWHM	Full width at half maximum
GTV	Gross tumor volume
IAEA	International Atomic Energy Agency
IMRT	Intensity Modulated Radiation Therapy
LINAC	Linear accelerator
MC	Monte Carlo
MLC	Multi Leaf Collimator
MRI	Magnetic Resonance Imaging
MU	Monitor Units
OAR	Organ at risk
PBC	Pencil Beam Convolution
PDD	Percentage Depth Dose
PET	Positron Emission Tomography
PHSP	Phase-space
PTV	Planning Tumor Volume
QA	Quality Assurance
SBRT	Stereotactic Body Radiotherapy
SRS	Stereotactic Radiosurgery
SRT	Stereotactic Radiotherapy
SSD	Source to Surface Distance
TPS	Treatment Planning System
VRT	Variance Reduction Technique

List of Figures

Table of Contents

1 Introduction

1.1 Motivation

IMRT is a technique that has been progressively implemented since the 90s, in the United States and in Europe. Initially, it started as a technique only used in international reference institutions, but nowadays a number of smaller radiotherapy departments have it also implemented. In Portugal, the scenario is not different, with IMRT being implemented in more and more hospitals. This is a technique that allows the geometric conformation of the radiation beam to the target volume with a high accuracy. Simultaneously, it allows the modulation of the beam intensity, which creates fluence maps according to different tumor activity [1]. Thus, the results of IMRT clinical application were promising, with direct impact on the improvement of patient's life quality, decreasing some adverse effects of therapy [2].

However, IMRT treatments needs supplementary quality assurance tests before its application on patients, in addition to those necessary in other conventional radiotherapy techniques. These tests have as goal the comparison between the plans calculated by the treatment planning system (TPS) with its application to a phantom. Thus, the compatibility between them is estimated. The agreement between them is calculated based on the gamma index. If compatibility is higher than 95%, to a gamma index on 3% and 3mm, the treatment is approved.

Sometimes this compatibility is not achieved and, in some cases, there is no apparent reason to that. The usage of matrix detectors to the practical acquisition of dose fluence is pointed out as possible cause for this incompatibility, because the matrix has spaces with no detectors. In IPO Porto is used a PTW 27x27 matrix, which has 729 ionization chambers spaced by 1 cm. The spaces between chambers have to be interpolated which can be an error source. For this reason, more accurate systems to calculate the applied dose profiles would be helpful in this situation.

Nowadays, Monte Carlo simulations are pointed out as one of the most accurate methods to calculate dose distributions in radiotherapy, because of the high range of samples, which allows a dose calculation very close to reality. However, these methods require long time of computation and are not much user friendly. Recently, a new program of dose calculation using Monte Carlo, named PRIMO, was developed with the advantage of simplifying the calculation process to the users, becoming faster and user-friendly. PRIMO is an excellent tool of dose distribution calculation, which appears to be very useful in those cases of

IMRT treatment verification that are not compatible because no apparent reason. This fact arose as motivation for the development of this work, because it is believed that within this project interesting things about IMRT treatments simulation with Monte Carlo and about IMRT treatments verification could be found out, or at least, a big step in this direction.

1.2 Intensity modulated radiotherapy (IMRT)

Intensity Modulated Radiation Therapy (IMRT) is a high precision radiotherapy technique that enables the administration of high doses of radiation to the target volume, while minimizing the dose to normal surrounding tissue very effectively. This kind of dose distribution is achieved through application of several radiation beams with different incident angles and different radiation intensities. Thus, a non-uniform dose distribution is created, being conformed to the structures undergoing treatment, whether they are concave or convex [3]. When compared to conventional radiotherapy techniques, IMRT has the advantage of deliver higher intensity dose, minimizing the side effects in healthy tissues and organs surround.

The treatment process begins with the planning Computed Tomography (CT) scan, which is sent to the 3D planning system, so that the medical oncologists could delineate the target volumes and organs at risk. In some cases other image modalities are needed to plan an IMRT treatment, such as Magnetic Resonance Imaging (MRI) or Positron Emission Tomography (PET), which are fused with the CT planning to help doctors to delineate the volumes of interest.

In IMRT the plan is made by a technique called “inverse treatment planning”, which means that minimum and maximum doses, required for tumor control, are prescribed in the target volumes. The same thing happens to healthy tissues, in which are also prescribed maximum doses. Thus, the dose distribution fits precisely around the tumor or target volume, saving the healthy tissues.

In general, this modality of radiotherapy uses about five to nine radiation fields oriented around the patient and administered by linear accelerators (LINAC) collimation systems with multiple leaves, which are called MLC (Multi Leaf Collimator). The dose distribution adapted to the volumes to treat is achieved because of the movement of the MLC leaves and because of the incidence angle of the beams [4], as already referred.

It is a highly complex technique in which a large number of professionals are involved, such as radiation oncologists, dosimetrists, radiation technologists and medical

physicists. The complexity of the process involves a very accurate verification of the administered dose through quality checks performed by the medical physicists, for each plan, before apply it to a patient. These tests are performed using phantoms that are irradiated with the dose planed by dosimetrists in TPS. Then, the dose distribution obtained in the phantom is compared with the one calculated in TPS and if they are compatible, the planned treatment can be applied to the patient.

1.3 Monte Carlo LINAC simulation

Monte Carlo simulation is a statistical methodology that relies on a big random sampling to get similar results to reality. It allows you to experiment with variables a sufficiently large number of times to more accurately the chance of a result happen.

In practice, whenever you come across situations with some level of uncertainty and want to use Monte Carlo simulation, you will have to go through four steps. First, a model of the problem is done. Second, random values are generated for the uncertainties of the problem. Then, the third step, the values uncertainties are replaced to calculate the result. Finally, the solution of the problem is estimated. With the evolution of these methods, their application was extended to several fields of study, as for example in radiotherapy.

Monte Carlo simulations started to be used in radiotherapy dose calculations, becoming a common method to check other dose calculation methods in complex cases, where the simple methods were not able to work accurately. The development of a Monte Carlo beam model for linear accelerators (LINACs) was one of the first and most important step in Monte Carlo dose calculations. The calculation of the exact dose by Monte Carlo method requires accurate characterization of the radiation source [5].

To simulate the production of photon beams in a LINAC, the head components have to be precisely defined because they influence the output beam. Commonly, these components are the target, primary collimator and flattening filter, which have the greatest influence on the shape of the photon spectrum; and also the ionization chamber, the mirror and the secondary collimator. Information about components geometry and materials of the LINAC can be obtained from the manufacturer.

To evaluate the dose distribution in a particular geometry, it is necessary that the state of particles in the incident beam is precisely known, i.e. energy, orientations and positions of photons, electrons and positrons. This data set is called phase space files (PHSP). Obtain a phase space in MC simulations of LINACs is achieved by defining a sensitive volume that stores

information about particles passing through. Generally, this volume is a thin circular cylinder that sits above the secondary collimator. In this case the phase space becomes a virtual LINAC and can be used in different simulations, paying attention if the amount of particles stored in the file is a sufficient sample to obtain the required precision.

Phase space files (PHSP) are used as a primary generator in a simulation, which avoids the need for a detailed description of the geometry and materials, which are often a trade secret, and are rarely shared with the user`s machine. The availability of data PHSP also allows easy use of various beam qualities dosimetry studies, as detector characterization and the development of dose protocols.

The International Atomic Energy Agency (IAEA) has promoted a project to build a database to make public representative PHSP files of linear accelerators (and Co-60 units) used in external radiotherapy, compiling the existing data that has been properly validated. The IAEA PHSP format was designed and approved by a committee of international experts for use in medical applications [6]. This format was implemented in newer versions of general purpose MC codes as BEAMnrc / EGSnrc and Penelope, which are considered the state of -the -art for the electron-photon transport engaged in medical applications[7]. More recently, a Penelope based computer software named PRIMO was created, which is promising software in Monte Carlo LINAC simulation and will be used in this work.

PRIMO project was released in 2013 and it is a program that simulates linear accelerators and estimated absorbed dose distributions in water phantoms and CT scans (in dicom format). This software combines an appealing graphical interface to the user with computation processes based on the Monte Carlo code PENELOPE. The most of Varian and Elekta LINACs can be simulated by PRIMO, including electron applicators and multileaf collimators (MLC). The radiation fields may be stored in intermediate phase-space files which comply with the IAEA format. Thus, simulations can be done by steps and using information from other simulations already performed, saving computing resources and time. The program has also graphical and numerical tools to analyze phase-space files. Its graphical interface allows users to simulate and analyze results without performing very elaborate procedures [8]. Thereby, a prior very detailed knowledge of the Monte Carlo method or the inner LINAC operation is not a prerequisite to perform simulations at Primo, which does not occur in other such programs.

1.4 Objectives of this work

This project aimed to demonstrate the existence of an alternative method, based on Monte Carlo simulations, to calculate dose distribution profiles of IMRT treatments, since they require a verification process before applying the treatment to a patient. This study intends to demonstrate the usefulness of PRIMO in this context. Sometimes, IMRT treatments verification fail, i.e., the treatment plan does not correspond to the one irradiated in the phantom, without any apparent reason. That can happen due to physical limitations of MLC, which leads to LINAC incapacity to reproduces the generated plan in TPS. Another fact pointed out is related to the fact that the verification processing is performed using a matrix, which have ionization chambers separated by 1 cm. This makes the data acquisition of irradiations discrete in space, meaning that some results must be interpolated. This interpolation could not match exactly to the planned by TPS, being necessary to redo the verification process. Thus, this project aimed to demonstrate that PRIMO software has potential to simulate IMRT treatments and, perhaps, in the future, PRIMO can be used for IMRT verifications of dose distributions calculations, when there is no correspondence between TPS and LINAC irradiation. In order to achieve this major goal, it is necessary to structure the work in stages.

First of all, PRIMO software must be validated. At this stage the main goal is to demonstrate that the program can simulate a Clinac 2300, one of the LINACs used in IPO Porto. That is made by comparing basic dosimetry curves simulated and obtained with LINAC.

The second task is related to the validation of the MLC. Thus, a field with a given irradiation features and a given MLC conformation is simulated with Primo. At this stage, the objective is to demonstrate that simulation results are compatible with LINAC irradiation of the same field and with its calculation in TPS. As a result, there will be MLC validation and consistent evidence that the program can simulate a static irradiation field.

Ending the project, the last step has as objective the simulation of a single dynamic field and also, its comparison with LINAC irradiation and TPS calculation of this same field. If the three modalities are compatible, the main objective of this work is fulfilled, proving the potential of PRIMO software to simulate a complete IMRT treatment, once it successfully simulates a single irradiation field.

2 Experimental and theoretical background

2.1 Linear Accelerators

Radiation therapy consists on the usage of high energy radiation for tumors treatment, making them smaller by the destruction of tumor cells. In this technique, X-rays, gamma rays and charged particles could be used. Radiation can be applied by an external device to the body, which is called external radiotherapy, or inserting radioactive material into the body, near to cancer cells, which is called brachytherapy.

Most of the time, external radiation therapy sessions are made using a linear accelerator (LINAC), equipment that produces high energy x-rays. This radiation is applied to the patient, in the tumor region in a way that tumor cells are destroyed and healthy tissues around the tumor are saved.

The radiation production by a LINAC equipment is based on thermionic emission, similarly to what occurs in conventional x-rays. Thereby, an electron beam is emitted by an electron gun and accelerated in a tube due to high frequency microwaves generated by a Magnetron or a Klystron [9]. The electrons can be used directly to treatments on body surface or they can hit a metal target of high atomic number and be transformed into photons to use in deeper treatments (Figure 2.1). For this reason the LINACs make available two or more photon energies and several electron energies.

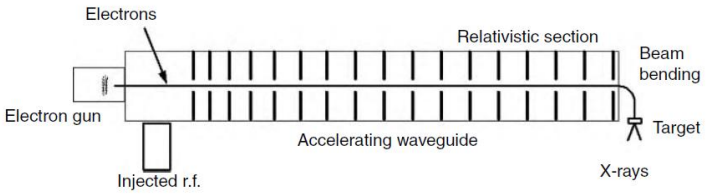

Figure 2.1 – Diagram of a linear accelerator in photon mode [10].

The beam modulation and its alignment are achieved by collimators in the inside of the LINAC head. All the LINACs have collimators, known as traditional collimators, which are distinguished between primary and secondary collimators. The primary collimator is made up of a relatively large lead block (or simply a heavy metal alloy), in order to produce a cross conical beam. The secondary collimator consists in pairs of metal blocks positioned in a perpendicular way between them. These blocks are called jaws and they control the field size for each treatment. This type of collimators only restrict rectangular fields [11].

However, the most recent models of LINACs have an additional type of collimation made of several thin leaves that allows a better conformation to the tumor shape. This system is called Multileaf Collimator (MLC) and it allows the irradiation of irregular fields without personalized protections for each patient (Figure 2.2). This system of collimation in a LINAC brings an increase on the initial investment but, in a long term this cost is overcome. This happens because individual protections hard to do are not needed, the treatment time is diminished, which increases the profitability of the LINAC and improve the treatments. Nowadays, the MLC used in clinical practice have 80 till 160 leaves, each one with some millimeters until 1 cm of wide. Every leaf is controlled with a computer, thus conformations with more than 1 mm of accuracy can be achieved and consequently irregular fields can be formed.

Figure 2.2 – Multileaf collimator [12].

In the LINAC head, ionization chambers are also present, which allow the dose monitoring and the end of the treatment when the prescribed dose has been delivered. The gantry is the LINAC component that moves around the table where the patient is lying down. The table movements can be longitudinal, lateral and rotational. In the LINAC positioning the isocenter has to be placed in a volume of millimeters for every movement. Multiple or rotational beams are applied but in all cases the tumor must be the key target. One way to ensure this happens is to locate the tumor on the isocenter on which everything runs around. In Figure 2.3 a blueprint of a LINAC is represented.

Several diseases can be treated with a LINAC, using several techniques such as conventional techniques, Intensity-Modulated Radiotherapy (IMRT), Imaging Guided Radiation (IGRT), Stereotactic Radiosurgery (SRS) and Stereotactic Body Radiotherapy (SBRT) [13].

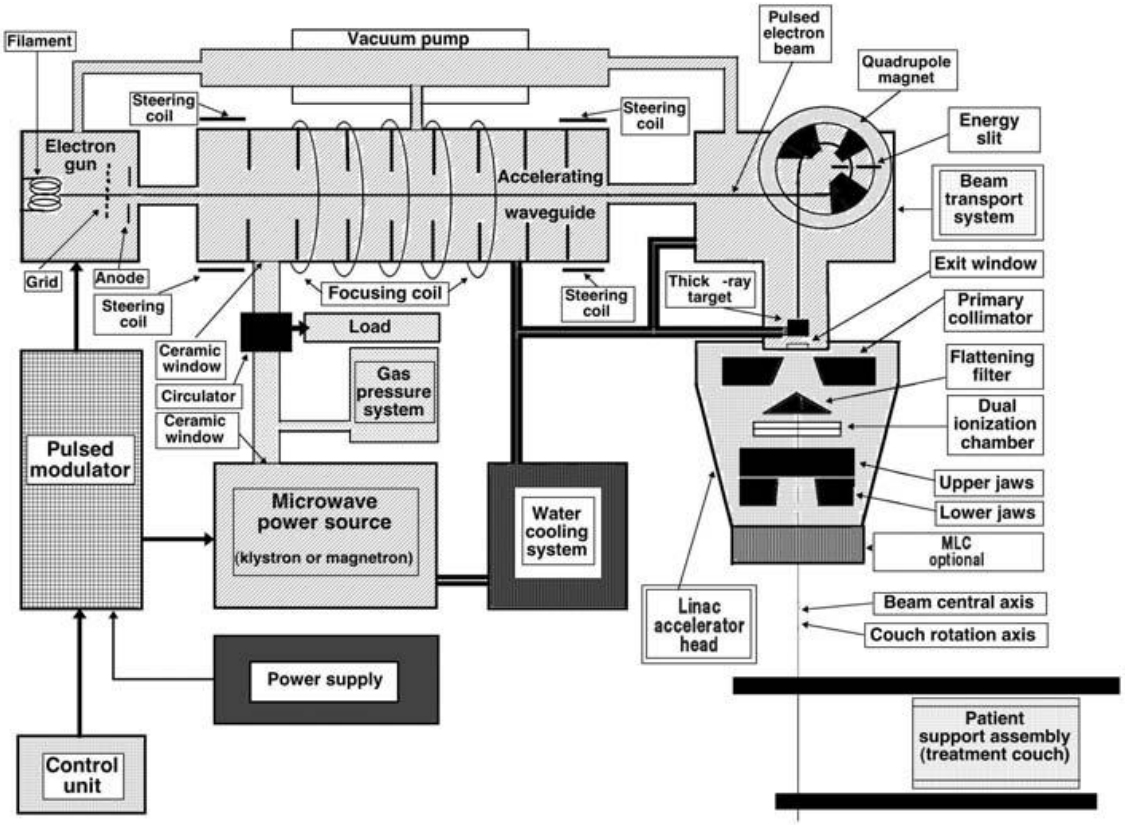

Figure 2.3 – Main components of a LINAC [11].

2.2 Dose measurement

Currently the biological effects produced in irradiated tissues are associated with a quantity called absorbed dose. This quantity is defined as the average energy deposited per mass unit of a certain volume element and it is measured in gray (1Gy = 1J / kg)[14]. Absorbed dose is a macroscopic quantity, not stochastic and therefore not described the sequence of microscopic energy deposition processes. However, it is the spatial distribution of ionization caused by the incident radiation that determines the biological effect.

Ionizing radiation itself cannot be measured directly. The detection is performed by the result produced by radiation interaction with sensitive means (detector). To be used as a dose meter for ionizing radiation (which is called dosimeter), a material must have certain properties such as: accuracy and precision in measurement, linearity, dose or dose rate dependence, energy dependence, directional dependence and spatial resolution [15].

In the measurement process of dose absorbed, several types of detectors of different materials and shapes can be used, in a radiotherapy context. The most common are the

ionization chambers, followed by dosimetric radiosensitive films, solid state detectors (as TLDs) and electronic devices, usually made of silicon.

In general, an ionization chamber is constituted by a center electrode (anode) and the chamber wall, which is coated with a conductive material that acts as cathode. The detector sensitive volume is delimited by the chamber wall, forming a cavity filled with a gas or a gas mixture at a relatively low pressure. Between the anode and the cathode, a potential difference is applied to separate the ion pairs produced. As a result, negative ions migrate to the anode and positive ions to the cathode. This ion flow produces an extremely low electric current which can be measured by an electrometer, a device that measures small currents [15].

The Farmer type ionization chambers (Figure 2.4) are widely used due to its accuracy in reading. It is recommended for MV photon beams and for electron beam with energies above between 10 MeV to 45 MeV [16].

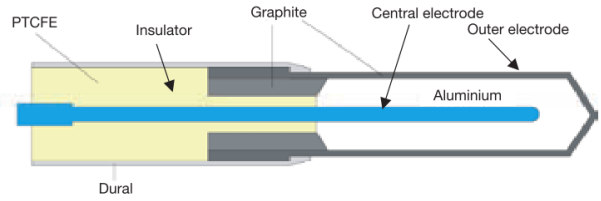

Figure 2.4 - Basic design of a cylindrical Farmer type ionization chamber [15].

2.3 Phantoms for basic dosimetry

The calibration of a LINAC consists in a set of procedures in order to getting depth curves yield and dose profile for each irradiation field, energy, type of radiation and for each beam modifier accessory. To obtain this dosimetric database for a radiation treatment unit is a meticulous experimental work, which is called basic dosimetry [17].

Usually, this calibration is performed in a cubic water phantom (Figure 2.5), whose dimensions are much greater than the irradiation fields dimensions used in clinical situations. The incidence of the beam is perpendicular to the water surface at a specific distance from the focus of the radiation. The set - up has ionization chambers to acquire the data.

Figure 2.5 – Water tank phantom for basic dosimetry[18].

2.4 Percentage Depth Dose (PDD)

The Percentage Dose Depth (PDD) is a curve that shows a ratio between the absorbed dose in several depths and the absorbed dose in a reference depth (Zmax). In Equation 1 is seen the quotient that defines a PDD, in which D_d represents the dose at any depth and D_{d0} represents the dose at a fixed reference depth (Figure 2.6) [19]. This curve is defined for a given material, for a specific field of irradiation, for a certain irradiation beam energy and Source to Surface Distance (SSD) [11].

$$\boldsymbol{P = \frac{D_d}{D_{d_0}} \times 100} \qquad \textbf{Equation 1}$$

The PDD curve has an initial point which represents the dose deposited on a patient skin (or phantom surface). The photons interact with the matter, which increase the dose in the patient (or phantom) until the maximum. That area, between incident surface and the point where the maximum dose is achieved is called build-up region. In this area the interaction between photons and tissues releases electrons, which leave their energy in a certain distance of their origin.

The percentage depth dose (beyond the depth of maximum dose) increases with beam energy. Higher-energy beams have greater penetrating power and thus deliver a higher-percentage depth dose (Figure 2.7). In the practice, the acquisition of these profiles is made by using a water phantom, which is a tank made of acrylic full of water with controlled height and leveling.

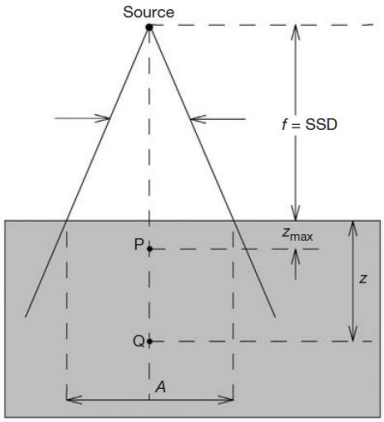

Figure 2.6 – Geometrical PDD definition. Q is an arbitrary point at depth Z and P is the point at Z_{max}. A corresponds to the field size [11].

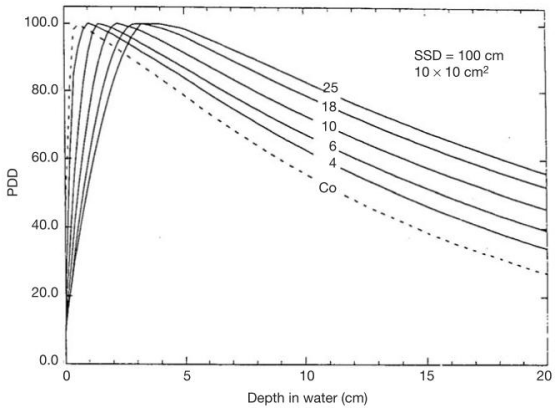

Figure 2.7 – PDD curves in water for various photon beams at SSD of 100 cm [11].

2.5 Lateral Profiles acquisition and characterization

The dose distribution (along the) the central axis is only a portion of the patient's dose distribution. For two or three dimensions the distribution is achieved by the combination of the central axis distribution with the off-axis profiles. The dose measurement of these last profiles is made on perpendicular axis to the central one using some depths of acquisition. The most used depths dose of measurement are the depth of maximum dose , and the 5, 10 cm, 20 and 30 cm, which are used for the planning systems.

The profile of a megavoltage radiation beam is composed by three distinct regions: the central region, the umbra, and the penumbral region (Figure 2.8). The central region goes from the central axis to 1 cm or 1.5 cm of the geometric field border. The umbra is the region outside the radiation field. The penumbral region is the one that suffers the source penumbra

influence, the collimator radiation transmission and radiation scatter, which together make the physical penumbra. In this region the dose change abruptly and depends on the source size, on the collimation position and the lateral electronic scatter.

The beam profile analysis is based on some parameters that define its uniformity, which are the flatness and symmetry.

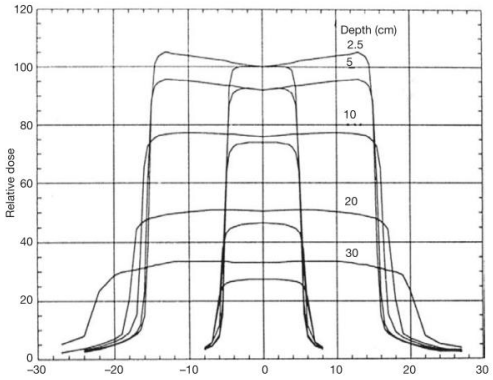

Figure 2.8 – Beam profiles of 10 MV at various depths in water, for field sizes of 10 cm x 10 cm and 30 cm x 30 cm[11].

2.5.1 Flatness

The flatness is a parameter calculated using the maximum and minimum dose values of 80% of the beam profile central part, as can be seen at Equation 2.

$$F = 100 \times \frac{D_{max} - D_{min}}{D_{max} + D_{min}} \qquad \textbf{Equation 2}$$

According to the LINAC components and details of its beam an excess of filtration can be seen on the central axis for the maximum dose depth. This fact occurs because the LINAC has a filter which will flat the beam. This effect will be less pronounced with the increase of the depth. In this situation the profile will present more rounded borders rather than peaks. The emission of lower energy photons outside the central axis explain this fact, when comparing to the ones emitted on the central axis [11].

The traditional LINACs for clinical use usually require that the flatness would be lower than 3%, for measurements with a 10 cm depth and a SSD of 100 cm and for the bigger field available (commonly 40 x 40 cm^2).

2.5.2 Symmetry

The symmetry is a parameter measured at the maximum dose depth, since it is the most critical area for this evaluation, because in that point the beam profile has the peaks already referred. According to Task Group 142 [20], for the same profile, the beam should present a symmetry with a maximum disagreement of 2% between two points at the same distance from the central axis.

Another way to measure beam symmetry is calculating the areas besides the central axis until the point of 50% dose value and compare them using Equation 3.

$$S = 100 \times \frac{A_{left} - A_{right}}{A_{left} + A_{right}} \qquad \textbf{Equation 3}$$

2.6 Modern Radiotherapy Techniques

2.6.1 3DCRT

The tridimensional conformal radiotherapy (3D-CRT) is a technique that uses multiple beams with uniform radiation intensity to irradiate the exact treatment area, according to the security margins [21]. This exact targeting makes it possible to use higher levels of radiation in treatment, which are more effective in shrinking and killing tumors.

2.6.2 IMRT

Intensity Modulated Radiotherapy is an evolution of 3D-CRT, because the applied fields have variable intensities (**Figure 2.9**). It is a modality of external radiotherapy extremely accurate that allows the administration of high radiation doses on the target volume, reducing the dose in the healthy tissues around. The radiation is applied according to the tridimensional shape of the tumor, which is achieved by the beam modulation (Figure 2.10). Similarly to 3D-CRT, IMRT allows a geometrical conformation adding a dosimetric adjustment to the irradiated area [17]. Therefore, the toxicity of the treatment, the side effects in a short and long term will be reduced [22].

Despite the benefits of IMRT in relation to the 3D-CRT, this technique requires a more severe treatment plan. In both techniques the targets and structures to protect are

selected by the doctor, which are called the volumes of interest for the treatment. However, in IMRT a technique called inverse planning is introduced, while in 3D-CRT a common planning is used. In 3D-CRT simple beams are shaped considering field margins that will compensate the daily variations in configuration and the beam characteristics. In this case, the quantity and angle of incidence of beams and its configuration are chosen and then the dose in the volumes of interest is calculated. Then the plan is analyzed in terms of dose, confirming if the maximum dose in the organs at risk is not achieved. The plan can be remade changing some parameters in order to find the best treatment plan: the one with lower dose in the organs at risk and higher dose at the tumor. On the other hand, in the IMRT treatment planning the opposite process occurs. The dose in the target and in the structures to be protected is prescribed by the doctor. For this purpose tolerance levels for each organ have to be determined [23]. Then, the program used to planning creates a series of modulation patterns in order to find the configuration that best match to the desired plan [21]. In general, 5 to 9 irradiation fields are used in an IMRT treatment, which are administered to the patient by linear accelerators with multi-leaf collimation systems.

According to the way of delivering IMRT, there are two techniques that can be distinguished: IMRT with segmental MLC, which is known as step and shoot; and IMRT with Dynamic MLC. The step and shoot technique is a discrete mode of IMRT delivery, in which the MLC leaves move to their next position while the beam is off [24]. In this case, the sum of all radiation segments will produce the intensity modulated field. In contrast, with the dynamic MLC technique the MLC leaves are in continuous motion during all treatment. The desired intensity of radiation in a specific point is achieved by a variation on MLC leaves motion speed and the changes in their position[21].

Even though IMRT has emerged in the beginning as an experimental technique, mainly in academic environment, nowadays there are a growing number of centers in Europe using IMRT in clinical practice [25]. Currently, IMRT is particularly indicated to the treatment of prostate tumors, head and neck, gynecological, gastrointestinal and central nervous system tumors.

This technique requires many resources and time to its implementation. A large number of professionals are necessary from treatment planning, until its implementation and also some procedures have to be done. Thus, acceptation and commissioning tests are needed to implement IMRT, but also quality assurance tests of the treatments are a requisite to apply an IMRT treatment to a patient.

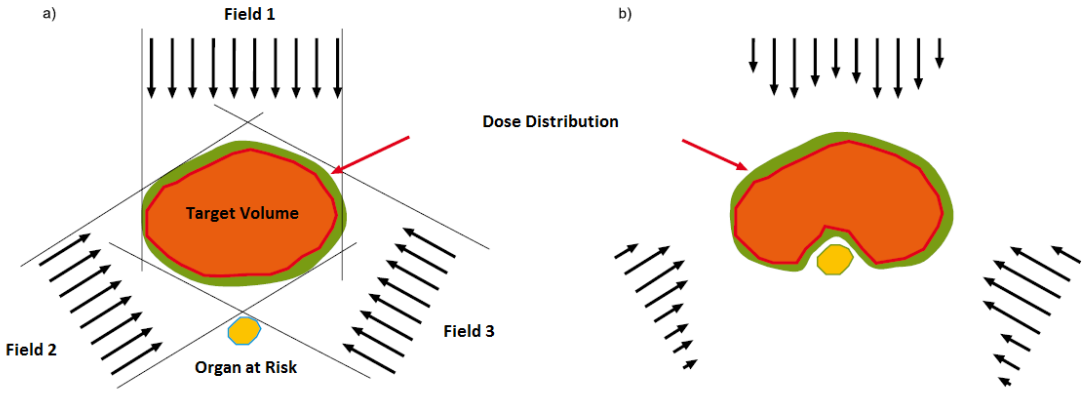

Figure 2.9 – a) 3D Conformal RT technique using uniform beams; b) IMRT technique using non uniform beams [17].

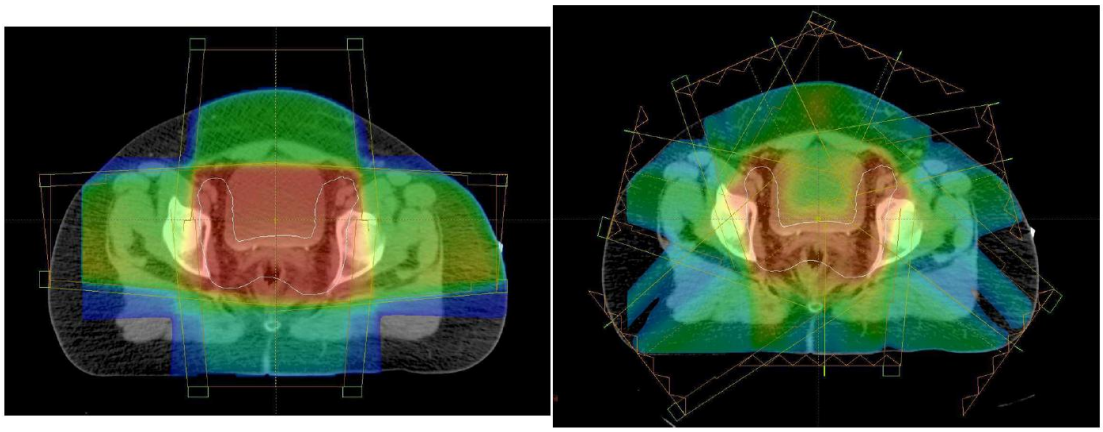

Figure 2.10 – Beam incidence and dose color wash on 3D-CRT (on the left) and Beam incidence and dose color wash on IMRT(on the right) [21].

2.6.3 Volumetric Modulated Arc Therapy - VMAT

VMAT allows carrying intensity modulated treatment only in one arc. This is achieved through the simultaneous variation of several parameters, as MLC leaves pattern, dose rate and rotation speed of the gantry. This treatment technique produces high compliance absorbed dose distributions and is quite effective in terms of treatment time [26].

RapidArc ™ (Varian Medical Sistems, Palo Alto, CA, USA) is one of the solutions already in the market for this type of treatment [27]. RapidArc™ has recently been introduced in clinical practice in various institutions after an intensive validation [28]. This introduction requires a new work methodology, being necessary introduce a quality assurance program and systematic dosimetric verification.

2.6.4 Tomotherapy

Tomotherapy is a type of image-guided IMRT that combines imaging and treatment capabilities in one unit [29]. The part of tomotherapy machine that delivers radiation for both imaging and treatment can rotate completely around the patient in the same manner as a normal CT scanner. This equipment can capture MV CT images of the patient's tumor immediately before treatment sessions, to allow for very precise tumor targeting and sparing of normal tissue. The intensity modulation is obtained by a binary collimator that opens and closes, according to computer control. Meanwhile the fan beam runs continuously around the patient and bed moves at a predetermined rate[30].

2.6.5 SRS, SRT and SBRT

Stereotactic Radiosurgery (SRS), Stereotactic Radiotherapy (SRT) and Stereotactic Body Radiotherapy (SBRT) are three techniques closely related. All of them are delivered on a LINAC and require extreme precision in patient positioning, because they are normally used when exist the need of spare immediately adjacent normal tissue[31].

In SRS a high radiation dose is given to a certain brain region of a patient in one or a few fractions. The goal of SRT is to disrupt cell division processes without completely destroying the local tissue. SRS, on the other hand, is an ablative technique where the goal is to deliver sufficient dose to the target area to kill all the cells in the target region. In this technique a fractionated schedule of delivery is used, although that schedule may be accelerated in a hypofractionated regime of as few as 3-5 treatment sessions. The difference between this technique and SBRT is the body region where the technique is applied. Thus the first one treats brain and spine tumors , the second one treats other body regions as lungs, liver, pancreas and kidneys, for example [32].

2.6.6 Treatment monitoring

In radiotherapy treatments the periodic verification of radiation fields is important, which is achieved through the use of images. In the most common LINACs, the image acquisition systems comprise a robotic arm having a panel with a matrix of detectors, called portal imaging system. With these detectors it is possible to obtain images, resulting from patient output radiation, due to the attenuation caused by tissues. These images contain

anatomical information of the patient and are used to verify the effects of the treatment. Thus, in treatment monitoring by portal images periodic information on target position and movement are obtained (within the same session or between consecutive sessions). Then it is compared with reference imaging, giving feedback to correct the patient setup and optimize target localization. These images also have the potential to provide feedback that may help to adapt subsequent treatment sessions according to tumor response [33].

2.6.7 Image guided patient positioning techniques

Image Guided Radiotherapy is a technique that allows checking the patients positioning while they are in the treatment table. Images can be acquired through the portal imaging system or with the Megavoltage Cone-Beam CT technique. In the first case, the patient is irradiated with a very low dose in two orthogonal directions (one above and one side), which will create 2D images that can be compared with the corresponding image in the planning computed tomography (CT). In the second case, the LINAC rotates around the patient allowing the creation of a 3D image, which is also compared to the CT planning, which gives information about the patient position in relation to the isocenter.

The imaging scans obtained are processed by computers to identify changes in a tumor's size and location due to treatment. They allow the position of the patient or the adjustment of the planned radiation dose during treatment. The imaging repetition can increase the accuracy of radiation treatment and may allow reductions in the planned volume of tissue to be treated, thereby decreasing the total radiation dose to normal tissue [34].

2.7 Treatment Planning System (TPS)

2.7.1 Treatment planning

The treatment planning systems (TPS) are used on external radiation therapy to simulate the radiation beams and its dose distribution. Consequently, the tumor control is maximized and the complications with healthy tissues are minimized. The help of complex calculation systems are needed to elaborate the patients' treatment plans [35].

To start the planning phase patients CT scans are performed, in which they are in the same position of the external radiation treatment. Sometimes, when the gross tumor volume

(GTV) location is hard to define, other types of images are required, as PET or MRI for example. Thus, the physician has to delineate the several volumes [36]:

- **GTV (*Gross Tumor Volume*)** – Tumor or tumor extent detected and / or visible by medical palpation or identified in complementary diagnostic images (CT, MRI, PET / CT).
- **CTV (*Clinical Tumor Volume*)** – Volume of treating tissue which comprises the GTV associated with microscopic disease extent.
- **PTV (*Planning Tumor Volume*)** – Defined by CTV and safety margins (about 1 cm). These margins compensate for changes due to the variation in size and shape of the CTV tissues and daily variations of the patient's face.
- **OAR (*Organ at risk*)** – Healthy tissues/ organs close to the tumor, whose tolerance doses might influence the volume and / or the dose levels to irradiate.

After this selection, the treatment plan is made using the TPS. The treatment plans for each patient have information about the position of the gantry, collimators and treatment table. The field dimensions, protections to use and dose are also information on the treatment plan. Based in all selected mechanical properties and dose values assigned to each treatment plan are found the Monitor Units (MU) that should be applied in each irradiation field of treatment. In the final phase of the planning process dose volume histograms are created, which are evaluated by doctors for approval of treatment plan.

There are several planning systems available in the market, but in the context of this project the Eclipse system is the most important to refer, because is the one used in IPO Porto. With this system the radiotherapy treatment plan is a faster and easily process. In the particular case of IMRT treatments, Eclipse combines tools from 3D-CRT with a fast, accurate and interactive dose optimization. Furthermore this system also allows automatic optimization of beam geometry, simplifying the task of select the best incidence angles of beam radiation in IMRT [37].

2.7.2 Dose calculation algorithms

One of the most used dose calculation algorithm is the pencil beam. This technique assumes that any collimated photon beam incident on the patient is a group of lots of smaller, narrow pencil beams. Each of these pencil beams has a central axis ray along which it deposits

some dose. The dose deposition pattern varies with the intensity and the spectrum of the beam that is incident on the patient [38].

The Anisotropic Analytical Algorithm (AAA) is a considered a 3D Pencil Beam superposition-convolution model [26] and it was the first algorithm of this kind being implemented on Eclipse Treatment Planning System from Varian Medical Systems.

The superposition-convolution algorithms are explained by a model in which the dose deposition is seen as weighted responses (kernels) superposition for specific radiations. Kernels represent the transport and dose deposition energy of secondary particles coming from the irradiation point. When kernels are spatially invariant, this superposition can be evaluated using convolutions [26].

AAA applies kernels derived from Monte Carlo calculations, which are sized to be adjusted to local density. This algorithm considers tissues heterogeneity anisotropically by dispersing kernels in multiple lateral directions. The final dose distribution is obtained by superposition of the doses from the photon and electron convolutions[39]. Comparing AAA with other algorithms as Pencil Beam Convolution (PBC), it presents a better performance, because AAA is able to model with higher precision the electrons transport in a heterogeneous medium [40]. The computation time to calculate this algorithm is reduced, and similar to PBC, when calculated in Eclipse.

2.7.3 Isodose distributions

A dose distribution in a three-dimensional volume cannot be characterized only by depth dose distribution in the central axis. To represent a planar or volumetric variation in absorbed dose, the distributions are represented by lines passing through points with the same dose values, which are called isodose curves [19].

The planning systems calculate for each field configuration the dose distribution, given by a set of isodose curves, which are quantitatively evaluated from dose volume histogram (DVH). The DVHs are statistic dose tools that allow knowing the dose reaching a certain volume of a given anatomical structure [17]. With the help of DVHs, a planning evaluation is made, based on dose distribution analysis around the PTV and OARs. For this reason, in each image slice, the isodose distributions must be inspected [41].

2.7.4 Dose distribution verification techniques

Before the first treatment session, the MUs generated in planning system should be checked using an independent verification system. In the case of IMRT treatments, the correlation between MUs and dose delivered to each intensity modulated field is not much evident, and problems that can occur cannot be predicted by these means [42]. Therefore, for purposes of dose administered quality control, the achievement of absolute dose and relative dose verification tests are requirements for IMRT planning.

The purpose of absolute dosimetry is measure the deviation between the dose planned and dose in a point, typically the isocenter, while relative dosimetry has as goal to determine the accuracy of dose distribution. The relative dose verification consists on the comparison between the irradiation of a field planed for the patient on a cubic phantom (always with the angle of the gantry at 0 °) and the planar image provided by the Electronic Portal Imaging Device (EPID) (or other verification system) after its irradiation according to the respective patient's treatment parameters. The dose distribution plan adapted to a geometric phantom should also be compared with the resulting dose distribution in irradiated films (or in other detector) after patient's treatment simulation. To be considered absolute dose verification, the absorbed dose in films should be normalized to the isocenter dose value, obtained with the plan irradiation using a calibrated ionization chamber[43].

These tests are protocolled in order to ensure the reliability in the execution of each patient planning. These protocols include pre-treatment verifications and periodically verifications over the treatment.

2.8 Phantoms for IMRT verification

A phantom is an object that can represent a patient in terms of absorption and scattering properties of radiation. A phantom can be geometric or anthropomorphic and can be filled with water, homogeneous solid material or materials equivalent to human tissue. All of them allow the access to relevant dosimetry information, by the introduction of some kind of detector therein. This makes phantoms an essential tool in the evaluation of equipment operating conditions or in quality control checks.

In daily IMRT treatments verification, a geometric phantom made by solid water slabs is widely used (Figure 2.11), which simulates the radiation absorption and diffusion properties in human tissues. The solid water slabs reproduce the dosimetric properties of the

tissues, in a simple way, reducing anatomy complexity and presenting regular geometries. These slabs are made of water-equivalent plastic and have holes for different types of ionization chambers, in particular for Farmer type, allowing that absolute or relative dose measurements be achieved [44].

Figure 2.11 – Solid water phantom used in IMRT treatments quality control [45].

2.9 Monte Carlo dose distribution calculations

Stochastic methods are known since before the advent of computers, however only in 1947 the name of Monte Carlo Methods has been assigned [46]. This term encompasses a class of numerical methods based on random numbers usage. These methods are very used in areas as physics and mathematics, in particular at large number of independent variables problems [47].

In Monte Carlo simulations of radiation transport, a particle is seen as a random sequence of free paths, which ends with an interaction. Therefore, the particle could change its direction of movement, loses energy, and occasionally produce secondary particles. This simulation is the numerical generation of random events and a model to describe them is needed. Thus, a set of differential cross sections (DCS) are created for the relevant interaction mechanisms. The DCSs determine the probability distribution function (PDF) of the random variables that characterize an event, such as interaction between successive events of a free path particle, the type of interaction occurred, and the loss of energy and angular deflection due to an interaction [48]. As these PDF are known, it is possible to generate random events by using appropriate sampling methods.

Monte Carlo algorithm includes some components that should be highlighted: the probability distribution, since the system has to be described by one or more PDFs; the

random number generator from where the entire process begins, which must be fast and reliable.

The Monte Carlo calculations can take a long time, especially in radiotherapy applications. For this reason, techniques to increase simulations speed are needed, which are called variance reduction techniques [46]. Particle splitting, Russian roulette and forced interaction are three techniques that worth to be highlighting in this context.

In particle splitting, the particle to being controlled is divided into several particles, which are followed individually. Mathematical aspects of particle splitting are the other variance reduction techniques basis.

Russian roulette is a mathematical tool essential to the other variance reduction techniques implementation. This technique combines several particles at once, but only a single particle at a time is followed. Accordingly to this, the probability of 1-p (typically 90-99%) is assigned for the death of a particle, but its weight is increased by a factor of 1/p when the particle survives. The necessity of this tool is evident when used with the forced interaction (discussed below), since without the particle "death" in russian roulette, the first interaction would never end. This is a method performed when the particle weight is below a certain "cut" value. In Russian roulette the variance of the problem is increased, but Monte Carlo calculation efficiency is also increased. Therefore computer time is saved, which would be spent on low-weight particles.

Forced interaction technique forces a collision on a given segment of the particle path, which is located inside the region under study. This should make particles live longer and have more chance of being counted.

Several Monte Carlo codes are available for simulation of many types of particles transport and in a wide range of energies. The most general Monte Carlo codes, as GEANT, MCNPX or FLUKA, simulate the transport of various types of particles (electrons, positrons, photons, protons, neutrons, heavy ions, etc.) to a wide range of energy[49]. Those programs have various applications such as detectors simulation response; medical treatments simulations; radiological protection dosimetry; study of the radiation effects in microelectronics, etc. More specific codes, such as PENELOPE, EGS, ETRAN, ITS, they focus on electrons and photons transport [50].

Monte Carlo methods are considered the most accurate methods for dose calculation in radiotherapy [51]. They can model realistic radiation transport through the LINAC head, the MLC and the patient anatomy accurately. In this context, several programs directly indicated to radiotherapy have been developed such as: VMC/XV MC, DPM, MCV and MCDOSE [50]. These codes use multiple variance reduction techniques and complete

calculations with a reduce CPU time, in comparison with ordinary EGSnrc calculations [52]. Most recently, another simulation program of radiotherapy treatments came up, known as PRIMO, which will be studied next.

2.10 PRIMO (Penelope based MC code)

PRIMO is a Monte Carlo program to simulate a wide range of Varian and Elekta linear accelerators [53], as well as their electron applicators and multi-leaf collimators. This program allows the calculation of the dose distribution in the patient in a simple way, without being required deep computing knowledge. This is possible because PRIMO is made of a combination of several programs [54], which work together in order to make PRIMO a potential tool in radiotherapy treatments simulations. Also for this reason, PRIMO is interactive, intuitive and simple to use, in contrast to other Monte Carlo simulation programs.

The PRIMO codebase for physical aspects is PENELOPE. It allows the simulation of radiation transport in a LINAC, as well as the absorbed dose distributions in a phantom or patient. The remaining constituents of PRIMO programs and their respective functions are shown in Figure 2.12.

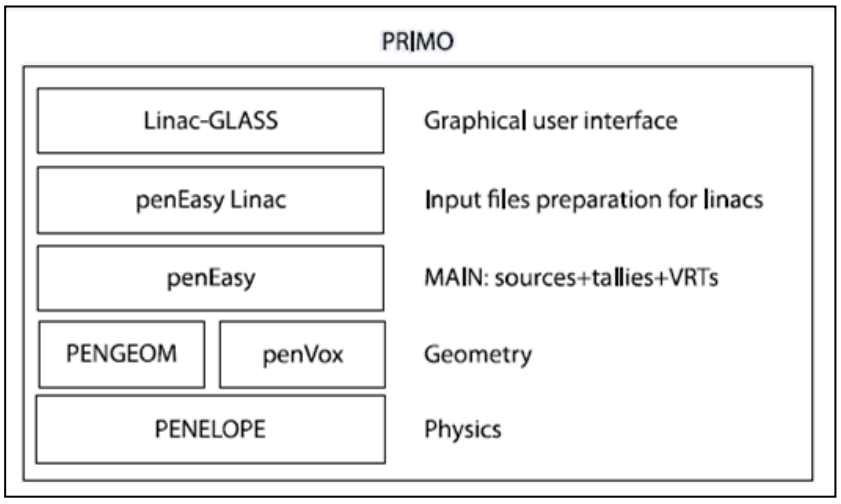

Figure 2.12 – Scheme that has all the components of PRIMO [55].

To begin the project, a device model to simulate as well as the operation mode (electrons or photons) must be chosen. Then, the calculations performed by this program can start selecting other parameters of interest, which are divided into three phases. In the first one (s1) are determined the energy of irradiation (nominal energy), the initial energy, the energy of FWHM, the focal spot of FWHM and the beam divergence. In this step is created a

phase-space file that contains information about the particles created and its interaction on the LINAC head. In the second stage (s2) the interaction in the bottom of the LINAC of all particles generated in S1 is simulated. The interaction occurs between particles and the jaws, MLC and air space until the phantom (or patient). In s2 are determined the presence or absence of MLC, the number of fields, its size and configuration. In the third and final stage (s3) the interaction between particles coming from previous segments with the phantom (or patient) is simulated. Here is chosen the use of a phantom (and its definitions) or a patient CT image and the SSD. These three segments can be launched one at a time or all together, but before parameters relating to the variance reduction techniques, simulation time, number of particles, number of cores used and with random numbers must be chosen.

Once all simulation steps are finished, the dose profiles in the phantom (or patient) are obtained. The generated files can be analyzed using tools provided by PRIMO. To s1 and s2 the generated phase space files can be accessed and analyze. In s3, the dose distribution profiles can be seen, studied and compared with other calculated or experimental curves. This comparison tool is based on the gamma test that will be explained next [55].

2.11 Use of Gamma Index function for MC simulations validation

A simple way to evaluate the obtained results is overlapping two dose distributions: for example, compare a distribution from the TPS with a measured in the LINAC. With this analysis it can be seen that the areas are not totally coincident in both images, compatible regions and less compatible regions can be distinguished. However, obtain more accurate results, meaning quantitative data, can be a hard task to do.

The first criterion used to perform a quantitative evaluation was the dose difference, which is good for regions with low gradient dose. However, for areas with a high gradient dose this criterion is not suitable, since small space deviation brings a big dose difference. For this reason, another criterion, called DTA (Distance-To-Agreement), has been admitted in order to evaluate the high dose gradient regions.

The analysis of dose distributions (fluence) is performed comparing the dose and DTA, which determines if the dose distribution measured with LINAC is in accordance with the one that was planned. In this context, a function called Gamma Analysis or Gamma index has appeared.

The dose analysis [56] is a method that combines the dose difference and DTA criterions for comparing two dose distributions (e.g., a simulated curve and a curve obtained

experimentally). The dose difference is evaluated by exploring the dose distribution in the neighborhood of the experimental points. For a given experimental point P, where the dose in the point is $d_e(p)$, the gamma index, Γ, is given by:

$$\Gamma = \min \left\{ \sqrt{\left(\frac{\Delta d_i}{\Delta D}\right)^2 + \left(\frac{\Delta s_i}{\Delta S}\right)^2} \right\}, \qquad \textbf{Equation 4}$$

where are arbitrary constants known as the acceptance criteria for dose difference and DTA (values used are typically 2% and 2 mm for ΔD and ΔS, respectively). The term Δd_i is the difference between $d_e(p)$ and the simulated dose at a certain point p_i; and Δs_i is the distance between p and p_i. Evaluating the set of points p_i and finding the minimum value of the expression in brackets the gamma index value is discovered [57]. Through this analysis it is possible to obtain information about the zones where the dose distribution is in according, or not, to the acceptability criteria [58].

3 Methodology

3.1 Basic Dosimetry

The validation of the program in study requires the comparison of basic dosimetry curves generated by PRIMO with the ones acquired in the LINACs every six months. When both curves match according to the gamma index test, PRIMO is validated and other studies can be started.

To acquire the PDD, in a LINAC, a setup with a water phantom has to be mounted. First of all, the gantry and collimator must be in 0º and the table on 90º. Then the tank can be centered under the gantry and filled with water. After that the controller and the electrometer should be connected to the tank cables and all the equipments can be turned on. The next step is level the tank, align it with the lasers, put the thermometer in the water to stabilize, and adjust the SSD to 100 cm. At that moment, the measuring and reference ionization chambers (PTW Semiflex Ionization Chamber 31010) can be connected to the electrometer. The measuring chamber is dipped until the limit of water surface and the reference chamber stay in the support above the water tank in the limits of the irradiation field. Finally the pressure and temperature values are noted and the practical acquisition of PDD and lateral profiles is started.

With the purpose of finding the best curve to use on the validation process, the variation of the PDD curve over time (to the same LINAC) will be studied. To reach that goal the maximum of the curves will be calculated and compared with the ones obtained in the acquisition program, called MEPHYSTO.

3.1.1 Basic Dosimetry Curve Analysis

To analyze the PDD curves the first thing to do is to calculate the curve that better fits the maximum of the PDD. This is done in order to discover the accurate value of depth to the maximum dose, once in practical acquisition the curve obtained is made of discrete points. The maximum value is found by an interpolation of the points made by Mephysto. This process of interpolation is not known, that is why it is so important to calculate the PDD maximum using a known procedure.

The first step in this procedure is to select the maximum values of each curve (approximately the twelve maximum values) and choose the degree and parameters of the

function. The adjustment of these parameters is made by using the solver tool from excel. The function selected was the one in which the sum of the residue difference (between values from Mephysto and the ones calculated by the new function) was minimal. With this step the function is founded for each PDD curve. Calculating the first derivative of the function the maximum values of the curve were found. Those values were compared with the ones obtained with Mephysto and both were analyzed regarding the parameters: quality index (Qi or QI), the depth of the maximum dose (R100) or 80% and 50% of dose (R50, R80) and percentage dose at a depth of 100 mm (D100). The quality index parameters are calculated based on help documents from Mephysto using Equation 5 and Equation 6, where D_{200} is the dose at depth of 200 mm [59]. The same kind of analysis was made to the lateral profiles x and y. In this case the profiles flatness and symmetry along the years were calculated and compared with the ones given by Mephysto. This calculation was made using the equations already showed in Flatness and Symmetry on the Theoretical Background, also present in Mephysto help documents [60]. Ending this procedure the curves for comparison and validation of PRIMO can be chosen, which are considered in this context reference curves.

$$\boldsymbol{Q_I = \frac{D_{200}}{D_{100}}} \qquad \textbf{Equation 5}$$

$$\boldsymbol{Q_i = 1.2661 \times Q_I - 0.0595} \qquad \textbf{Equation 6}$$

3.2 PRIMO Simulation

To start a PRIMO simulation the first thing to do is write the simulation name on Project ID space that can be seen in Figure 3.1. In the same window is chosen the folder where the project is saved, and most important, the LINAC to simulate and the operation mode are selected. In this work, a Clinac 2300 with operation mode in photons will be always used. The simulations were performed in an Intel(R) Xeon(R) CPU E5-2660 v3 @ 2.60GHz 2.60GHz with 16GB of RAM, with 32 CPU cores working at the same time.

After that, the simulation segment 1 can be set up as shown in Figure 3.2. In this stage, parameters as nominal energy, initial energy, energy FWHM, focal spot FWHM and beam divergence are defined. The nominal energy used was 6 MV for all the simulations performed. The other parameters were changed until the best simulation results were achieved. After validate PRIMO these parameters did not suffered changes. In Figure 3.2 are the parameters that get the best accordance with practical results. To simulate this segment a check signal must be put in the check box of S1. Other parameters related to S1 should be configured

before launch the simulation. The variance reduction techniques configuration will not change for all simulations (Figure 3.3). At S1 is chosen the splitting roulette for the splitting above jaws, since all simulations have initial energy lower than 15 MV. For size of splitting region the second option will be selected (fitted to the field size), because in this work only fields with 10x10 cm^2 will be simulated. In simulation configuration, the simulation time or the number of histories is defined as stopping criteria, as can be seen in Figure 3.4. These parameters affect statistics, that's why after finding the best parameters for S1, a new simulation with a higher number of histories should be done. In this window is also configurable the refresh time for simulation partial report and the number of processors used in calculations. The random seeds should also be switched before any simulation beginning, in order to obtain more reliable results, which change randomly clicking on dices. Then the save button should be pressed and the simulation of S1 launch.

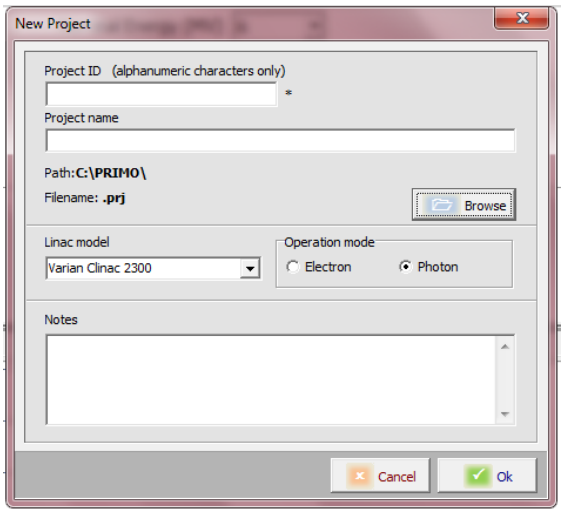

Figure 3.1 – PRIMO window that opens when new Project is selected.

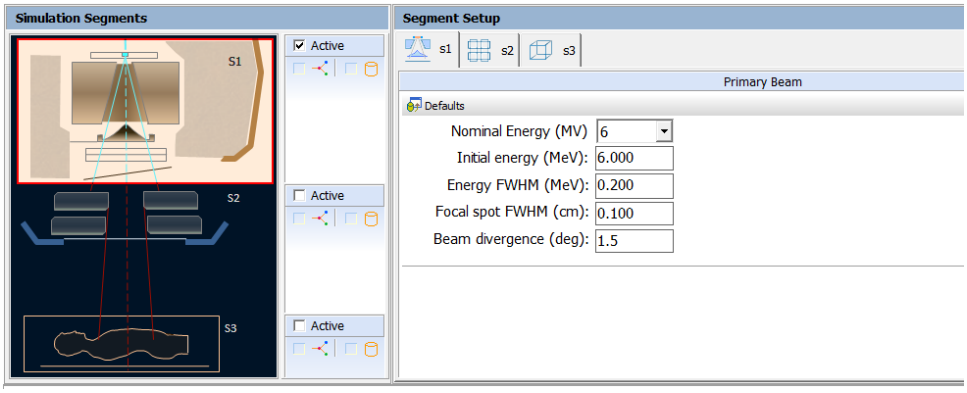

Figure 3.2 – Parameters of Segment 1.

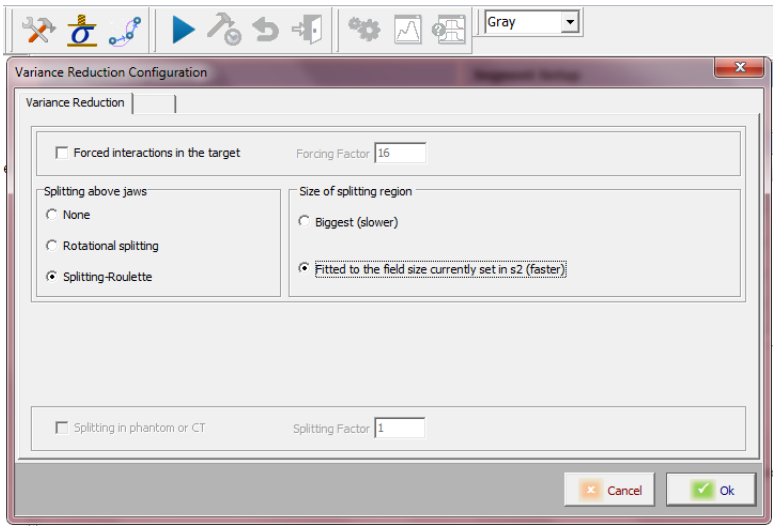

Figure 3.3 – Variance reduction configuration for s1.

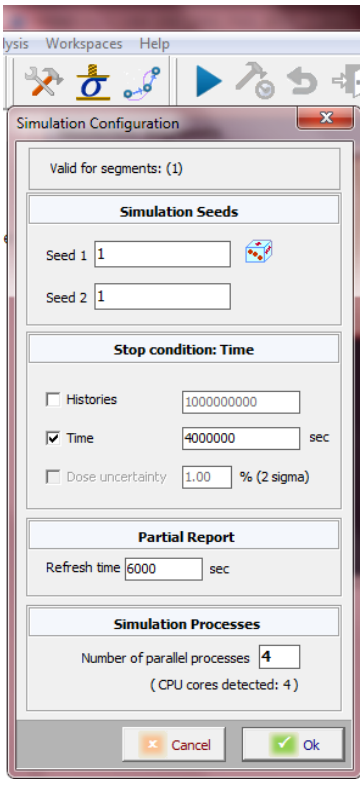

Figure 3.4 – Simulation configuration.

In segment 2 is defined the data related to the jaws, MLC and gantry. To simulate this step, similarly to what occurred in S1 it is necessary to check the S2 box, as shown in Figure 3.5. In this work, only the boxes related to MLC and jaws will suffer changes, the remaining ones will not. For all PRIMO simulations in the context of this project, the field size will be 10 x 10 cm^2 (Figure 3.6). After validate PRIMO, MLC should be introduced. In the MLC box it is selected the same MLC present in the simulated LINAC. In this particular case, once it is

intended to simulate the 6MV beam of a DHX HP LINAC from Porto IPO, the millennium 120 MLC will be choose. After all parameters be defined, the simulation configuration window should be opened and select the stopping criteria number of histories that came from S1. Then, all configurations are saved and S2 simulation is launched.

Segment 3 is the simulation part related to the dose distribution on the phantom or patient, thereby is at this stage that information about the receptors of radiation are defined. In Figure 3.7 a layout of the configuration window of s3 can be seen. There are the options to simulate a dose distribution on a water phantom, on a slab phantom or in a CT. In this work only simulations with a water phantom and with a CT were performed. To validate PRIMO the simulations were made using the water phantom. For this reason, it was necessary to define the grid of calculation: the total size and the bin size. Otherwise, in simulations after PRIMO validation a CT scan of a phantom used in practical measurements was used. In this case there is no need to complete anything, because CT scan already brings all the information about the calculation grid. Defining all this, and the box of S3 with a check signal it is time to configure the variance reduction parameters for S3 (Figure 3.8). In this window is checked the splitting in a phantom or CT with a splitting factor of 200. This value was used by recommendation of PRIMO project authors. After that, the simulation configuration window is opened and once again is selected the stopping criteria on the number of histories. Then, this entire configuration is saved and S3 is launched, finishing all the simulation steps.

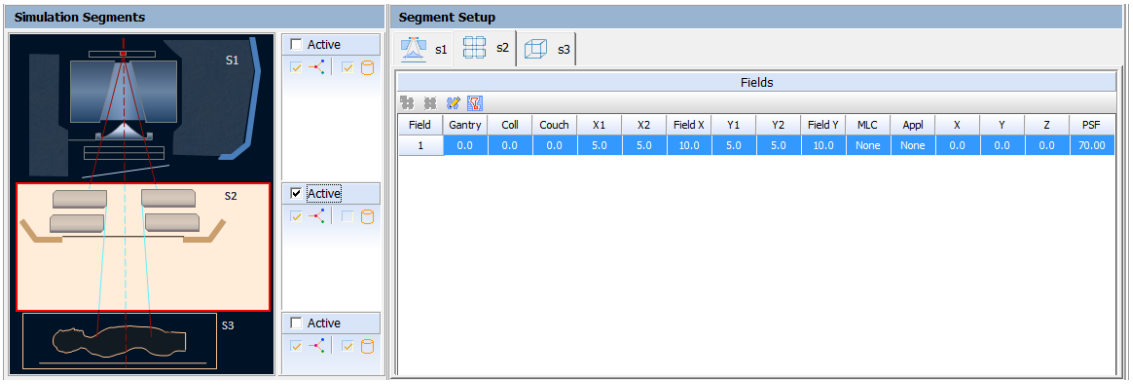

Figure 3.5 - Parameters of Segment 2.

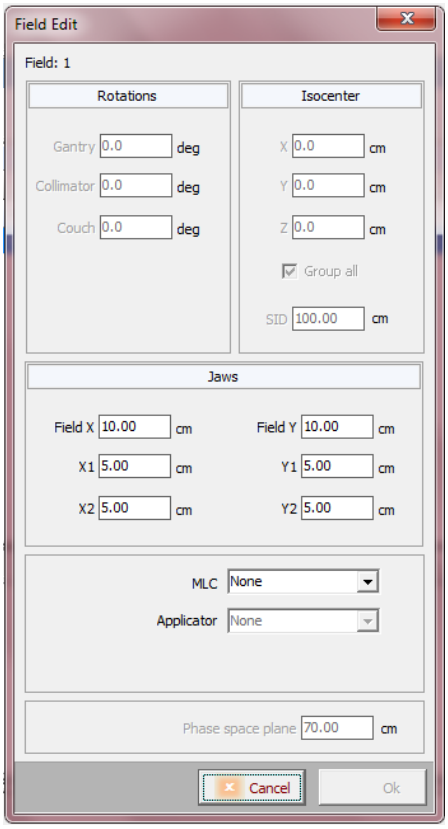

Figure 3.6 – Configuration of the irradiation field.

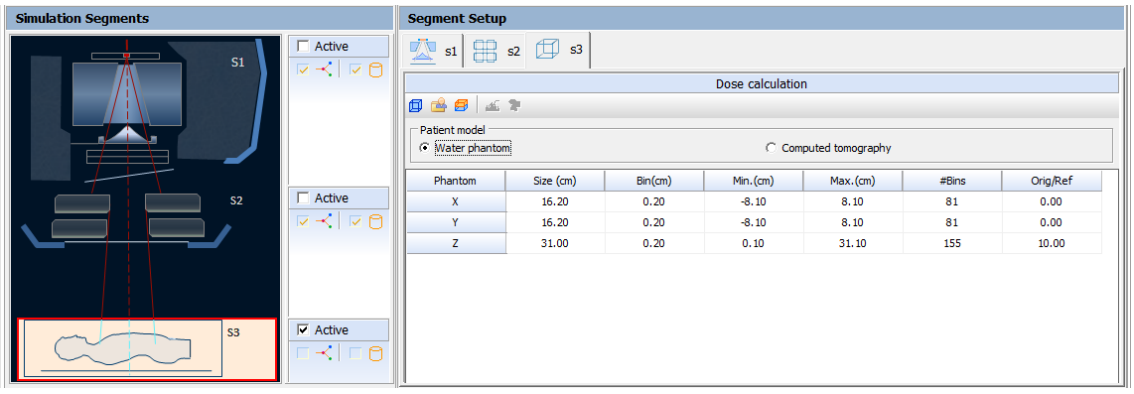

Figure 3.7 - Parameters of Segment 3.

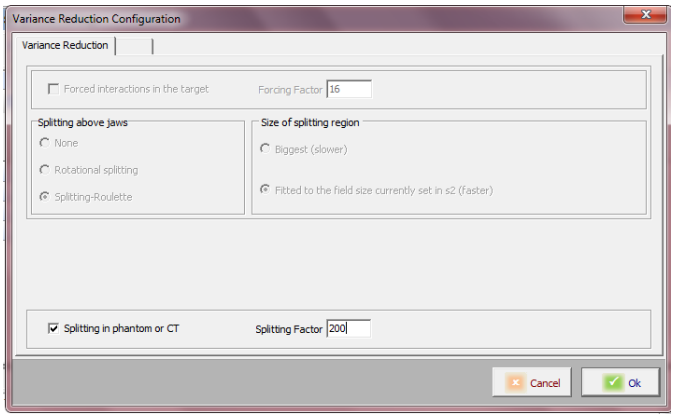

Figure 3.8 - Variance reduction configuration for s3.

3.3 PRIMO validation

To validate PRIMO software, the basic dosimetry curves simulated must be compatible to the ones selected before, from the biannual LINAC tests. With this correlation PRIMO is validated, the parameters of s1 are found and there is no need to redo simulations of the LINAC head.

The discovery of the parameters is done by trial and error, trying one by one all the parameters that can be adapted by PRIMO and comparing the simulation with the reference curves. First of all, the variation of the simulation results according to the number of histories will be studied. In order to do that, it will be checked if the simulation time is proportional to the number of histories. Simulations with an increase on time will be done and the number of particles checked. Then, the statistical uncertainty will be also studied. In that case, it will be chosen the minimal simulation time to obtain results with acceptable statistical uncertainties, which is a parameter connected to the number of particles.

The energy of the electrons in the electron gun is another parameter that has to be studied. The nominal energy was for all simulations 6MV, but for the initial energy simulations with energies between 5.4 MeV and 6.26 MeV were made. The best value of initial energy is the one that the PDD curves simulated and obtained are most coincident. The beam divergence, energy FWHM and focal spot FWHM also suffer changes in their values. Although these parameters are related to S1, the three segments have to be simulated in order to check the results. This happens because only the last simulation segment gives curves that can be compared with the ones from the LINAC.

As nominal energy was constant for all simulations the variance reduction techniques does not suffer many alterations. The variance reduction technique splitting roulette is more

efficient to low energies simulations (above 15 MeV) when compared to rotational splitting [57]. Thus, as the only energy used in simulations was 6 MeV the variance reduction technique used was always splitting roulette with the parameters suggested in the PRIMO's user manual for the example of a Varian Clinac 2100 simulation [57].

To validate PRIMO software the coincidence of the lateral profiles simulated and acquired in practice must exist. This step is not as easy as the coincidence between PDD curves. In PDD curves the parameter that most affects the result is the energy of the beam, but in lateral profiles this question is not so obvious. Lateral profiles will be affected by factors that are not directly connected to the first simulation segment (S1). Parameters controlled in S2 and S3, as field dimensions and visualization grid of dose distributions, respectively, have a major importance in this question. Therefore, the field dimension must be confirmed, which was 10 cm x 10 cm for all simulations made in this work. If penumbra regions where coincident the fields have the same size. The size is confirmed by the position of the penumbra region in the position axis. However, dose distribution simulation grid controlled in S3, in the voxels dimensions, can affect this result. Consequently, some grids should be tried in order to obtain the best coincidence between lateral profiles. All of these simulations were made using a water phantom in S3, which the voxels size and number of primary histories will be optimized to obtain statistical uncertainties below 2% in suitable calculation time.

When this process is finished, PRIMO software is validated and more complex simulations can be done.

3.4 PRIMO output problem

The PRIMO output is shown in the program as images and graphs. However, the data is not easily accessible using other programs. The only file that is exportable to other programs is a text file with all the values generated by PRIMO. As this document is not easy to understand, interpret the file and convert it into an image is imperative. This transformation is important to compare PRIMO output with data from other programs or practical data, which is a big goal in this project.

In addition to the fact that the output document can be of complex interpretation, comparing to other programs than PRIMO, it can present two layouts according to the simulation type. If the simulation is with a water tank phantom the data organization is different than if the simulation were with a slab phantom CT (the one used in practical

measurements). This situation complicates the output data conversion to other programs, such as Verisoft from PTW Freiburg.

To solve this problem a set of Matlab functions was created (Appendix A). They have as final objective to manipulate the PRIMO output in order to create dose images at specific locations in DICOM format, independently of the data output type. For a simple field, i.e. only one field no matter its configuration, this task is not much difficult. The output data is read by a Matlab function and converted into a matrix for a given depth (or for a given value of x or z, accordingly to the final goal). Then, this matrix is transformed into a dicom image which can be introduced in Verisoft to be compared with another image from TPS or from LINAC.

However, if the simulation contains more than one field, this process of conversion needs more steps. Thereby, before convert PRIMO data into a matrix, a merge of all fields must be done, for a given depth. In order to achieve that, a weighted mean of all fields is made. This transforms the data from several fields in data with similar structure of the initially obtained from one field. After that, the procedure is the same used to one field: convert data into a matrix and transform it in a dicom image.

3.5 Quality Assurance (QA) Test

A verification of the dose distribution to be administered to the patient in an IMRT treatment needs to be performed by physicist for every treatment plan. This procedure is made using quality control software, such as PTW-Verisoft. Thereby, after being completed the treatment plan the physicists will verify if the plan (adapted to a water phantom) is coincident with the measurements on the phantom. This comparison is made based on the gamma index test. When the distribution dose profiles simulated and measured have a compatibility higher than 95%, with a gamma index to 3% and 3mm, the treatment is approved and administered to the patient. Otherwise is necessary to find what was wrong and redo the QA. In this part of the work, the same thing will be done, with the addition of PRIMO output comparison.

After performed simulations in PRIMO, the same irradiation set-up will be calculated in TPS in order to be scheduled and sent to the equipment to be applied. Then, practical measurements on the LINAC will be acquired using the same set-up of QA tests for IMRT treatments. A phantom of 30 cm x 30 cm x 15 cm is placed on the top of the bed. The phantom is made of a material with similar physical properties to the water, in this case the slabs are the PTW RW3, which have an epoxy resin coverage. There are 4 slabs of 1 cm and 1 slab of 0.2 cm above the detectors (Figure 3.9) and 10 slabs beside them. Between the slabs is placed a PTW

Octavius® I (RW3729 array) (Figure 3.10). This is a 27 x 27 cm^2 matrix with 729 ionization chambers that will obtain de dose distributions.

Figure 3.9 – Solid water phantom used in IMRT treatments quality control in Porto IPO being mounted on the LINAC table for a verification procedure.

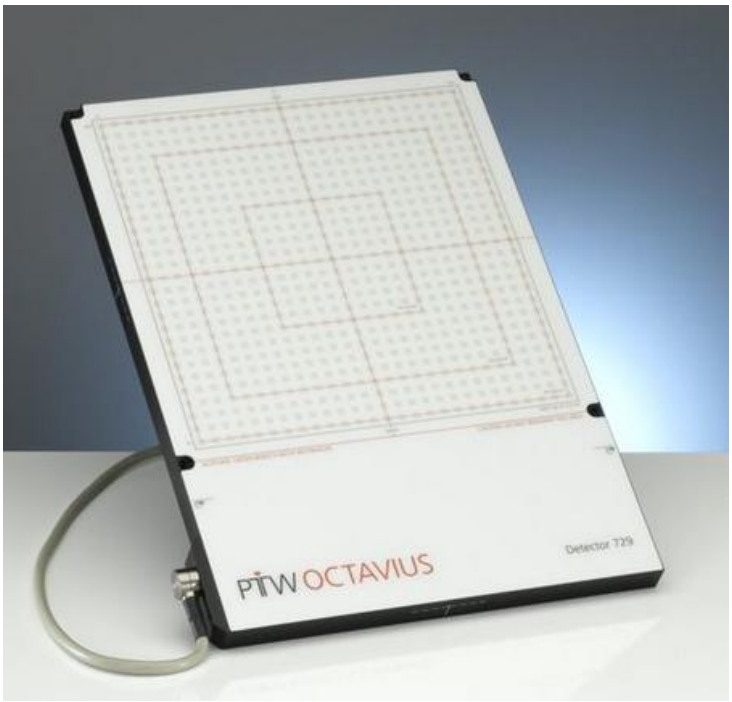

Figure 3.10 – PTW matrix of 27 x 27 cm^2 formed by 729 ionization chambers, spaced by 1 cm, which is used in the solid water phantom at IMRT treatments quality control [45].

3.6 MLC Tests

Once PRIMO is validated the MLC is added. This is crucial to the aim of this project, since there is no IMRT without MLC. Thus, MLC tests will be made in order to prove that PRIMO has potential to simulate IMRT treatments.

At this stage some tests with MLC will be done, but all of them will have the same logistics. A PTW Octavius® I (RW3+729 array) was imaged by a GE LightSpeed CT scan, introduced in PRIMO and used as the voxelized phantom. Then, PRIMO simulation is launched using the same parameters that validated PRIMO software. The obtained data is converted in dicom images, using the procedure already exposed in PRIMO output problem. In second place the same test is made in TPS and irradiated in a LINAC, using the set-up of IMRT QA tests, which were already described. At last, the three results are compared using Verisoft, to see if they are compatible according to gamma test. This procedure is made for every MLC test, before proceed to the next one.

The first test made was to see the influence of MLC addition in simulations with an open field. The same MLC present in the LINAC was selected in PRIMO without any configuration, i.e., maintaining an open field of 10 x 10 cm^2. In the institute, the LINACs 2300 have an MLC of type Millenium 120 MLC, which was used in simulation. After that, the same configuration was used in TPS calculation and was irradiated in a LINAC.

Keeping the same MLC, the second test consists in adding a configuration to it. This represents an irradiation of a static field. The configuration was chosen in order to test both sides of MLC leaves. Therefore, some leaves staid opened and others closed, as represented in Figure 3.11.

After validation of static MLC, the most important step for this project can be done: a test with dynamic MLC. This will be the concept proof that PRIMO can potentially be used to verify IMRT treatments. At this stage, a dynamic IMRT plan was calculated by the Eclipse™ TPS and irradiated. Based on this plan, a dynamic MLC delivery was split into 89 static segments and simulated on solid water phantom as reported in Figure 3.12 and Figure 3.13. The dynamic IMRT plan was delivered on a solid water phantom, in the same condition of the routinely Quality Assurance (QA) measurements: solid water phantom centered and positioned at SSD 95 cm with the 729 array placed at 5 cm of depth in the phantom. This represents the irradiation of one IMRT field in a LINAC, when is used the step and shoot technique.

Given the matrix design, which has 1 cm spaces between ionization chambers, it was used also gafchromic for the last test. This would assure the compatibility or not between the three images, since its spatial resolution is better than the one associated to the matrix.

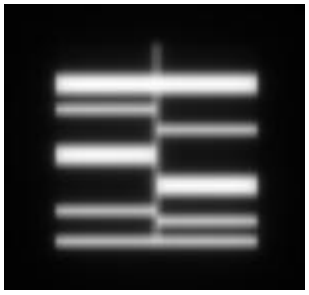

Figure 3.11 – MLC static configuration.

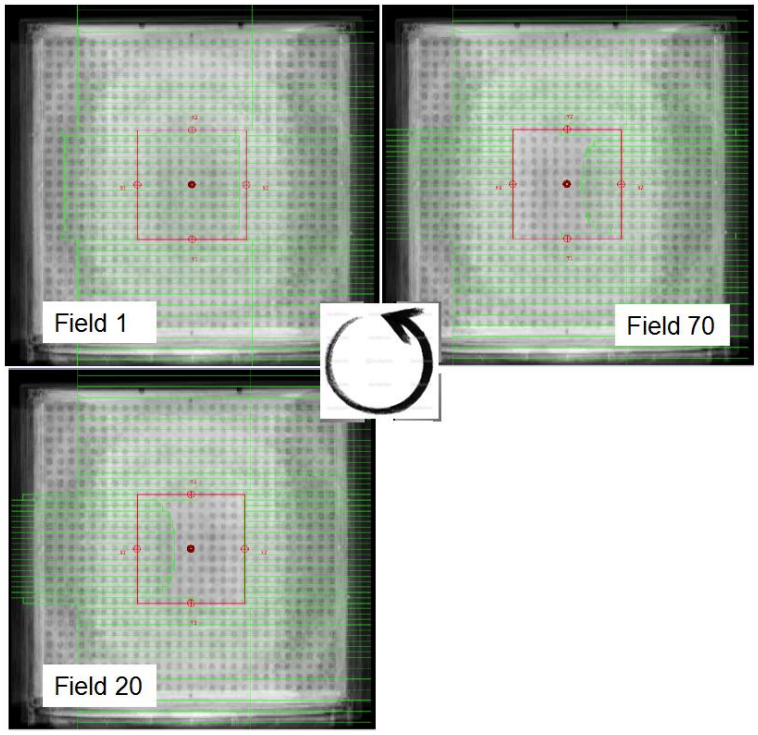

Figure 3.12 – Example of Dynamic IMRT divided into 89 static MLC shaped fields.

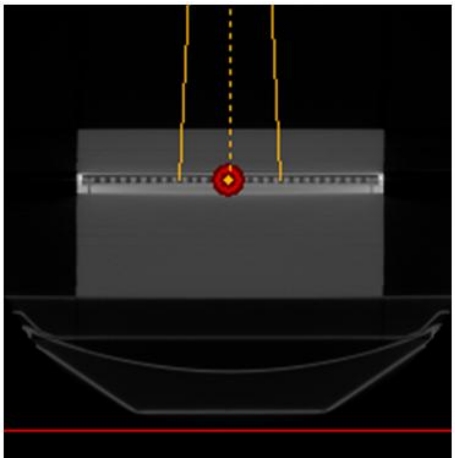

Figure 3.13 – Simulation Setup. The red mark indicates the isocenter placed at the center of the ion chamber array. The isocenter is at 100 cm distance from the beam source. The numerical voxelized phantom is created by the internal conversion tool of PRIMO, once the CT scan calibration curve is introduced.

4 Results and Discussion

4.1 Basic Dosimetry Curves Analysis

Every six months, LINAC tests using water tank are performed to verify PDD curve, lateral profiles and other parameters. The curves obtained in these tests are the ones used in PRIMO comparisons, for validation purposes. However, over the years many curves were obtained from these verifications. Thus, a study about them had to be made in other to choose the best curves to use in PRIMO validation. Thinking in PDD curves, it is obvious that from those measurements is not possible distinguish the maximum value, since the curve is made by discrete points. Thus, the maximum value of these PDD curves has to be calculated according to the methodology already presented in the previous chapter. From calculations of the curve that best fits the maximum PDD curve points it was obtained, for every curve analyzed, a three degree polynomial equation. Calculating the first derivative, the zeros are obtained and consequently the depth of the maximum dose for that set of points, which is one of the zeros. In Figure 4.1 the points calculated and given by Mephysto are shown and the differences are visible. R100 from Mephysto and R100 adjusted oscillate around a midline and they are limited by a margin of 2σ, which means twice the standard deviation (k = 2; Prob(2σ) = 95.4%). The values suffer variations that seem to be random over time, not being possible to distinguish any trend.

All values are in the considered range, but some of them are near the borders. The first values of R100 and R100 adjusted are the most compatible and they are in the middle line. All the other values suffer variations in relation to each other. Although in the end they tend to the first value, the one from commissioning, because LINACs are adjusted when out of the limits in accordance to those values.

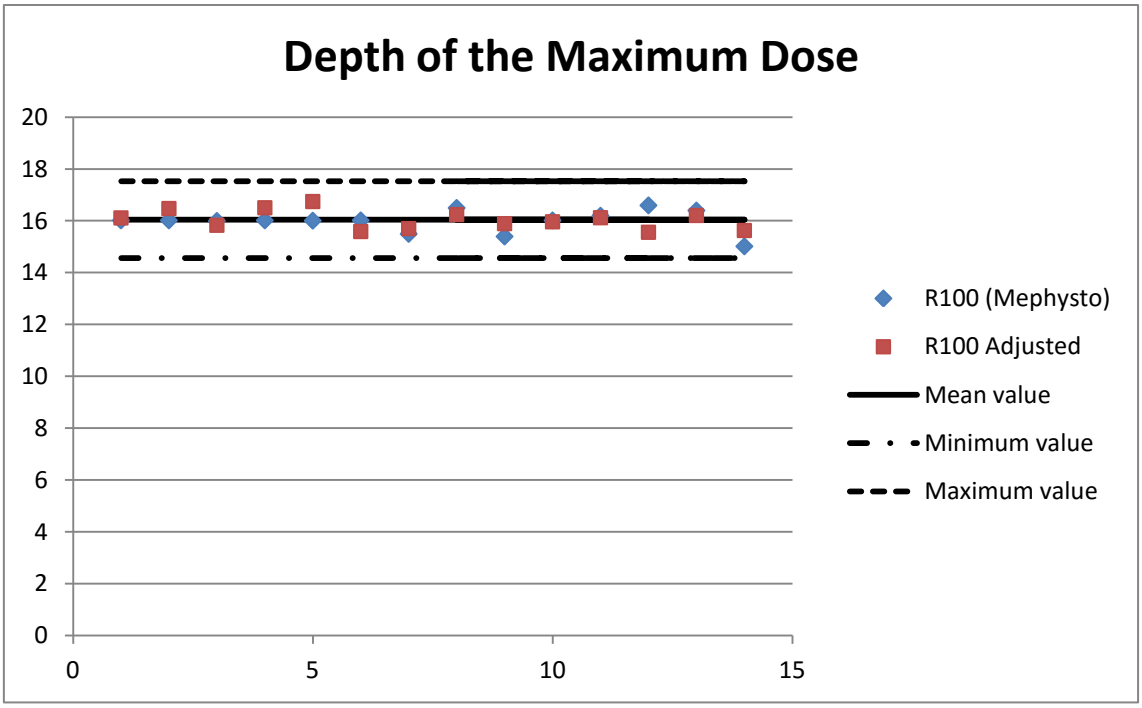

Figure 4.1 - Maximum dose depth.

Regarding to the lateral profiles x and y a variation in the values of flatness and symmetry also occurs. This variation occurs between the calculated and Mephysto values as well as between the symmetry and flatness values over time. This fact can be observed in Figure 4.2 and Figure 4.3 for lateral profile X; in Figure 4.4 and Figure 4.5 the variations in lateral profile Y. The differences among calculated and Mephysto values are explained for the expressions used to calculate the data, since the expressions used in the program are unknown. However, the variations over time in flatness and symmetry calculated and from Mephysto are the same. Similarly to what occurs with PDDs the changes over time are random around a central middle line. Although, the values increase and decrease over the years always tending for the values from commissioning.

After this analysis of the PDD curves and lateral profiles over the years, the data chosen for simulations comparison were the ones from commissioning. They were selected because the reference for adjustments that LINAC suffers over time and data analyzed proves this fact.

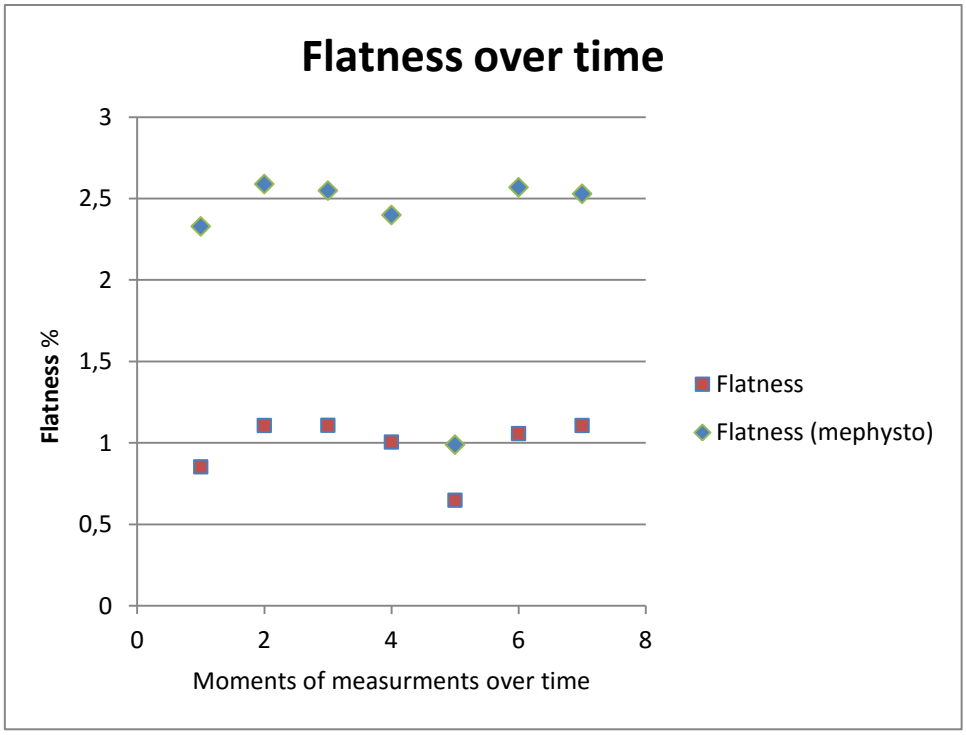

Figure 4.2 – Flatness over the years for lateral profile X.

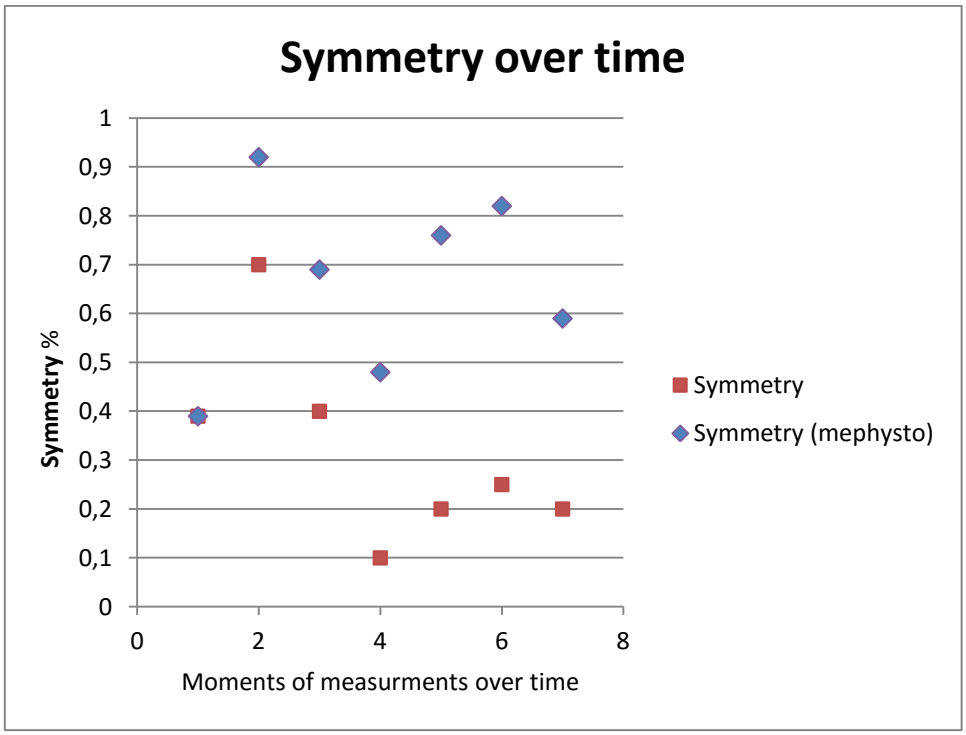

Figure 4.3 – Symmetry over the years for lateral profile X.

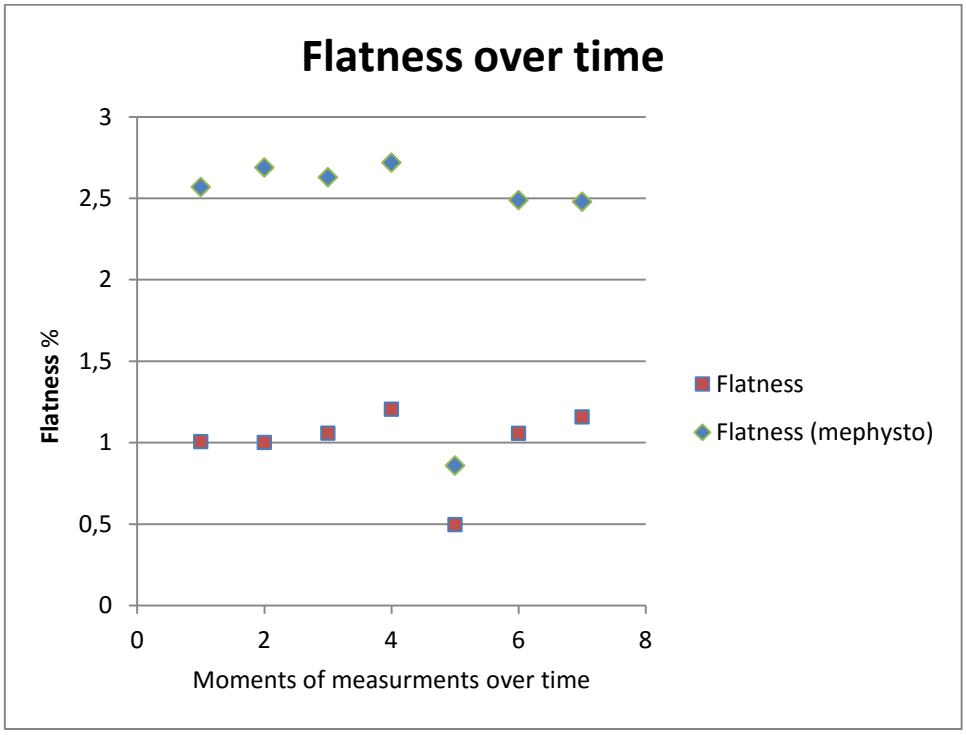

Figure 4.4 - Flatness over the years for lateral profile Y.

Figure 4.5 - Symmetry over the years for lateral profile Y.

4.2 PRIMO validation

The validation of PRIMO requires the study of many parameters, in order to understand how they change the basic dosimetry curves simulated by the program. The first parameter to be studied was the number of histories. First of all, the relationship between the number of histories and simulation time should be optimized. After running several simulations with different time lengths, a graph with the relationship between the number of histories and the simulation time was built. In this graph, shown in Figure 4.6, an increase of the histories number can be seen when the simulation time also increases. However, some points differ of this linear correlation. This happens because the processor activity influences these parameters, meaning that if the computer is running other task while simulation is running, the number of histories will not be the same as if the processor was only doing the simulation, considering an equal duration. Sometimes, this question is hard to overcome because the computer software (Windows 7) has some hidden processes running during Monte Carlo simulations that come from other tasks, which reduces the computer processing capacity. For this reason, if a previous number of histories have to be achieved, it is not convenient simulation time to be used as stopping criteria. For this purpose it is better to select the number of histories instead. This technique was adopted, but the amount of time wasted to a given simulation was too big and the results did not show a big difference. In fact, they were similar to the ones obtained in simulations based on time. For example, to get a simulation with about $1x10^8$ histories, it would take about a month, which is not reasonable for a project with this dimension. However, for a simulation with a week of duration the obtained results were very satisfactory. In this analysis it was perceptible that simulations with a major number of histories had better statistic, i.e., the curves generated were smoother (Figure 4.7). It happens that the higher the number of histories, the better the statistics, but only up to a point in which the improvement was not noticeable. However, there is no number of histories that give an ideal simulation curve, with the less oscillation as possible. Thus, a balance between time consumed and simulation results in statistic terms must be made. Because of this, the stopping criteria time was chosen as work method in this task, since it obtained an acceptable number of histories and consequently a good simulation statistics in a time interval controlled by us. This will bring similar results with a smaller waste of time. To minimize the influence of the hidden processes referred before, and get a number of histories proportional to the simulation time, the computer should be restarted before launch any simulation. The proportionality between the number of histories and the correlation of calculated and

measured data (based on gamma index) is also studied, as shown in Figure 4.8. As can be seen, there is no relation between both variables. The increment of the number of histories generates more points, more statistics, smoother curves, but not necessarily accurate profiles. The precision of the profiles is affected by other factors, which will be studied forward.

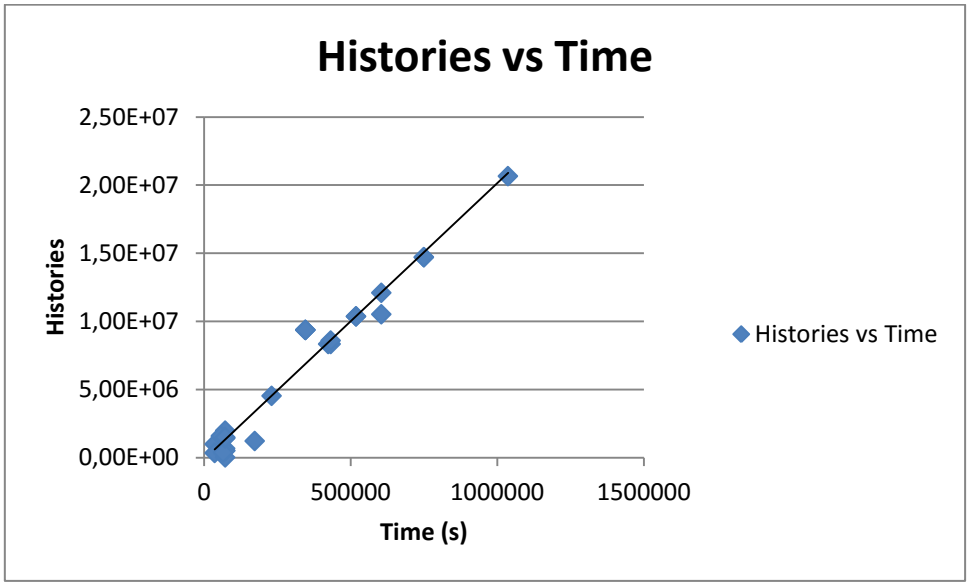

Figure 4.6 – Number of histories in function of the simulation time.

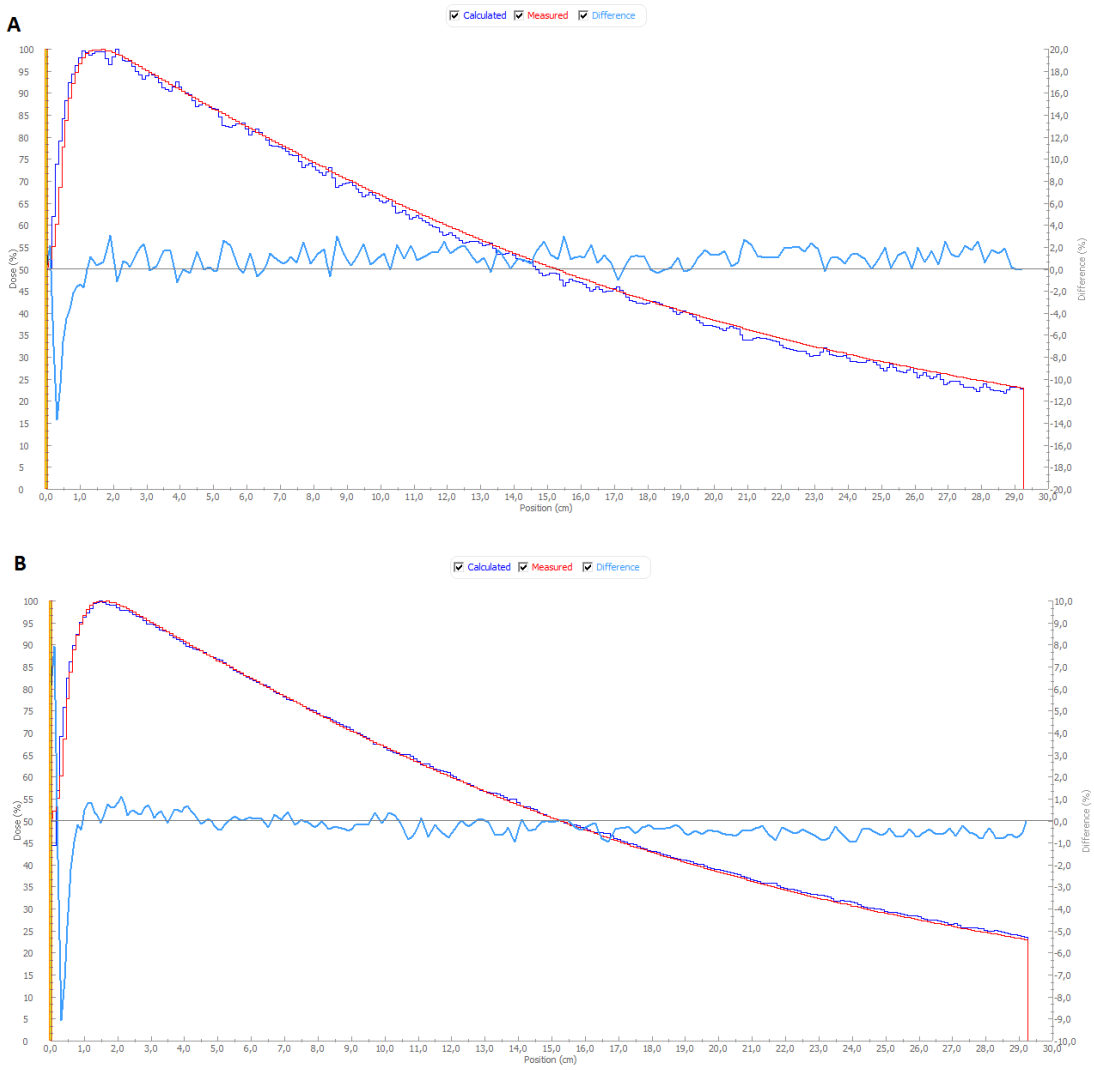

Figure 4.7 – PDDs from simulations with the same conditions but with different time as stop criteria. A – PDD from simulation with 1.97 x 10^6 histories. B – PDD from simulation with 9.37 x 10^6 histories.

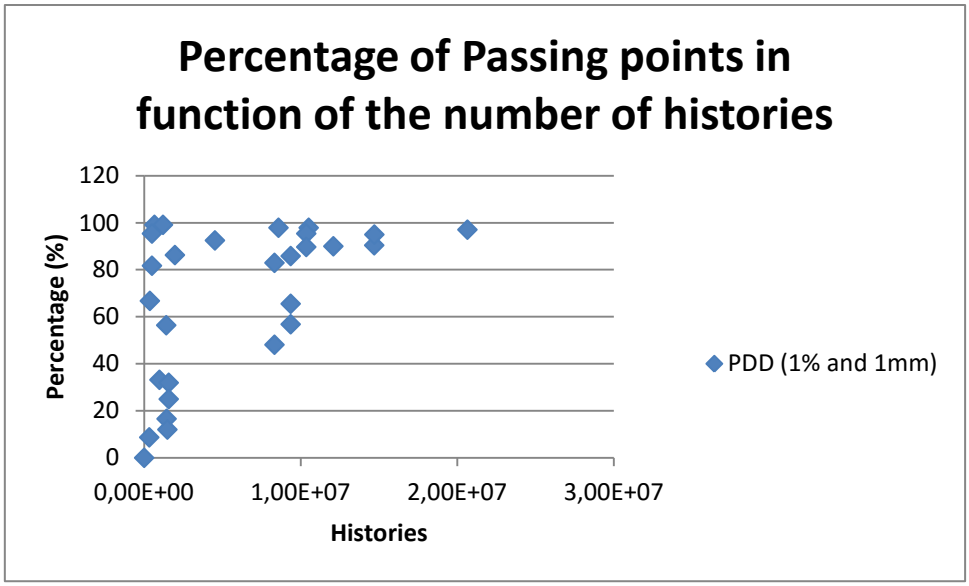

Figure 4.8 – Percentage of passing points in function of the number of histories.

The next parameter to study was the energy of the electrons when they leave the electron gun. This is a parameter analyzed through comparison of PDDs calculated and measured on Varian Clinac 2300. In the user's guide it is suggested to use as energy value the 5.4 MeV and that was the initial value used for most simulations. However, the results were not the desired ones because the PDDs do not overlap completely, there was always a deviation indicating that the energy value of the electrons in the electron gun would be higher. Thereby, the energy of 6.26 MeV was experienced, because it was the energy used in the examples on the user's guide manual. However, from the comparison with the Clinac 2300 measured curves, it was concluded that the energy of the electrons would not be that one, because the calculated PDD was positioned slightly above the measured PDD. Thus, a new value of energy was experienced. In this case it was the 5.9 MeV. Here, the curves were quite coincident, but the calculated PDD still appeared to be slightly below the measured one. For this reason the procedure was repeated. At this time, the new value of energy tested was 6 MeV. The comparison between PDD curves calculated and measured on the LINAC were very coincident, the most compatible so far. In Figure 4.9 is shown the percentage of passing points when calculated and measured PDD curves were compared in function of the energy. Looking to this graph it is not possible to clearly distinguish which are the best energies, because for all the energies there are percentages of passing points close to 100%, but there were also very bad results. This study was made by looking directly to every PDD curve obtained. This happens because the percentage of compatible values is influenced by other factors than the electrons energy, as we have seen previously. For example, in the case of the 6 MeV of energy,

it can be distinguished in the graph a simulation with a percentage of passing points less than 20% and another in which the compatibility between both PDDs is around 100%. This occurred because in one of the simulations, the number of histories was much smaller than in the other. Consequently, it brings a lower statistics for the calculated PDD and therefore less consistent results, even when the simulation parameters are in accordance with the LINAC parameters in study. This change in energy affects essentially the PDD curve, not affecting much the lateral profiles. To adjust the lateral profiles, it is necessary to change another parameter in simulation S1 step, the focal spot. This change was done but it was observed that if the focal spot is too big, the lateral profiles lose their shape, showing with a more round shape (Figure 4.10). The best value found for this parameter was 0.1 cm, in which the lateral profiles calculated and measured showed the same shape. The energy FWHM and the beam divergence also affects the calculated curves, in particular the lateral profiles. After the study of the variations in these two parameters they were fixed in 0.2 MeV and 1.5 deg, respectively.

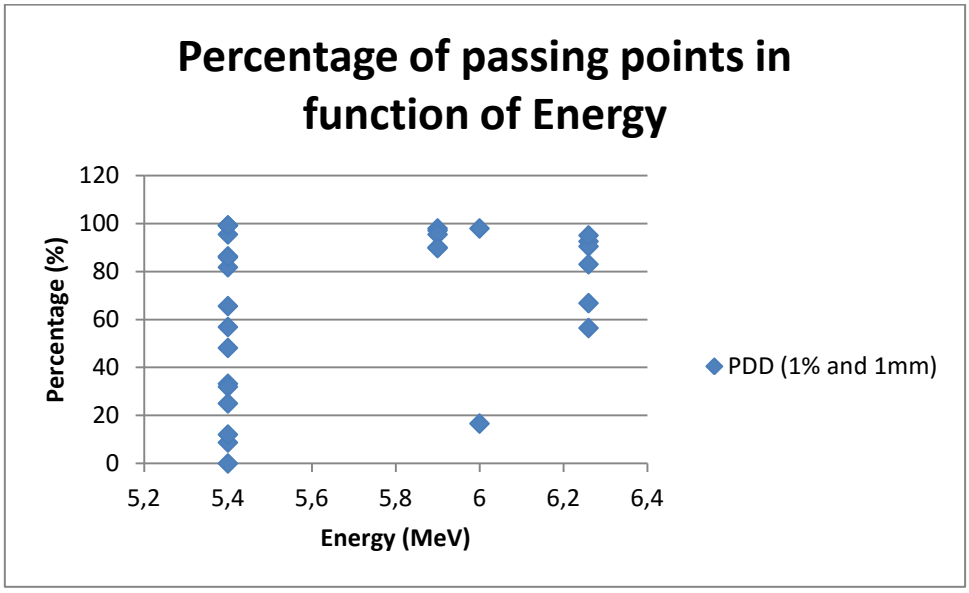

Figure 4.9 - Percentage of passing points as function of the energy.

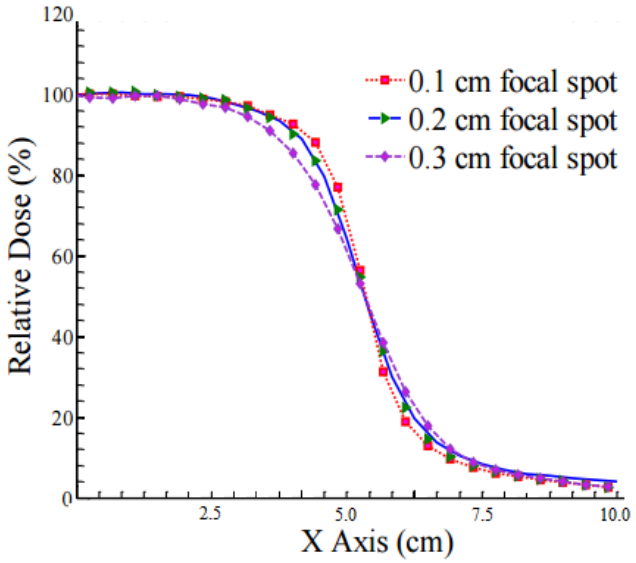

Figure 4.10 – Illustration of lateral profile variation when increasing focal spot.

Another parameter that needs our attention is the Variance Reduction Technique (VRT), since it affects the simulation results and speed. As these are simulations in whose nominal energy value remains constant in 6 MV, the VRT used will always be splitting roulette. This VRT is more efficient for energies below 15 MV than the rotational splitting option. The simulated field length was always the same (10x10 cm^2). As this happens, the option "fitted to the field size" is chosen, which makes the simulation shorter. For this VRT the splitting factor parameter must be set, which in the user's guide indicates the value of 200. However, a study around this variable was performed in order to confirm that this was indeed the best value for splitting factor. In Figure 4.11 is shown how the variation of the splitting factor affects the agreement between the curves in comparison. It can be seen that a higher splitting factor doesn't mean that the correlation between both curves will be higher. As a matter fact, it is possible to see that the best results occurred, in general, with a splitting factor below 500. Because of this, the splitting factor of 200 was maintained to all simulations, as suggested in the user's guide manual, because it gives good results in a good amount of time.

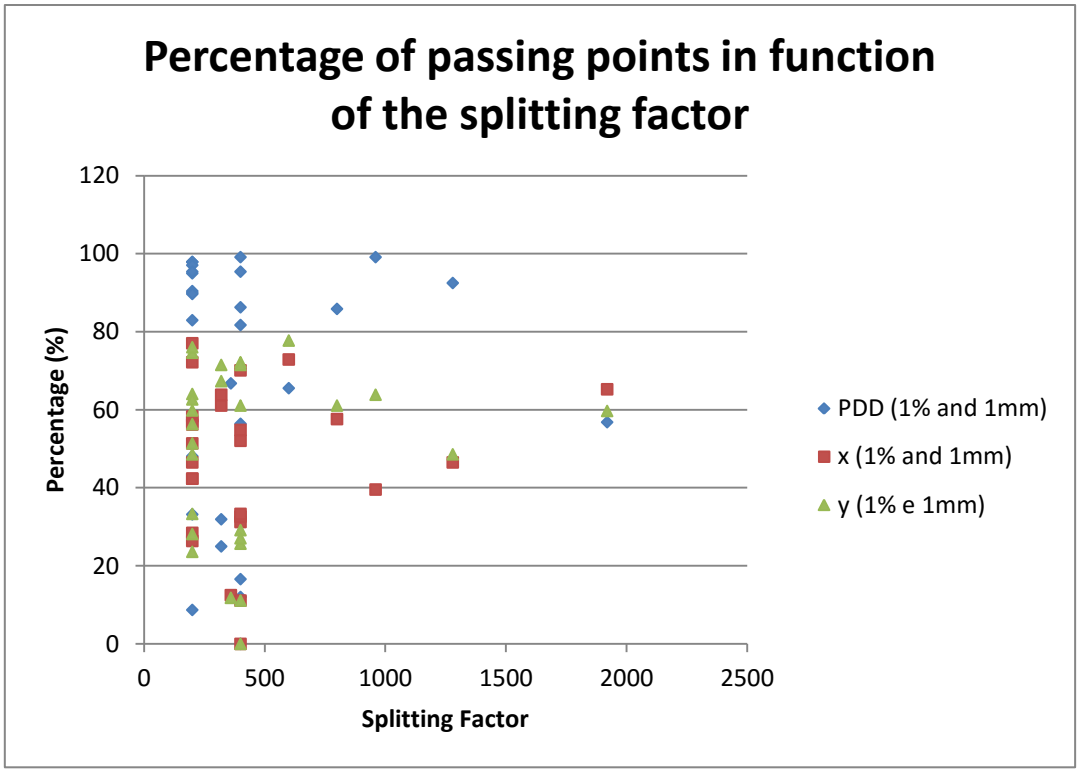

Figure 4.11 - Percentage of passing points in function of splitting factor.

Once these steps are completed, a PDD quite coincident with those acquired on Clinac 2300, in Porto IPO was achieved (Figure 4.12). But, to validate the software configuration, it is necessary that the simulated and measured lateral profiles are also compatible, which did not occur in the first simulations performed (Figure 4.13). Thus, it had to be confirmed if the simulated field size was in agreement with the measured field size. That was corroborated because the penumbra of both curves was compatible, which means that the calculated and measured field dimensions were the same. The differences between the lateral profiles were more based the umbra, which didn't present the exactly shape in both curves. For this reason it was necessary to check the simulation grids defined in s3, because it is a parameter that has a big influence in the simulation results, because it can distort the examination of the obtained results. Thus, after several tests regarding the phantom setup, the conformation of Figure 4.14 was used. The main change made in this Setup was to check the box "shift phantom half bin along Z" and set the "depth of measurement" in 10.000 cm. This step changed the calculation grid making the previously calculated results well visible after this alteration. Therefore, curves which were not in agreement previously, making this small change became compatible, because the LINAC parameters were already well defined (according to Clinac 2300) and the calculation grid was properly adjusted.

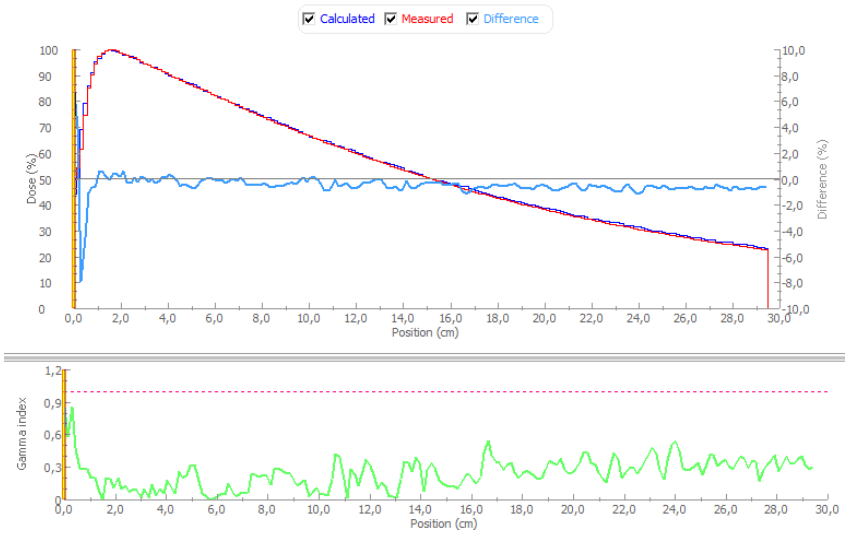

Figure 4.12 - Comparison between Clinac 2300 (DHX5) PDD from 2011 and corresponding PRIMO simulation. The gamma function analysis (2%, 2mm) showed that 100% of the points was lower than 1.

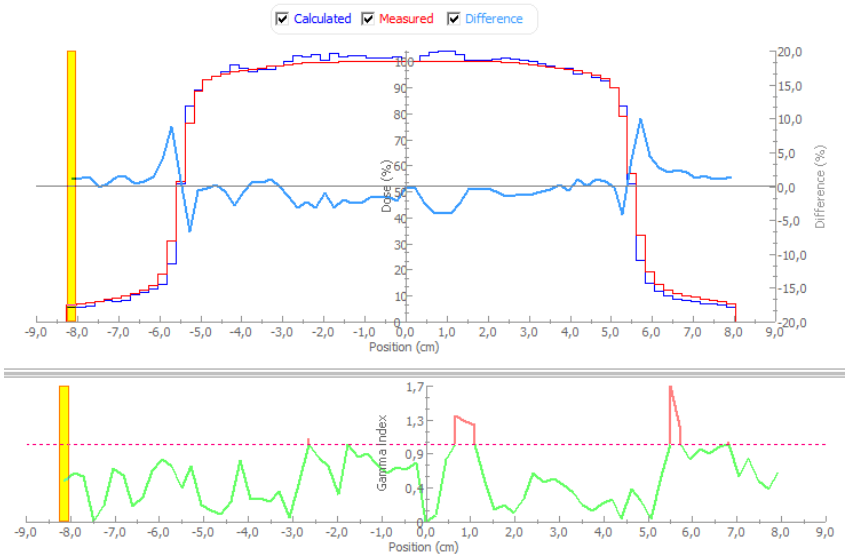

Figure 4.13 - Comparison between Clinac 2300 (DHX5) lateral profile Y from 2011 and corresponding PRIMO simulation. The gamma function analysis (2%, 2mm) showed that 90.54% of the points was lower than 1.

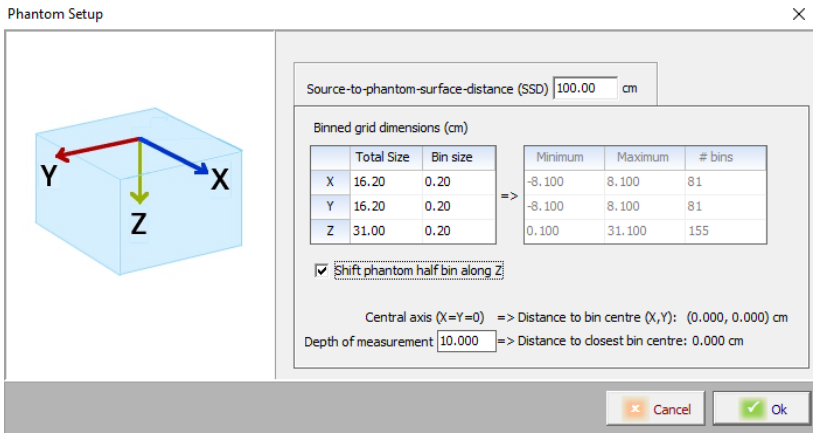

Figure 4.14 – Phantom Setup.

Ending the study of all these parameters, PRIMO software was validated with a simulation of 2 weeks that resulted in 8.6×10^8 histories simulated using the parameters already referred. This simulation generated the PDD presented in Figure 4.15 and the lateral profiles in Figure 4.16 and Figure 4.17. As can be seen there the curves simulated and measured are highly compatible, which makes possible PRIMO validation. These results are also the basis for all the remaining simulations to be carried out to complete the goals of this work.

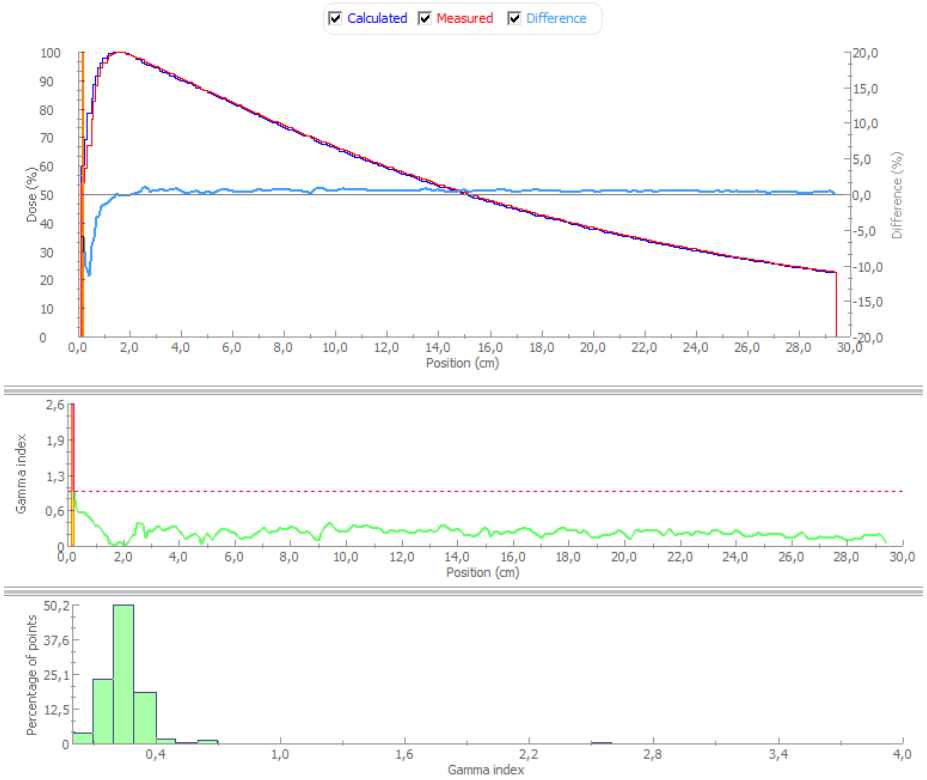

Figure 4.15 – Comparison between Clinac 2300 (DHX5) PDD from 2011 and corresponding PRIMO simulation. The gamma function analysis (2%, 2mm) showed that 99.66% of the points was lower than 1.

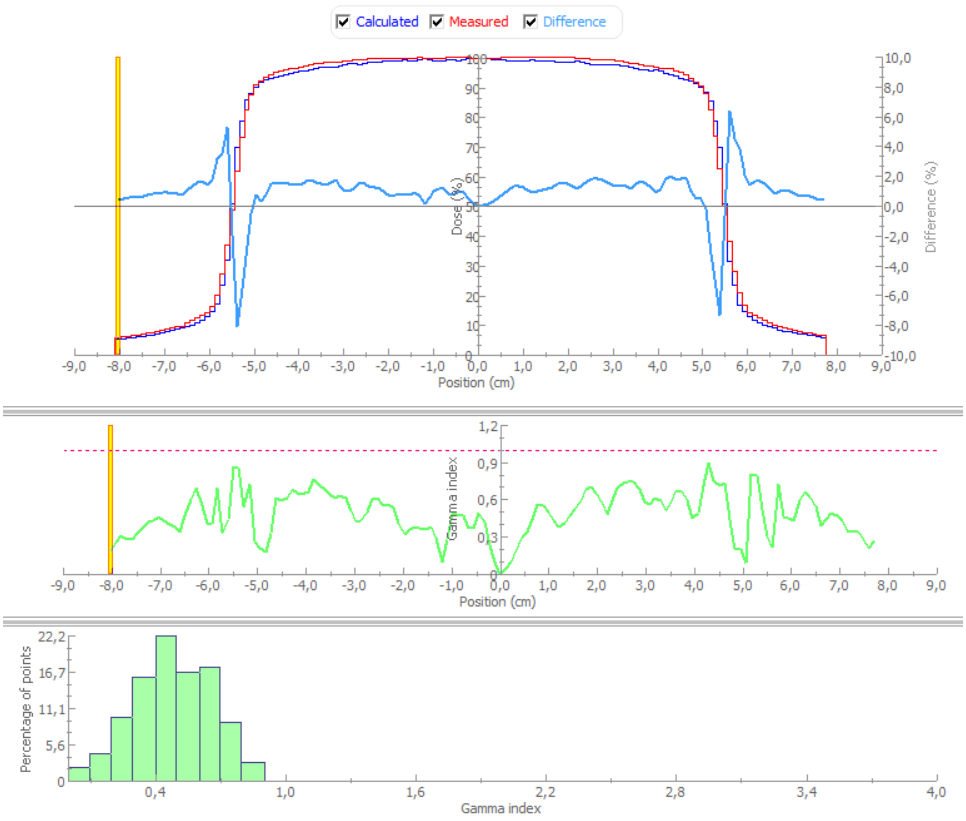

Figure 4.16 – Comparison between Clinac 2300 (DHX5) lateral profile X from 2011 and corresponding PRIMO simulation. The gamma function analysis (2%, 2mm) showed that 100% of the points was lower than 1.

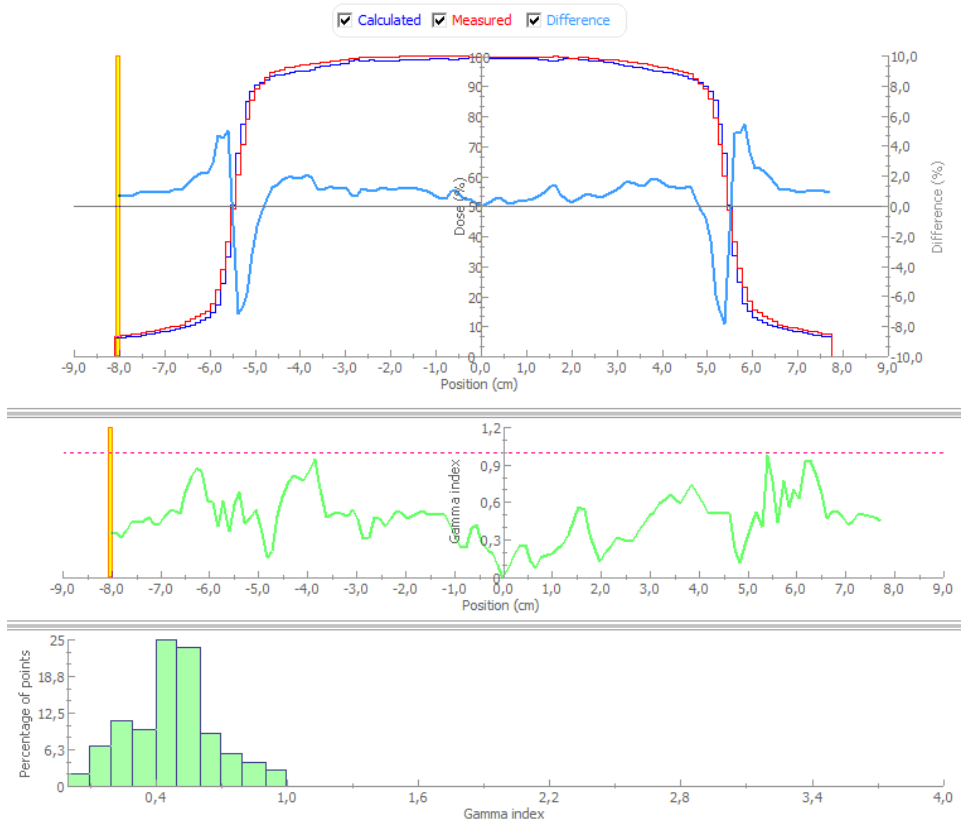

Figure 4.17 - Comparison between Clinac 2300 (DHX5) lateral profile Y from 2011 and corresponding PRIMO simulation. The gamma function analysis (2%, 2mm) showed that 100% of the points was lower than 1.

4.3 PRIMO output problem

The simulation results made with PRIMO are shown in images and graphs, as can be seen in Figure 4.18. This output shows a dose distribution with a 10x10 cm^2 open field simulated by PRIMO, for a given depth. However this output is given with an extension *.dat*, which means that a note pad document with a list of numbers is created. However, the most common programs used in radiotherapy to analyze these dose distributions does not read files with extension dat. or with this kind of data organization. Thus, the study of PRIMO results is a hard task to do using tools that do not belong to the program. Consequently, the comparison between PRIMO results with data from other programs is also difficult to perform because PRIMO only compares PDD curves and lateral profiles, but do not compare, for example, an image of a open field dose distribution. In the radiotherapy service, the majority of data from other programs come in *dicom* images or similar. For this reason, a way to convert the files from PRIMO to dicom images is necessary in order to compare both data and overcome this problem. This transformation is made based on Matlab functions, as it was already explained in Methodology. The process is a little bit complex and long because PRIMO notepad documents showed different data organization when the simulation is made using a CT scan of a slab phantom or a model from a water phantom. To reach these conclusions, it was necessary to previously analyze various PRIMO outputs, which are a big time consumer task, but an essential step to proceed with this work.

In Figure 4.19 is shown the output of PRIMO already converted. Looking to both images (Figure 4.18 and Figure 4.19) it can be seen that they are the same image but with a different color scheme. However, as the image from Figure 4.19 was transformed in a dicom image it can be used in comparison tests with other programs as Verisoft or Doselab, which are used in clinical radiotherapy.

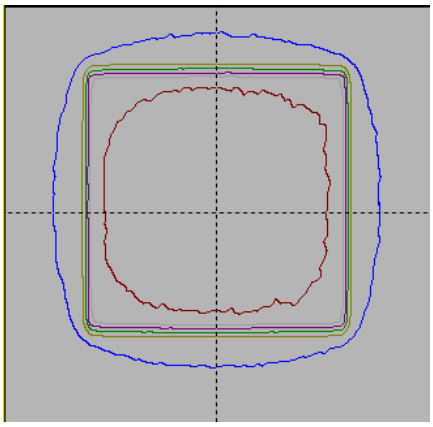

Figure 4.18 – PRIMO simulation results.

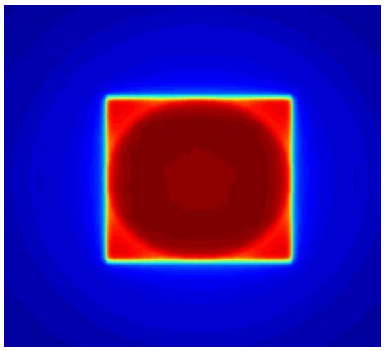

Figure 4.19 – Image output created by MATLAB from PRIMO notepad document.

4.4 MLC Tests

Following the procedure described in the Methodology for MLC tests, the influence of the addition of an MLC was checked in an open field simulation. This simulates an irradiation in a Clinac 2300 with an open field, because the LINAC didn't have only the jaws but also have the MLC and that's what it is so important to do this test. The simulation performed didn't show relevant differences from simulations with only the jaws present. Thus, the simulation performed was also compatible with the dose distribution acquired from a LINAC irradiation (Figure 4.20), as occurred with the simulation performed without the presence of the MLC. The dose distribution of an open field in a Clinac 2300 was also calculated in TPS and compared with the simulation in PRIMO (Figure 4.21) and with the irradiation in the LINAC (Figure 4.22). As expected, the results from the three modalities were compatible between them. The PRIMO simulation shown an agreement of 100% with the LINAC irradiation and of 96,7% with TPS, using gamma index in clinical conditions (3%, 3mm). In its turn, the comparison between irradiated field and TPS had also an agreement of 100% using the same comparison conditions. The purpose of this test was to confirm the compatibility of the three

modalities, in order to be able to perform more complex tests, once the agreement between them was assured for open fields.

Gamma 2D - Parameters

3,0 mm Distance- To- Agreement
3,0 % Dose difference with ref. to local dose
Suppress dose below 10,0 % of max. dose of calculated volume
Option "Use 2nd and 3rd pass" selected

Statistics

Number of Dose Points	729
Evaluated Dose Points	121 (16,6 %)
Passed	121 (100,0 %)
Failed	0 (0,0 %)
Result	100,0 % (Green)

Settings

Passing criteria	Gamma ≤ 1,0
Green	95,0 % to 100,0 %
Yellow	75,0 % to 95,0 %
Red	0,0 % to 75,0 %

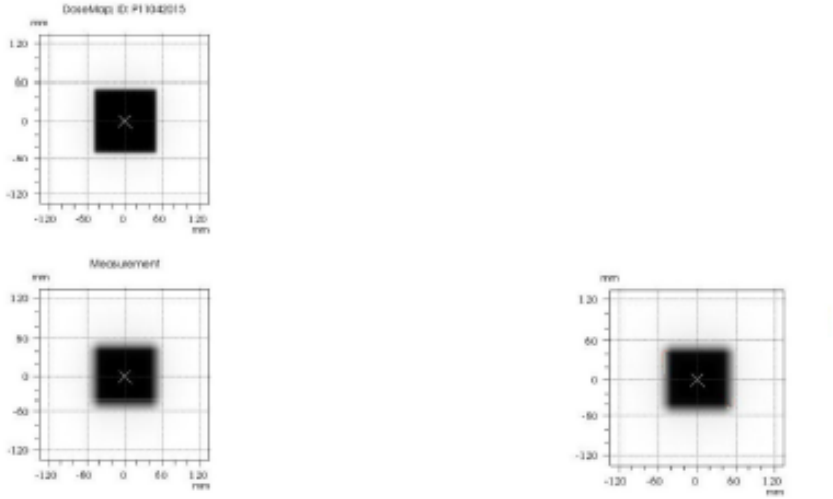

Figure 4.20 - Comparison between PRIMO simulation and LINAC irradiation of an open field.

Gamma 2D - Parameters

3,0 mm Distance- To- Agreement
3,0 % Dose difference with ref. to local dose
Suppress dose below 10,0 % of max. dose of measured slice

Statistics

Number of Dose Points	729
Evaluated Dose Points	121 (16,6 %)
Passed	117 (96,7 %)
Failed	4 (3,3 %)
Result	96,7 % (Green)

Settings

Passing criteria	Gamma ≤ 1,0
Green	95,0 % to 100,0 %
Yellow	75,0 % to 95,0 %
Red	0,0 % to 75,0 %

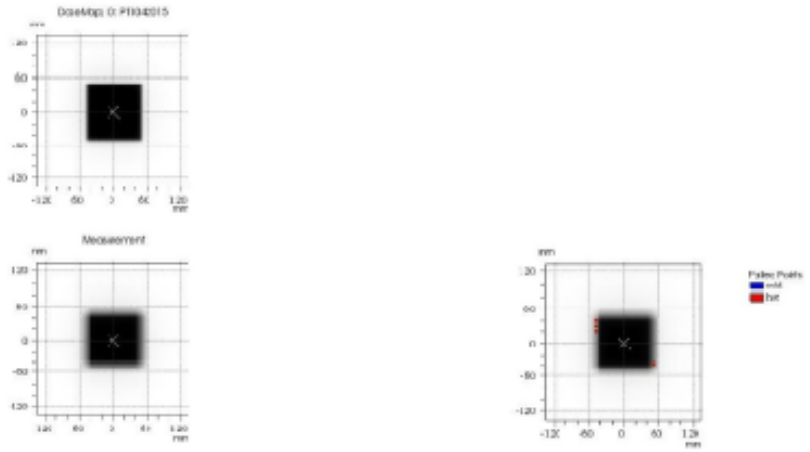

Figure 4.21 - Comparison between PRIMO simulation and TPS of an open field.

Gamma 2D - Parameters

3,0 mm Distance- To- Agreement
3,0 % Dose difference with ref. to local dose
Suppress dose below 10,0 % of max. dose of calculated volume
Option "Use 2nd and 3rd pass" selected

Statistics

Number of Dose Points	729
Evaluated Dose Points	121 (16,6 %)
Passed	121 (100,0 %)
Failed	0 (0,0 %)
Result	100,0 % (Green)

Settings

Passing criteria	Gamma ≤ 1,0
Green	95,0 % to 100,0 %
Yellow	75,0 % to 95,0 %
Red	0,0 % to 75,0 %

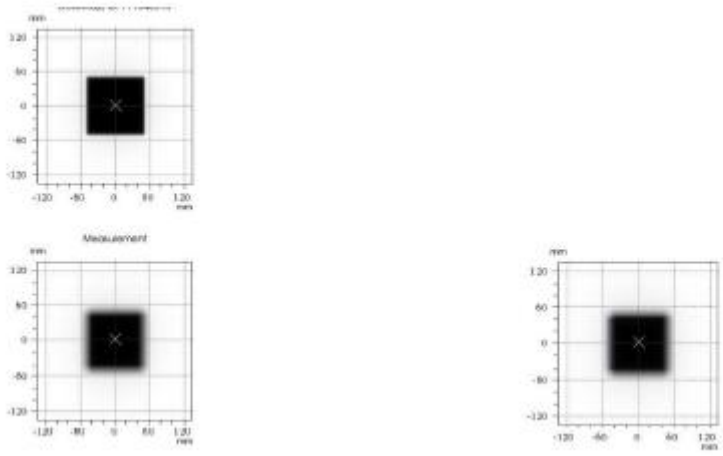

Figure 4.22- Comparison between TPS and LINAC irradiation of an open field.

The next step in this process is to add a conformation to the MLC and perform compatibility tests for static fields. In this section will only be discussed one example of a static field, since it reflects the results from the other tests performed. This static field was chosen because the MLC leaves present the major variation tested. In this example the field borders were tested with close leaves in the top of the field and with open leaves in the opposite extreme and the remaining field was tested with all types of conformations for the different pairs of MLC leaves. The simulation results from PRIMO were transformed in dicom images and compared with the same static field irradiation in a Clinac 2300 and with a dose distribution from TPS. In Figure 4.23 is shown the comparison between a static field simulated on PRIMO with the same field calculated with TPS. The comparison result shows a compatibility of 98.1%. This comparison was made using the gamma test with DTA of 3 mm and dose difference of 3 %, which are the criteria used in clinical practice. Looking to this result, the fields are in agreement, with compatibility bigger than 95% meaning that the simulation made with PRIMO, using Monte Carlo, is in accordance with the dose distribution

calculated by TPS. In Figure 4.24 the comparison between practical dose distribution and PRIMO results can be seen. They present an agreement of 100%, which means that the dose distribution calculated in PRIMO was the same irradiated by LINAC. Finally, in Figure 4.25 is shown a comparison between TPS calculation and a LINAC irradiation in order to prove by clinical means that both modalities have the same dose distribution. These results demonstrate that PRIMO works very well in dose distribution calculation for static fields, which makes possible to proceed the study, in order to prove the potentiality of PRIMO for IMRT treatments verification. At this stage, PRIMO simulation of conventional radiation therapy treatments was checked.

Gamma 2D - Parameters

3,0 mm Distance- To- Agreement
3,0 % Dose difference with ref. to local dose
Suppress dose below 10,0 % of max. dose of calculated volume
Option "Use 2nd and 3rd pass" selected

Statistics

Number of Dose Points	73.441
Evaluated Dose Points	8.309 (11,3 %)
Passed	8.154 (98,1 %)
Failed	155 (1,9 %)
Result	98,1 % (Green)

Settings

Passing criteria	Gamma ≤ 1,0
Green	95,0 % to 100,0 %
Yellow	75,0 % to 95,0 %
Red	0,0 % to 75,0 %

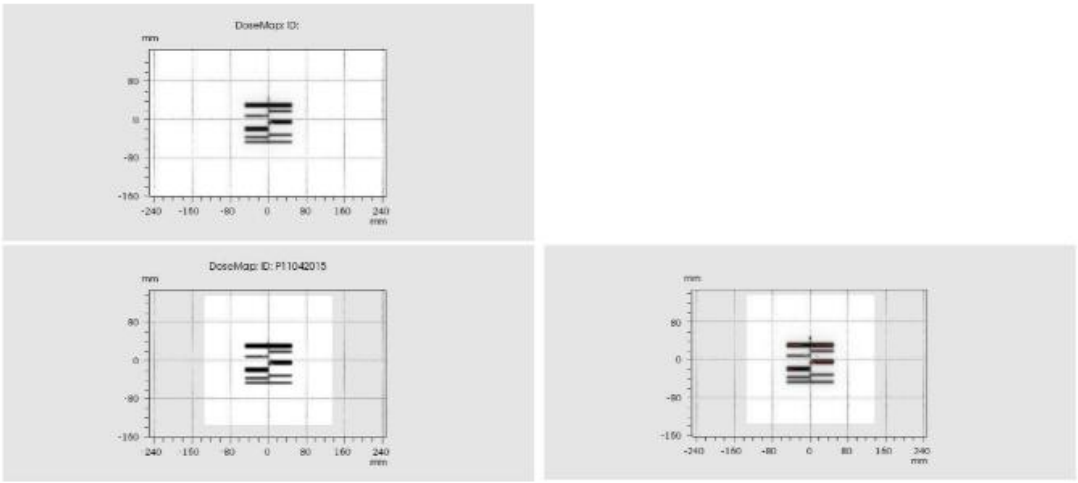

Figure 4.23 – Comparison between PRIMO simulation and TPS of a static MLC field.

Gamma 2D - Parameters

3,0 mm Distance- To- Agreement
3,0 % Dose difference with ref. to local dose
Suppress dose below 10,0 % of max. dose of calculated volume
Option "Use 2nd and 3rd pass" selected

Statistics

Number of Dose Points	729
Evaluated Dose Points	87 (11,9 %)
Passed	87 (100,0 %)
Failed	0 (0,0 %)
Result	100,0 % (Green)

Settings

Passing criteria	Gamma ≤ 1,0
Green	95,0 % to 100,0 %
Yellow	75,0 % to 95,0 %
Red	0,0 % to 75,0 %

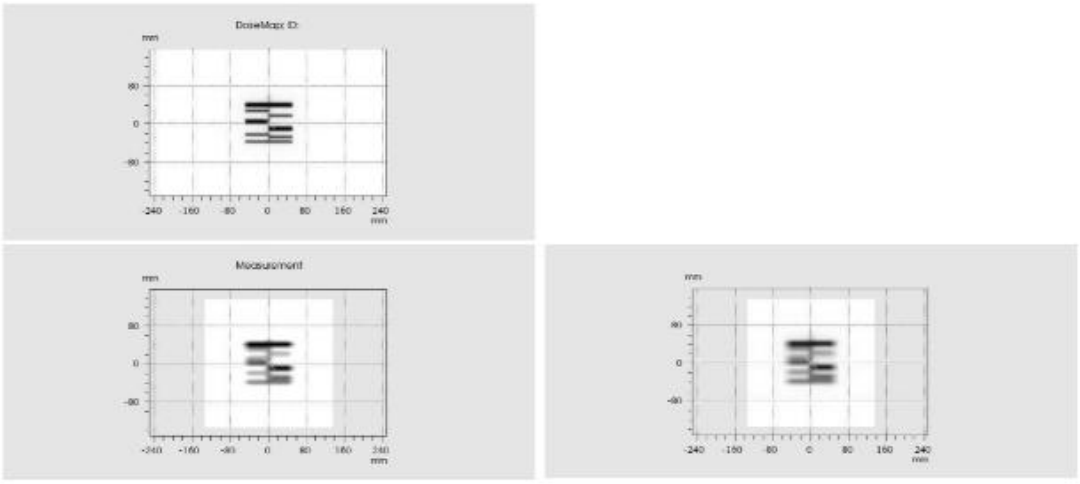

Figure 4.24 - Comparison between PRIMO simulation and LINAC irradiation of a static MLC field.

Gamma 2D - Parameters

3,0 mm Distance- To- Agreement
3,0 % Dose difference with ref. to local dose
Suppress dose below 10,0 % of max. dose of calculated volume
Option "Use 2nd and 3rd pass" selected

Statistics

Number of Dose Points	729
Evaluated Dose Points	87 (11,9 %)
Passed	87 (100,0 %)
Failed	0 (0,0 %)
Result	100,0 % (Green)

Settings

Passing criteria	Gamma ≤ 1,0
Green	95,0 % to 100,0 %
Yellow	75,0 % to 95,0 %
Red	0,0 % to 75,0 %

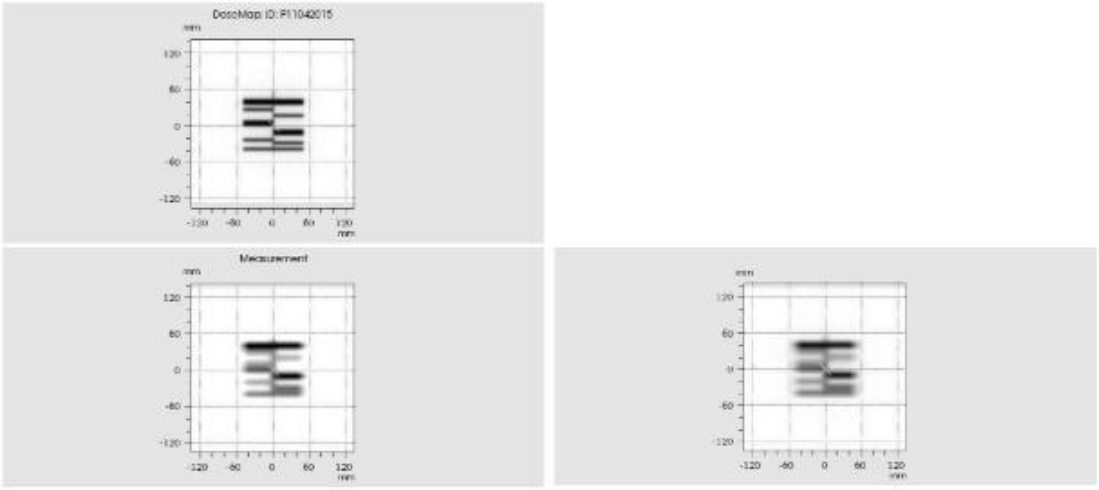

Figure 4.25 - Comparison between TPS and LINAC irradiation of a static MLC field.

Continuing this work, it was time to begin the simulation of dynamic fields. This type of irradiation field intends to represent one IMRT field in step and shoot technique, which the dose is not uniform. In PRIMO, it is not possible to simulate one field with a non - uniform dose distribution. To accomplish this dynamic field it is necessary to simulate the superposition of several fields with different positions of the MLC leaves. In the end of the simulation, a non-uniform dose distribution is obtained and it is composed by the sum of these 89 fields calculated. The same dynamic field simulated was also irradiated by LINAC in the PTW ion chamber matrix. The obtained results were compared with simulations using Verisoft. However, compatibility between them was hard to obtain and tests with gafchromic films were made to confirm dose distribution in the irradiated field. This technique was adopted since it is a more accurate way to analyze dose distributions, because gafchromic spatial resolution is higher than ion chamber matrix spatial resolution. Thus, a gafchromic film was irradiated with the dynamic field in study (Figure 4.26), and the ion chamber matrix was also irradiated with the same plan. The comparison of both showed an agreement of 98.8%, using

gamma test with 3%, and 3mm as criteria, the values used in clinical practice (Figure 4.27). After confirming that the dose distribution obtained with gafchromic films and with the matrix were compatible, the comparison tests with the matrix were repeated because it is less complicated to obtain and analyze results. When gafchromic is used the film irradiation is made in one day, and its analysis just can be done in the day after, adding the fact that gafchromic films require some care in its use. In its turn, using the PTW matrix, the field is irradiated and in a few minutes the results can be seen and analyzed, which for this type of work is more advantageous since the work scheme doesn't change. Comparing the data from PTW matrix with PRIMO simulation, compatibility between both results was not the intended, revealing that data normalization has to be done. This normalization was made to the highest dose value, directly in Verisoft. In Figure 4.28 are the results from this process. The measured with the ion chamber matrix and simulated dose distributions show good agreement. The gamma function analysis (2%, 2mm) showed that 96% of the points were lower than 1, confirming that the simulated and experimental data were compatible. With this step was proved that PRIMO software has potential to be used in IMRT treatments verification, since it simulates with a good agreement IMRT fields in the IMRT step and shoot technique.

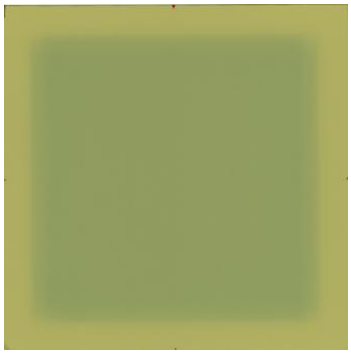

Figure 4.26 – Gafchromic film after the dynamic field irradiation.

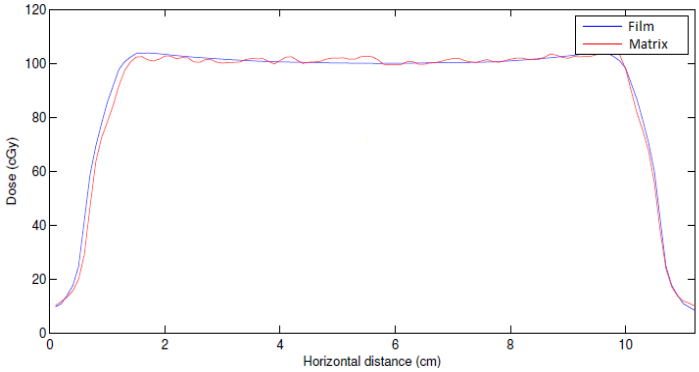

Figure 4.27 – 2D Comparison obtained in Doselab between dynamic field measured with a gafchromic film and with the same measurement in ion chamber matrix. The gamma function analysis (3%, 3mm) showed that 98.8% of the points was lower than 1.

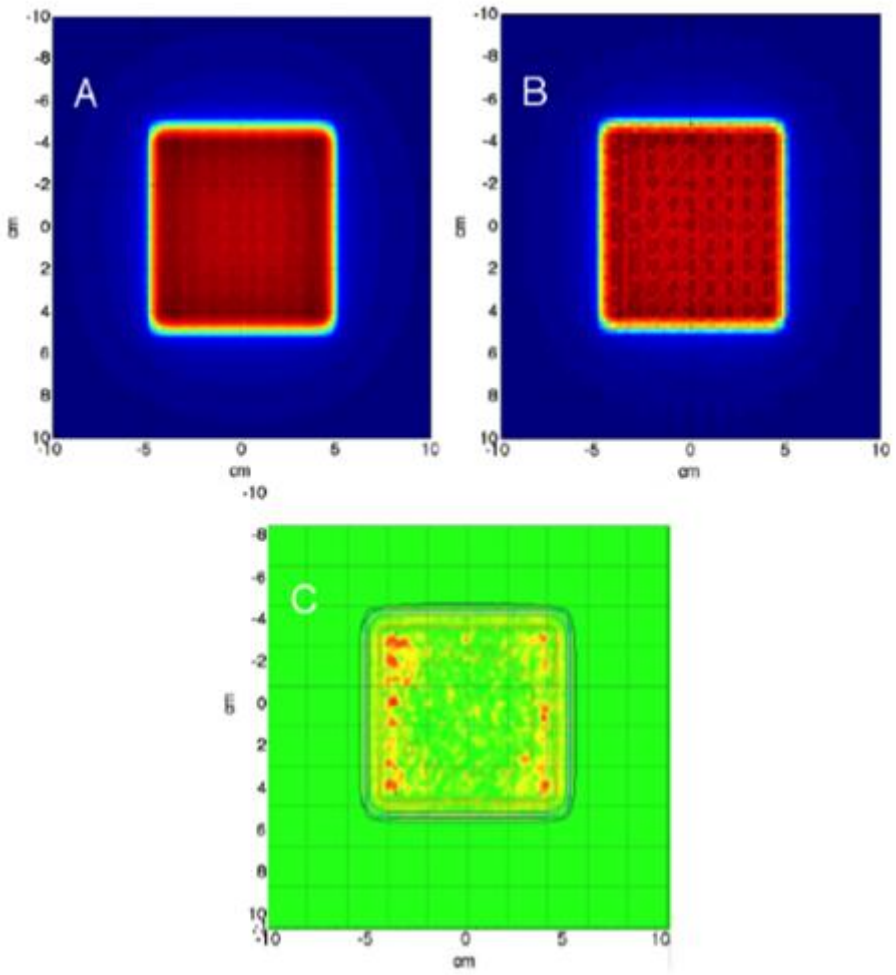

Figure 4.28 – A - Dose distribution for the dynamic IMRT treatment, measured with ionization chamber array, placed at 100 cm distance from the LINAC head under 5 cm of water equivalent. B – Dose distribution at the matrix for the simulated dynamic plan. C - Comparison between PRIMO simulation and LINAC irradiation of a dynamic MLC field.

5 Conclusions and Future Work

IMRT is a radiation therapy technique that is widely used in Europe biggest radiotherapy centers. However, many smaller hospitals still not have this technique in their treatments, and others are dealing, only at this moment, with their implementation. Thus, although this is no longer a totally new technique, it still has a very great clinical significance. Therefore, nowadays the need of improving and developing the IMRT technique still exist.

As mentioned before, IMRT is a conformal therapy technique, highly accurate, that allows the administration of high doses of radiation to the target volume, while dose is minimized, very effectively, to normal surrounding tissue. To achieve this goal, a verification process is necessary before applying the treatment to a patient, in order to confirm if the TPS planned treatment and irradiated by LINAC are compatible. This compatibility, which is based on the gamma index at 3% and 3 mm, must be greater than 95%, which does not always occur. Completed this preliminary analysis it was concluded that combining Monte Carlo calculations to the verification process may be a way to reduce cases of non-compatibility. This was the reason why this project began, using PRIMO software, which is a program that promised to calculate dose distributions in a faster and more user friendly way.

As PRIMO is a recent program, and once it was necessary to validate the LINAC to simulate, in the first work phase was unable to test the program in terms of simulation speed (when comparing it to other programs with the same purpose). However, on PRIMO first utilization, its user-friendly aspect is evident. Any person with minimal knowledge in informatics and MC simulations of a LINAC can perform a simulation, thinking that it is a program very simple to use and very intuitive. After a few times of utilization, it was realized that to obtain satisfactory results, it was necessary larger simulation times. However, compared to other programs it was concluded that this could be faster and more efficient, because PRIMO creates intermediate phase-space files (PHSP files) in each simulation stage, which could be reused. For example, in a simulation of s1, the reused of a PHSP file save weeks of simulation. However, until the program validation, simulations would have to be completed, to be able to identify the best parameters to use as LINAC parameters.

The software validation was the most time-consuming task in this project, because it required longer simulations. For the obtainment of good statistical results, simulations performed in about 2 weeks were need. The validation process was the most time-consuming also because, as expected, the default data in PRIMO, for the simulated LINAC (the Clinac 2300), did not have the desired compatibility degree with the IPO device used for comparisons.

For this reason, a discovery process of ideal parameters ideas begun by a trial error routine. After several simulations and elapsed many time, the ideal parameters to validate the PRIMO software were found. Thus, a longer simulation was performed with these parameters in order to be able to use the PHSP file in the following steps, saving the time used in s1 simulations. At the end of this first step, it was concluded that PRIMO user-friendly feature made the program validation much easier, giving that parameters influencing dose distributions were quite explicit: they were the only parameters that could be altered directly in PRIMO program. All other parameters that did not influence this task, such as those relating to LINAC construction are in a PHSP file that the program uses but does not give to the user the option to change. This saves time, because no simulations are carried out with alterations that do not directly affect the dose distribution. Looking to this fact, PRIMO can appear to be a "closed box" program, which for a kind of software like this is not an add-value. However, this PHSP files that PRIMO launch can be open as a text file and directly changed, avoiding this question of "closed box". In conclusion, this first step, besides validating PRIMO for simulation of the LINAC 2300 present in Porto IPO, also allowed an adaptation and understanding of the program.

In the second step of the project, MLC validation was performed, through the simulation of a field with a static MLC conformation. At this stage, problems in PRIMO results exportation were found. This situation forced the creation of alternatives to interpreting these results, including the creation of various MATLAB functions to read and transform PRIMO results in DICOM images. Another issue which is worth highlighting is the fact that PRIMO do not had all kind of MLC that could be present in the devices which PRIMO proposes to simulate. This is a question that must be taken into account initially, during the first uses of the program, in order to avoid the LINAC validation, and then the desired MLC does not exist in PRIMO, which requires that the validation process must be started over. Apart from these issues, this was a quick phase to execute, in which no adversities were found, in terms of compatibility between PRIMO simulations, TPS calculations and LINAC irradiation. Ending this phase, it is concluded that a conventional radiation treatment simulation would be perfectly performed using the PRIMO, given the compatibility obtained for static MLC.

To complete this work, the simulation of a field using a dynamic MLC was performed. As PRIMO was not built with the initial idea of simulate non-conventional radiotherapy treatments, this was a more complicated task. For this reason, alternatives that allow going around this issue had to be found. Since IMRT treatments fall into two categories: the step and shot (also known as IMRT with MLC in segments) and IMRT with dynamic MLC; it was decided to focus only on step-and-shoot mode. As this mode not has a continuous irradiation, it can, in theory, be simulated quite reliably by PRIMO, even it not being predestined to non-

conventional treatments simulation. The simulation of only one field of this modality is a long-lasting process due to the amount of MLC position that needs to be acquired in each field. Once simulated the IMRT field (in step-and-shoot mode), the comparison between simulation, TPS and LINAC data was made. After some adjustments and according to a gamma index of 3% and 3mm (which are used in clinical practice), compatibility between the three modalities was found. Thus, it was concluded that PRIMO is able to simulate a complete IMRT treatment, since it can simulate a field of IMRT in step-and-shoot mode. Being possible the simulation of an IMRT treatment, it is also proved that PRIMO can be used in IMRT verification process, but with the disadvantage that it is a slower process than the current one. However, for more complex verification cases, this program can be very useful, given that the time to redo the treatment plan can be used to perform verification with PRIMO. Thus, it would be possible to better realize if the plan was or not the appropriate, or if the non-compatibility is due to an inadequate matrix interpolation.

In the end of this project, it can be concluded that these were preliminary studies in order to use PRIMO in clinical practice into the future. This Master`s project proved the potential of PRIMO within IMRT radiotherapy technique (in step-and-shoot mode), but further work is required for simulating a complete IMRT treatment of a patient. An important issue that should be taken into account, at an earlier stage of testing, would be to perform simulations with different field sizes and more variations in MLC position. This wasn't possible to achieve, due to the time needed to carry out these tests, and given the time predicted for this project realization. In the context of the work developed, it also should be done more dynamic field simulations, with a big variety of conformations, which was not made due to the reasons already explained.

To continue this work from here, I leave as suggestion the simulation of various IMRT treatment fields of a patient (in step-and-shoot mode), using their CT and subsequent comparison with data from TPS and LINAC. This way, it will be effectively verified an IMRT treatment, proving not only the program potential for this purpose, but its present implementation. Another suggestion, a bit more complex, would be the simulation of IMRT treatments with dynamic MLC. Subsequently, the simulation of VMAT, another radiotherapy treatment technique, would be easier to perform, which would be a big step in MC simulation of non-conventional treatments. However, this is a work that, if being developed, will need many more tests and also some imagination to circumvent some program issues derived from its user-friendly feature, which is presented to the user as a kind of "closed box".

As understood with this essay, PRIMO software presents a great potential in MC simulations field. Combine this software with IMRT treatments, which are one of the most

revolutionary radiotherapy techniques, could only end as an innovative idea, which brought new topics of discussion to this investigation field. Proving this fact, a communication coming from this master thesis was presented in ESTRO 35, one of the most important conferences in radiotherapy around the world, organized by the European Society for Radiotherapy & Oncology (ESTRO).

Bibliography

[1] K. Chao, S. Apisarnthanarax, and G. Ozyigit, *Practical Essentials of Intensity Modulated Radiation Therapy*. Lippincott Williams & Wilkins, 2005.

[2] L. Veldeman, I. Madani, F. Hulstaert, G. O. De Meerleer, M. Mareel, and W. De Neve, "Evidence behind use of intensity-modulated radiotherapy: a systematic review of comparative clinical studies.," *Lancet Oncol*, vol. 9, no. 4, pp. 367–75, 2008.

[3] S. I. Gutiontov, E. J. Shin, B. Lok, N. Y. Lee, and R. Cabanillas, "Intensity-modulated radiotherapy for head and neck surgeons," *Wiley Online Libr.*, vol. 119, no. 6, pp. 377–382, 2015.

[4] P. C. Williams, "IMRT: Delivery techniques and quality assurance," *Br. J. Radiol.*, vol. 76, no. 911, pp. 766–776, 2003.

[5] A. Mesbahi, A. J. Reilly, and D. I. Thwaites, "Development and commissioning of a Monte Carlo photon beam model for Varian Clinac 2100EX linear accelerator," *Appl. Radiat. Isot.*, vol. 64, no. 6, pp. 656–662, 2006.

[6] R. Capote, R. Jeraj, C.-M. Ma, D. W. O. Rogers, F. Sánchez-Doblado, J. Sempau, J. Seuntjens, and J. V. Siebers, "Phase-Space Database for External Beam Radiotherapy," Vienna, 2006.

[7] M. A. Cortés-Giraldo, J. M. Quesada, M. I. Gallardo, and R. Capote, "An implementation to read and write IAEA phase-space files in GEANT4-based simulations," *Int. J. Radiat. Biol.*, vol. 88, no. 1–2, pp. 200–208, 2012.

[8] L. Brualla, M. Rodriguez, and J. Sempau, "PRIMO Project," 2013. [Online]. Available: https://www.primoproject.net/primo/.

[9] J. Pope, *Medical Physics: Imaging*. Oxford: Heinemann Educational Publishers, 1999.

[10] P. Mayles, A. Nahum, and J. C. Rosenwald, *Handbook of radiotherapy physics: theory and practice*. Taylor & Francis Group, 2007.

[11] E. B. Podgorsak, *Radiation Oncology Physics: A Handbook for Teachers and Students*. Vienna: IAEA, 2005.

[12] J. M. Michalski, C. A. Perez, and J. A. Purdy, "Three-Dimensional Conformal Radiation Therapy (3DCRT) for Prostate Cancer," *The Prostate Cancer InfoLink*, 1996. [Online]. Available: http://www.phoenix5.org/Infolink/Michalski/Part2.html. [Accessed: 26-Jun-

2015].

[13] “Linear Accelerator,” *RadiologyInfo.org*, 2013. [Online]. Available: http://www.radiologyinfo.org/en/info.cfm?pg=linac. [Accessed: 23-Jun-2015].

[14] ICRP, “ICRP 103: The 2007 Recommendations of the International Commission on Radiological Protection,” *Ann. ICRP*, vol. 37, p. 330, 2007.

[15] J. Izewska and G. Rajan, *Review of Radiation Oncology Physics: A Handbook for Teachers and Students; Chapter 3 - RADIATION DOSIMETERS*. IAEA, 2012.

[16] PTW, “PTW Farmer® Ionization Chambers.” [Online]. Available: http://www.ptw.de/farmer_chambers0.html. [Accessed: 13-May-2016].

[17] M. C. Lopes, “Um século de terapia com radiação,” *Gaz. Física*, vol. 30, no. 14, pp. 14–29, 2005.

[18] “MP3-M,” *PTW*. [Online]. Available: http://www.ptw.de/2038.html. [Accessed: 05-Apr-2016].

[19] F. M. Khan, *The Physics of Radiation Therapy*, 3rd ed. 2003.

[20] E. E. Klein, J. Hanley, J. Bayouth, F.-F. Yin, W. Simon, S. Dresser, C. Serago, F. Aguirre, L. Ma, B. Arjomandy, C. Liu, C. Sandin, and T. Holmes, “Task Group 142 report: quality assurance of medical accelerators.,” *Med. Phys.*, vol. 36, no. 9, pp. 4197–4212, 2009.

[21] A. Taylor and M. E. B. Powell, “Intensity-modulated radiotherapy - What is it?,” *Cancer Imaging*, vol. 4, pp. 68–73, 2004.

[22] T. S. Hong, M. a Ritter, W. a Tomé, and P. M. Harari, “Intensity-modulated radiation therapy: emerging cancer treatment technology.,” *Br. J. Cancer*, vol. 92, pp. 1819–1824, 2005.

[23] M. T. Milano, L. S. Constine, and P. Okunieff, “Normal Tissue Tolerance Dose Metrics for Radiation Therapy of Major Organs,” *Semin. Radiat. Oncol.*, vol. 17, pp. 131–140, 2007.

[24] T. Bortfeld, “IMRT: a review and preview.,” *Phys. Med. Biol.*, vol. 51, no. 13, pp. R363–R379, 2006.

[25] M. Alber, S. Broggi, C. De Wagter, I. Eichwurzel, P. Engström, C. Fiorino, D. Georg, G. Hartmann, T. Knöös, A. Leal, H. Marijnissen, B. Mijnheer, M. Paiusco, F. Sánchez-

Doblado, R. Schmidt, M. Tomsej, and H. Welleweerd, *GUIDELINES FOR THE VERIFICATION OF IMRT*. Brussels, 2008.

[26] L. Gomes, "Estudo dosimétrico comparativo do Acuros ® XB – Algoritmo Avançado de Cálculo de dose com o AAA – Anisotropic Analytical Alghorithm , em tratamentos de Radioterapia Externa com a técnica de RapidArc ™ Estudo dosimétrico comparativo do Acuros ® XB – Algori," Escola Superior de Tecnologia da Saúde de Lisboa, 2013.

[27] M. Scorsetti, A. Fogliata, B. Castiglioni, C. Bressi, M. Bignardi, P. Navarria, P. Mancuso, L. Cozzi, F. Alongi, and A. Santoro, "Early clinical experience with volumetric modulated arc therapy in head and neck cancer patients," *Radiat. Oncol.*, 2010.

[28] K. Otto, "Volumetric Modulated Arc Therapy: IMRT in a single arc," *Med. Phys.*, vol. 35, pp. 310–317, 2008.

[29] N. A. Detorie, "Helical Tomotherapy: A New Tool for Radiation Therapy," *J. Am. Coll. Radiol.*, vol. 5, no. 1, pp. 63–66, 2014.

[30] C. X. Yu and G. Tang, "Intensity-modulated arc therapy: principles, technologies and clinical implementation," *Phys. Med. Biol.*, vol. 56, 2011.

[31] G. MacLennan, "Precision Therapy Acronym Soup: SRS, SRT, SBRT, SAbR," 2015. [Online]. Available: http://www.grayden.info/precision-therapy-acronym-soup-srs-srt-sbrt-sabr.html. [Accessed: 06-Apr-2016].

[32] "Radiation Therapy for Cancer," *National Cancer Institute*, 2010. [Online]. Available: http://www.cancer.gov/about-cancer/treatment/types/radiation-therapy/radiation-fact-sheet. [Accessed: 25-Jun-2015].

[33] S. Goyal and T. Kataria, "Image Guidance in Radiation Therapy: Techniques and Applications," *Radiol. Res. Pract.*, vol. 2014, pp. 1–10, 2014.

[34] S. Noda, T. Lautenschlaeger, M. R. Siedow, D. R. Patel, A. El-Jawahri, Y. Suzuki, J. S. Loeffler, M. R. Bussiere, and A. Chakravarti, "Technological advances in radiation oncology for central nervous system tumors.," *Semin. Radiat. Oncol.*, vol. 19, no. 3, pp. 179–186, 2009.

[35] *Commissioning and Quality Assurance of Computerized Planning Systems for Radiation Treatment of Cancer*. Austria, 2004.

[36] D. Hinckley, "Prescribing, recording and reporting photon beam therapy (ICRU report 50)," *ICRU Rep.*, no. September, pp. 357–360, 1993.

[37] "Eclipse™ Treatment Planning System," *Varian*. [Online]. Available: https://www.varian.com/oncology/products/software/treatment-planning/eclipse.

[38] M. G. Carolan, "Pencil Beam Dose Calculation Algorithm," 2010.

[39] I. M. Gagné and S. Zavgorodni, "Evaluation of the analytical anisotropic algorithm in an extreme water-lung interface phantom using Monte Carlo dose calculations," *J. Appl. Clin. Med. Phys.*, vol. 8, no. 1, pp. 33–46, 2007.

[40] A. Sá, "Comparação entre o pencil beam convolution algorithm e o analytical anisotropic algorithm em tumores de mama," 2013.

[41] NCI, "The National Cancer Institute Guidelines for the Use of Intensity-Modulated Radiation Therapy in Clinical Trials."

[42] A. W. Beavis, "Is tomotherapy the future of IMRT?," *Br. J. Radiol.*, vol. 77, pp. 285–295, 2004.

[43] C. da S. Barros, "Estudo, avaliação e optimização em Radioterapia - IMRT," *Lisboa Univ. Nov. Lisboa*, 2010.

[44] A. L. D. S. Carvalho, "Implementação de um sistema de dosímetria 'in-vivo' em Radioterapia Externa – aplicação no cancro da mama," Minho, 2009.

[45] PTW, "OCTAVIUS® 729." [Online]. Available: http://www.ptw.de/3099.html?&cId=3498. [Accessed: 29-Jun-2015].

[46] J. Seco and F. Verhaegen, *Monte Carlo Techniques in Radiation Therapy*. Taylor & Francis, 2013.

[47] M. H. Kalos and P. a. Whitlock, *Monte Carlo Methods*. 2008.

[48] F. Salvat, J. Fernández-Varea, and J. Sempau, *PENELOPE-2006: A code system for Monte Carlo simulation of electron and photon transport*, no. 6416. 2006.

[49] R. Panait, I. Butuc, C. Constantin, M. Grivole, and D. Mihailescu, "Monte Carlo codes for use in medical radiation physics," *Lucr. în Ext.*

[50] L. Livermore, A. Bielajew, C. Hartmann-Siantar, I. Kawrakow, P. J. Keall, C.-M. Ma, A. Nahum, F. Salvat, and M. C. White, "MONTE CARLO TRANSPORT IN RADIOTHERAPY - CURRENT STATUS AND PROSPECTS , AND PHYSICAL DATA NEEDS," no. 8, 2000.

[51] L. A. V. Quino, C. I. H. Hernandez, N. Papanikolaou, A. Gutierrez, C. Esquivel, T. Eng, M. Manciu, and S. Stathakis, “A Monte Carlo model for independent dose verification in IMRT and VMAT for the Varian Novalis TX with high definition MLC,” *Int. J. Cancer Ther. Oncol.*, vol. 3, no. 3, pp. 1–7, 2015.

[52] T. Goetzfried, M. Rickhey, M. Treutwein, O. Koelbl, and L. Bogner, “Monte Carlo simulations to replace film dosimetry in IMRT verification.,” *Z. Med. Phys.*, vol. 21, no. 1, pp. 19–25, 2011.

[53] M. F. Belosi, M. Rodriguez, A. Fogliata, L. Cozzi, J. Sempau, A. Clivio, G. Nicolini, E. Vanetti, H. Krauss, C. Khamphan, P. Fenoglietto, J. Puxeu, D. Fedele, P. Mancosu, and L. Brualla, “Monte Carlo simulation of TrueBeam flattening-filter-free beams using varian phase-space files: comparison with experimental data.,” *Med. Phys.*, vol. 41, no. 2013, p. 051707, 2014.

[54] J. Sempau, A. Badal, and L. Brualla, “A PENELOPE-based system for the automated Monte Carlo simulation of clinacs and voxelized geometries—application to far-from-axis fields,” *Med. Phys.*, vol. 38, no. 2011, p. 5887, 2011.

[55] M. Rodriguez, J. Sempau, and L. Brualla, “PRIMO: A graphical environment for the Monte Carlo simulation of Varian and Elekta linacs,” *Strahlenther Onkol*, vol. 189, pp. 881–886, 2013.

[56] D. a Low and J. F. Dempsey, “Evaluation of the gamma dose distribution comparison method.,” *Med. Phys.*, vol. 30, pp. 2455–2464, 2003.

[57] L. Brualla, M. Rodriguez, and J. Sempau, *PRIMO User ’ s Manual*. 2014.

[58] T. Depuydt, A. Van Esch, and D. P. Huyskens, “A quantitative evaluation of IMRT dose distributions: Refinement and clinical assessment of the gamma evaluation,” *Radiother. Oncol.*, vol. 62, pp. 309–319, 2002.

[59] Mephysto, “Appendix D : Analysis Parameters for Photon Depth Dose Curves.” 2014.

[60] Mephysto, “Appendix B : Analysis Parameters for Profiles.” 2014.

Appendices

Appendix A

In Appendix A is presented all the Matlab functions used to transform PRIMO output in DICOM images. These functions also allow the sum of several fields, if needed, building one IMRT field.

A.1. Functions to write a new PRIMO file

```
%Function to write new PRIMO File

function WritePRIMOFile(inputAddressList, WeightList, outputAddress,
WhichIsLast, selection)

switch selection
    case 'CT'
        [MatMedia, Voxels, VoxelsDim, VoxelsPos, nParticlesSum] =
ReadPRIMOAllFileCT(WhichIsLast, inputAddressList, WeightList);
    case 'Box'
        [MatMedia, Voxels, VoxelsDim, VoxelsPos, nParticlesSum] =
ReadPRIMOAllFile(WhichIsLast, inputAddressList, WeightList);
    otherwise
        error('invalid selection')
end

fid = fopen(outputAddress,'wt');

switch selection
    case 'CT'
        SavePhantomFileCT(MatMedia, Voxels, VoxelsPos, VoxelsDim,
nParticlesSum, WhichIsLast, fid);
    case 'Box'
        SavePhantomFile(MatMedia, Voxels, VoxelsPos, VoxelsDim,
nParticlesSum, WhichIsLast, fid);
    otherwise
        error('invalid selection')
end

fclose(fid);


%Function to write PRIMO File Header

function WritePRIMOFileHeader(Voxels, MinValues, BinWidths, fid)

fprintf(fid, '%s\n',
'#>>>>>>>>>>>>>>>>>>>>>>>>>>>>>>>>>>>>>>>>>>>>>>>>>>>>>>>>>>>>');
fprintf(fid, '%s\n', '# [SECTION REPORT SPATIAL DOSE DISTRIB]');
fprintf(fid, '%s\n', '# Dose units are: eV/g per history');
fprintf(fid, '%s\n', '# No. of bins in x,y,z directions:');
fprintf(fid, '#   %d %d %d\n', Voxels);
fprintf(fid, '%s\n', '# Min values and bin widths for x,y,z(cm):');
fprintf(fid, '#    %7.5E  %7.5E  %7.5E  %7.5E  %7.5E  %7.5E\n',
MinValues(1), BinWidths(1), MinValues(2), BinWidths(2), MinValues(3),
BinWidths(3));
fprintf(fid, '%s\n', '#');
```

```
fprintf(fid, '%s\n', '# For plotting purposes, two values per bin
coordinate are given, namely,');
fprintf(fid, '%s\n', '#   the low end and the middle point of each
bin');
fprintf(fid, '%s\n', '#');
fprintf(fid, '%s', '# xBinIndex : xLow(cm) : xMiddle(cm) : yBinIndex :
yLow(cm) : yMiddle(cm) : zBinIndex : zLow(cm) : zMiddle(cm) : dose :
+-2sigma');


%Function to write PRIMO File Footer


function WritePRIMOFileFooter(nParticles, WhichIsLast, fid)

fprintf(fid, '\n\n\n');

if WhichIsLast~=0
    fprintf(fid, '# Performance report\n');
    fprintf(fid, '#   Random seeds:\n');
    fprintf(fid, '#   1\n');
    fprintf(fid, '#   2\n');
    fprintf(fid, '#   No. of histories simulated [N]:\n');
    fprintf(fid, '#             %d\n', nParticles);
    fprintf(fid, '#   CPU time [t] (s):\n');
    fprintf(fid, '#    4.40843E+02\n');
    fprintf(fid, '#   Speed (histories/s):\n');
    fprintf(fid, '#    1.04991E+03\n');
    fprintf(fid, '#   Average uncertainty (above 1/2 max score) in %%
[uncert]:\n');
    fprintf(fid, '#    1.70386E+02\n');
    fprintf(fid, '#   Intrinsic efficiency [N*uncert^2]^-1:\n');
    fprintf(fid, '#    7.44211E-11\n');
    fprintf(fid, '#   Absolute efficiency [t*uncert^2]^-1:\n');
    fprintf(fid, '#    7.81352E-08\n');
    fprintf(fid, '#\n');
end

WritePRIMOFile2ndFooter(nParticles, fid);


%Function to write PRIMO File Second Footer


function WritePRIMOFile2ndFooter(nParticles, fid)

fprintf(fid, '#\n');
fprintf(fid, '# The dose was integrated from NNN parallel simulation
processes.\n#\n#\n#\n');
fprintf(fid, '# Final performance report\n');
fprintf(fid, '#   No. of histories simulated [N]:\n');
fprintf(fid, '#           %d\n', nParticles);
fprintf(fid, '#   Speed (histories/s):\n');
fprintf(fid, '#      12509.07\n');
fprintf(fid, '#   Average uncertainty (above 1/2 max score) in %%
[uncert]:\n');
fprintf(fid, '#      38.561\n');
fprintf(fid, '#   Intrinsic efficiency [N*uncert^2]^-1:\n');
fprintf(fid, '#      1.20287E-010\n');
fprintf(fid, '#   Absolute efficiency [t*uncert^2]^-1:\n');
```

```
fprintf(fid, '#      1.50468E-006\n#\n');
fprintf(fid, '# Have a nice day.\n');
```

A.2. Functions to read and interpret PRIMO files using a slab phantom in the simulation

```
%Function to read PRIMO complete File

function [MatMedia, Voxels, VoxelsDim, VoxelsPos, nParticlesSum] =
ReadPRIMOAllFile(WhichIsLast, inputAddressList, WeightList)

MatsList = cell(size(inputAddressList));
HeadersList = cell(size(inputAddressList));
FootersList = cell(size(inputAddressList));

nParticleList = zeros(size(inputAddressList));

S = size(MatsList);

Voxels = [0, 0, 0];
VoxelTest = [0 0 0];

VoxelsDim = [0, 0, 0];
VoxelsDimTest = [0 0 0];

VoxelsPos = [0, 0, 0];
VoxelsPosTest = [0 0 0];

WeightSum = 0;
nParticlesSum = 0;
FactorSum = 0;

for ii=1:1:S(2)

    sprintf('\nReading Field %d\n', ii)

    if WhichIsLast==0
        [Mat, Voxels, VoxelsDim, VoxelsPos, nParticles] =
ReadPRIMOFile(char(inputAddressList(ii)), 1);
    else
        if ii~=WhichIsLast
            [Mat, Voxels, VoxelsDim, VoxelsPos, nParticles] =
ReadPRIMOFile(char(inputAddressList(ii)), 1);
        else
            [Mat, Voxels, VoxelsDim, VoxelsPos, nParticles] =
ReadPRIMOFile(char(inputAddressList(ii)), 0);
        end
    end

    sprintf('\nEnd Reading Field %d\n\n', ii)

    if ii==1
        MatMedia = zeros(Voxels(1)*Voxels(2)*Voxels(3), 11, 'double');
        for nn=1:1:9
            MatMedia(:, nn) = Mat(:, nn);
        end
    end
```

```
    if ii==1
        VoxelTest = Voxels;
        VoxelsDimTest = VoxelsDim;
        VoxelsPosTest = VoxelsPos;
    else
        if ((isequal(Voxels, VoxelTest) == 0) || (isequal(VoxelsDim,
VoxelsDimTest) == 0) || (isequal(VoxelsPos, VoxelsPosTest) == 0));
            error('Voxel numbers are different.... Check carefully
your files!')
        end
    end
    WeightSum = WeightSum + WeightList(ii);

    nParticles;

    nParticleList(ii) = nParticles;
    nParticlesSum = nParticlesSum + nParticles;
    FactorSum = FactorSum + WeightList(ii)*nParticles;

    MatMedia = CalculatePRIMOMedia(MatMedia, Mat, nParticleList(ii),
WeightList(ii));

end

MatMedia(:, 10) = MatMedia(:,10)/FactorSum;


%Function to read PRIMO File (header and footer)

function [MatOut, Voxels, VoxelsDim, VoxelsPos, nParticles] =
ReadPRIMOFile(inputAddress, islast)

format shortG

fid = fopen(inputAddress);

LineWith_nVox = 5;

LineWith_VoxDim = 7;

HeaderRows = 12;

Voxels = [0, 0, 0];

[Voxels, VoxelsDim, VoxelsPos] = ReadHeader(HeaderRows, fid,
LineWith_nVox, LineWith_VoxDim);

delimiterIn = ' ';

MatOut = fscanf(fid, '%d %f %f %d %f %f %d %f %f %f %f', [11
Voxels(1)*Voxels(2)*Voxels(3)]);
MatOut = MatOut';

LineWith_nParticles = 0;
if islast == 0
    LineWith_nParticles = 12;
else
```

```
    LineWith_nParticles = 29;
end

FooterRows = 36;

nParticles = 0;

nParticles = ReadFooter(FooterRows, fid, LineWith_nParticles);

fclose(fid);


%Function to read header


function [Voxels, VoxelsDim, VoxelsPos] = ReadHeader(HeaderRows, fid,
LineWith_nVox, LineWith_VoxDim)

for ii=1:1:HeaderRows
    Row = fgetl(fid);
    if ii==LineWith_nVox
        Voxels = ReadNumVoxelsFromHeader(Row);
    end

    if ii==LineWith_VoxDim
        [VoxelsDim] = ReadVoxelDimFromHeader(Row);
        [VoxelsPos] = ReadVoxelPosFromHeader(Row);
    end
end

%Function to read voxel number from header


function [Voxels] = ReadNumVoxelsFromHeader(Row)

S = size(Row);
Row = strtrim(Row(1,2:S(2)));
Voxels = str2num(Row);


%Function to read voxel dimensons from header


function VoxelsDim = ReadVoxelDimFromHeader(Row)

S = size(Row);
Row = strtrim(Row(1,2:S(2)));
Num = str2num(Row);

VoxelsDim = [Num(2) Num(4) Num(6)];


%Function to read voxel position from header

function VoxelsDim = ReadVoxelPosFromHeader(Row)

S = size(Row);
Row = strtrim(Row(1,2:S(2)));
```

```
Num = str2num(Row);

VoxelsDim = [Num(1) Num(3) Num(5)];


%Function to read footer


function [nParticles] = ReadFooter(FooterRows, fid,
LineWith_nParticles)

FooterExt = '';

for ii=1:1:FooterRows
    Row = fgetl(fid);
   if ii==LineWith_nParticles
        nParticles = ReadnParticlesFromFooter(Row);
   end
end


%Function to read number of particles in footer

function [nParticles] = ReadnParticlesFromFooter(Row)

S = size(Row);
Row = strtrim(Row(1,2:S(2)));
nParticles = str2num(Row);


%Function to calculate PRIMO mean values

function MatMediaOut = CalculatePRIMOMedia(MatMedia, Mat, nParticles,
Weight)

sprintf('\nSumming up Weighted Matrixes\n');

MatMediaOut(:, 10) = MatMedia(:, 10) + (Weight*nParticles)*Mat(:, 10);
MatMediaOut(:, 11) = 0;

sprintf('\nMatrixes Summed\n');



%Function to save phantom file


function SavePhantomFile(MatMedia, Voxels, VoxelsPos, VoxelsDim,
nParticlesSum, WhichIsLast, fid)

WritePRIMOFileHeader(Voxels, VoxelsPos, VoxelsDim, fid);

MatDose = reshape(MatMedia(:, 10), Voxels);
MatUncertainty = reshape(MatMedia(:, 11), Voxels);

for ii=1:1:Voxels(3)
    for jj=1:1:Voxels(2)
        for kk=1:1:Voxels(1)
```

```
            fprintf(fid, '\n%d %7.5E %7.5E %d %7.5E %7.5E %d %7.5E
%7.5E %7.5E %7.5E', kk, VoxelsPos(1)+(kk-1)*VoxelsDim(1),
VoxelsPos(1)+(kk-1)*VoxelsDim(1)+VoxelsDim(1)/2, jj, VoxelsPos(2)+(jj-
1)*VoxelsDim(2), VoxelsPos(2)+(jj-1)*VoxelsDim(2)+VoxelsDim(2)/2, ii,
VoxelsPos(3)+(ii-1)*VoxelsDim(3), VoxelsPos(3)+(ii-
1)*VoxelsDim(3)+VoxelsDim(3)/2, MatDose(kk, jj, ii),
MatUncertainty(kk, jj, ii));
        end
        fprintf(fid, '\n');
    end
end

WritePRIMOFileFooter(nParticlesSum, WhichIsLast, fid);



%Function to create image

function CreateImageFromBox(inputAddress, filter, selection,
inputmetadata, islast, saveAddress)

[MatIn, Voxels, VoxelsDim, VoxelsPos, nParticles] =
ReadPRIMOFile(inputAddress, islast);

Voxels
VoxelsDim
VoxelsPos
nParticles

MatOut = zeros(VoxelsDim(1)*VoxelsDim(2)*VoxelsDim(3), 11);

x = zeros(Voxels(1));
y = zeros(Voxels(2));
z = zeros(Voxels(3));

for ii=1:1:Voxels(1)
    x(ii) = VoxelsPos(1) + (ii-1)*VoxelsDim(1);
end

for jj=1:1:Voxels(2)
    y(jj) = VoxelsPos(2) + (jj-1)*VoxelsDim(2);
end

for kk=1:1:Voxels(3)
    z(kk) = VoxelsPos(3) + (kk-1)*VoxelsDim(3);
end

for ii=1:1:Voxels(1)
    for jj=1:1:Voxels(2)
        for kk=1:1:Voxels(3)
            MatOut(ii + (jj-1)*Voxels(1) + (kk-
1)*Voxels(1)*Voxels(2),1) = ii;
            MatOut(ii + (jj-1)*Voxels(1) + (kk-
1)*Voxels(1)*Voxels(2),3) = x(ii) + VoxelsDim(1)/2;
            MatOut(ii + (jj-1)*Voxels(1) + (kk-
1)*Voxels(1)*Voxels(2),2) = x(ii);

            MatOut(ii + (jj-1)*Voxels(1) + (kk-
1)*Voxels(1)*Voxels(2),4) = jj;
```

```
            MatOut(ii + (jj-1)*Voxels(1) + (kk-
1)*Voxels(1)*Voxels(2),6) = y(jj) + VoxelsDim(2)/2;
            MatOut(ii + (jj-1)*Voxels(1) + (kk-
1)*Voxels(1)*Voxels(2),5) = y(jj);

            MatOut(ii + (jj-1)*Voxels(1) + (kk-
1)*Voxels(1)*Voxels(2),7) = kk;
            MatOut(ii + (jj-1)*Voxels(1) + (kk-
1)*Voxels(1)*Voxels(2),9) = z(kk) + VoxelsDim(3)/2;
            MatOut(ii + (jj-1)*Voxels(1) + (kk-
1)*Voxels(1)*Voxels(2),8) = z(kk);

            MatOut(ii + (jj-1)*Voxels(1) + (kk-
1)*Voxels(1)*Voxels(2),10) = MatIn(ii + (jj-1)*Voxels(1) + (kk-
1)*Voxels(1)*Voxels(2), 10);
            MatOut(ii + (jj-1)*Voxels(1) + (kk-
1)*Voxels(1)*Voxels(2),11) = MatIn(ii + (jj-1)*Voxels(1) + (kk-
1)*Voxels(1)*Voxels(2), 11);
        end
    end
end

metadata = load(inputmetadata);

S = size(selection);

for ii=1:1:S(2)
    selection(1, ii);
    switch filter
        case 'x'
            MatSelect =
MatOut(double(MatOut(:,3))==double(selection(1, ii)), :);
            Voxels2D = [1, Voxels(2), Voxels(3)];
            metadata.metadata.Rows = Voxels(2);
            metadata.metadata.Columns = Voxels(3);
            PixSpac = [VoxelsDim(1) VoxelsDim(2)];
            metadata.metadata.Width = Voxels(2);
            metadata.metadata.Height = Voxels(3);
        case 'xVoxIndex'
            MatSelect = MatOut(MatOut(:,1)==selection(1, ii), :);
            Voxels2D = [1, Voxels(2), Voxels(3)];
            metadata.metadata.Rows = Voxels(2);
            metadata.metadata.Columns = Voxels(3);
            PixSpac = [VoxelsDim(1) VoxelsDim(2)];
            metadata.metadata.Width = Voxels(2);
            metadata.metadata.Height = Voxels(3);
        case 'y'
            MatSelect =
MatOut(double(MatOut(:,6))==double(selection(1, ii)), :);
            Voxels2D = [Voxels(1), 1, Voxels(3)];
            metadata.metadata.Rows = Voxels(1);
            metadata.metadata.Columns = Voxels(3);
            PixSpac = [VoxelsDim(3) VoxelsDim(1)];
            metadata.metadata.Width = Voxels(1);
            metadata.metadata.Height = Voxels(3);
        case 'yVoxIndex'
            MatSelect = MatOut(MatOut(:,4)==selection(1, ii), :);
            Voxels2D = [Voxels(1), 1, Voxels(3)];
            metadata.metadata.Rows = Voxels(1);
            metadata.metadata.Columns = Voxels(3);
```

```
            PixSpac = [VoxelsDim(3) VoxelsDim(1)];
            metadata.metadata.Width = Voxels(1);
            metadata.metadata.Height = Voxels(3);
        case 'z'
            MatSelect =
MatOut(double(MatOut(:,9))==double(selection(1, ii)), :);
            Voxels2D = [Voxels(1), Voxels(2), 1];
            metadata.metadata.Rows = Voxels(1);
            metadata.metadata.Columns = Voxels(2);
            PixSpac = [VoxelsDim(2) VoxelsDim(1)];
            metadata.metadata.Width = Voxels(1);
            metadata.metadata.Height = Voxels(2);
        case 'zVoxIndex'
            MatSelect = MatOut(MatOut(:,7)==selection(1, ii), :);
            Voxels2D = [Voxels(1), Voxels(2), 1];
            metadata.metadata.Rows = Voxels(1);
            metadata.metadata.Columns = Voxels(2);
            PixSpac = [VoxelsDim(2) VoxelsDim(1)];
            metadata.metadata.Width = Voxels(1);
            metadata.metadata.Height = Voxels(2);
        otherwise
            error('invalid selection')
    end

    str = strcat(saveAddress, sprintf('_%d.dcm', selection(ii)))
    metadata.metadata.Filename = str;

    MatSelect = squeeze(reshape(MatSelect(:,10), Voxels2D));

    dicomwrite(imrotate(MatSelect, -90), str, metadata, 'CreateMode',
'Copy', 'PixelSpacing', 10*PixSpac, 'SOPClassUID',
'1.2.840.10008.5.1.4.1.1.2', 'MultiframeSingleFile', true);
end
```

A.2. Functions to read and interpret PRIMO files using a CT image in the simulation

```
%Function to read PRIMO complete File

function [MatMedia, Voxels, VoxelsDim, VoxelsPos, nParticlesSum] =
ReadPRIMOAllFileCT(WhichIsLast, inputAddressList, WeightList)

nParticleList = zeros(size(inputAddressList));

S = size(inputAddressList)

Voxels = [0, 0, 0];
VoxelTest = [0 0 0];

VoxelsDim = [0, 0, 0];
VoxelsDimTest = [0 0 0];

VoxelsPos = [0, 0, 0];
VoxelsPosTest = [0 0 0];

WeightSum = 0;
```

```
nParticlesSum = 0;
FactorSum = 0;

for ii=1:1:S(2)

    sprintf('\nReading Field %d\n', ii)

    if WhichIsLast==0
        [Mat, Voxels, VoxelsDim, VoxelsPos, nParticles] =
ReadPRIMOFileCT(char(inputAddressList(ii)), 1);
    else
        if ii~=WhichIsLast
            [Mat, Voxels, VoxelsDim, VoxelsPos, nParticles] =
ReadPRIMOFileCT(char(inputAddressList(ii)), 1);
        else
            [Mat, Voxels, VoxelsDim, VoxelsPos, nParticles] =
ReadPRIMOFileCT(char(inputAddressList(ii)), 0);
        end
    end

    sprintf('\nEnd Reading Field %d\n\n', ii)

    if ii==1
        MatMedia = zeros(Voxels(1)*Voxels(2)*Voxels(3), 11, 'double');
        for nn=1:1:9
            MatMedia(:, nn) = Mat(:, nn);
        end
    end

    if ii==1
        VoxelTest = Voxels;
        VoxelsDimTest = VoxelsDim;
        VoxelsPosTest = VoxelsPos;
    else
        if ((isequal(Voxels, VoxelTest) == 0) || (isequal(VoxelsDim,
VoxelsDimTest) == 0) || (isequal(VoxelsPos, VoxelsPosTest) == 0));
            error('Voxel numbers are different.... Check carefully
your files!')
        end
    end
    WeightSum = WeightSum + WeightList(ii);

    nParticles;

    nParticleList(ii) = nParticles;
    nParticlesSum = nParticlesSum + nParticles;
    FactorSum = FactorSum + WeightList(ii)*nParticles;

    MatMedia = CalculatePRIMOMediaCT(MatMedia, Mat, nParticleList(ii),
WeightList(ii));

end

MatMedia(:, 10) = MatMedia(:,10)/FactorSum;


%Function to read PRIMO File (header and footer)
```

```
function [MatOut, Voxels, VoxelsDim, VoxelsPos, nParticles] =
ReadPRIMOFileCT(inputAddress, islast)

format shortG

fid = fopen(inputAddress);

LineWith_nVox = 8;

LineWith_VoxelDim = 10;

HeaderRows = 11;

[Voxels, VoxelsDim, VoxelsPos] = ReadHeaderCT(HeaderRows, fid,
LineWith_nVox, LineWith_VoxelDim);

Voxels
VoxelsDim
VoxelsPos

MatOut = zeros(Voxels(1)*Voxels(2)*Voxels(3), 11, 'double');

for kk=1:1:Voxels(3)
    [zVoxIndex middleZ] = ReadCTsingleVoxLine(fid);
    for jj=1:1:Voxels(2)
        [yVoxIndex middleY] = ReadCTsingleVoxLine(fid);
        for ii=1:1:Voxels(1)
            index = ii + Voxels(1)*(jj -1) + Voxels(1)*Voxels(2)*(kk-
1);
            MatOut(index, 1) = ii;
            MatOut(index, 2) = VoxelsPos(1) - VoxelsDim(1)/2 + (ii -
1)*VoxelsDim(1);
            MatOut(index, 3) = MatOut(index, 2) + VoxelsDim(1)/2;
            MatOut(index, 4) = jj;
            MatOut(index, 5) = middleY - VoxelsDim(2)/2;
            MatOut(index, 6) = middleY;
            MatOut(index, 7) = kk;
            MatOut(index, 8) = middleZ - VoxelsDim(3)/2;
            MatOut(index, 9) = middleZ;
            MatOut(index, 10) = fscanf(fid, '%f', 1);
            MatOut(index, 11) = fscanf(fid, '%f', 1);
        end
        fscanf(fid, '\n');
    end
    fscanf(fid, '\n');
end

LineWith_nParticles = 0;
if islast == 0
    FooterRows = 18;
    LineWith_nParticles = 8;
else
    FooterRows = 35;
    LineWith_nParticles = 25;
end

nParticles = 0;

nParticles = ReadFooterCT(FooterRows, fid, LineWith_nParticles);
```

```
nParticles

fclose(fid);


%Function to read header

function [Voxels, VoxelsDim, VoxelsPos] = ReadHeaderCT(HeaderRows,
fid, LineWith_nVox, LineWith_VoxDim)

for ii=1:1:HeaderRows
    Row = fgetl(fid);

    if ii==LineWith_nVox
        Voxels = ReadNumVoxelsFromHeaderCT(Row);
    end

    if ii==LineWith_VoxDim
        VoxelsDim = ReadVoxelDimFromHeaderCT(Row);
    end
end

position = ftell(fid);

Row = fgetl(fid);
[Values count] = ReadVoxelzPosFromHeaderCT(Row);
VoxelsPos(3) = Values(1) - VoxelsDim(3)/2;

Row = fgetl(fid);
[Values count] = ReadVoxelyPosFromHeaderCT(Row);
VoxelsPos(2) = Values(1) - VoxelsDim(2)/2;

VoxelsPos(1) = -Voxels(1)*VoxelsDim(1)/2 +VoxelsDim(1)/2;

Voxels;
VoxelsDim;
VoxelsPos;

fseek(fid, position, 'bof');


%Function to read voxel number from header


function [Voxels] = ReadNumVoxelsFromHeaderCT(Row)

S = size(Row);
Row = strtrim(Row(1,2:S(2)));
Voxels = str2num(Row);


%Function to read voxel dimensons from header

function [VoxelsDim] = ReadVoxelDimFromHeaderCT(Row)

S = size(Row);
Row = strtrim(Row(1,2:S(2)));
```

```
VoxelsDim = str2num(Row);


%Function to read voxel position in y from header


function [index VoxelsPos] = ReadVoxelyPosFromHeaderCT(Row)

[index VoxelsPos] = sscanf(Row, '# yVoxIndex=%d yMiddle(cm)= %f');


%Function to read voxel position in z from header

function [index VoxelsPos] = ReadVoxelzPosFromHeaderCT(Row)

[index VoxelsPos] = sscanf(Row, '# zVoxIndex=%d zMiddle(cm)= %f');



%Function to read footer

function [nParticles] = ReadFooterCT(FooterRows, fid,
LineWith_nParticles)

FooterRows;
LineWith_nParticles;

FooterExt = '';

for ii=1:1:FooterRows
    Row = fgetl(fid);
   if ii==LineWith_nParticles
       nParticles = ReadnParticlesFromFooter(Row);
   end
end


%Function to read number of particles in footer

function [nParticles] = ReadnParticlesFromFooter(Row)

S = size(Row);
Row = strtrim(Row(1,2:S(2)));
nParticles = str2num(Row);


%Function to calculate PRIMO mean values

function MatMediaOut = CalculatePRIMOMediaCT(MatMedia, Mat,
nParticles, Weight)

sprintf('\nSumming up Weighted Matrixes\n');

MatMediaOut(:, 10) = MatMedia(:, 10) + (Weight*nParticles)*Mat(:, 10);
MatMediaOut(:, 11) = 0;

sprintf('\nMatrixes Summed\n');
```

```
%Function to save phantom file

function SavePhantomFileCT(MatMedia, Voxels, VoxelsPos, VoxelsDim,
nParticlesSum, WhichIsLast, fid)

WritePRIMOFileHeader(Voxels, VoxelsPos, VoxelsDim, fid);

MatDose = reshape(MatMedia(:, 10), Voxels);
MatUncertainty = reshape(MatMedia(:, 11), Voxels);

for ii=1:1:Voxels(3)
    for jj=1:1:Voxels(2)
        for kk=1:1:Voxels(1)
            fprintf(fid, '\n%d %7.5E %7.5E %d %7.5E %7.5E %d %7.5E
%7.5E %7.5E %7.5E', kk, VoxelsPos(1)+(kk-1)*VoxelsDim(1),
VoxelsPos(1)+(kk-1)*VoxelsDim(1)+VoxelsDim(1)/2, jj, VoxelsPos(2)+(jj-
1)*VoxelsDim(2), VoxelsPos(2)+(jj-1)*VoxelsDim(2)+VoxelsDim(2)/2, ii,
VoxelsPos(3)+(ii-1)*VoxelsDim(3), VoxelsPos(3)+(ii-
1)*VoxelsDim(3)+VoxelsDim(3)/2, MatDose(kk, jj, ii),
MatUncertainty(kk, jj, ii));
        end
        fprintf(fid, '\n');
    end
end

WritePRIMOFileFooter(nParticlesSum, WhichIsLast, fid);


%Function to create image

function CreateImageFromCT(inputAddress, filter, selection,
inputmetadata, islast, saveAddress)

[MatIn, Voxels, VoxelsDim, VoxelsPos, nParticles] =
ReadPRIMOFileCT(inputAddress, islast);

Voxels
VoxelsDim
VoxelsPos
nParticles

MatOut = zeros(VoxelsDim(1)*VoxelsDim(2)*VoxelsDim(3), 11);

x = zeros(Voxels(1));
y = zeros(Voxels(2));
z = zeros(Voxels(3));

for ii=1:1:Voxels(1)
    x(ii) = VoxelsPos(1) + (ii-1)*VoxelsDim(1);
end

for jj=1:1:Voxels(2)
    y(jj) = VoxelsPos(2) + (jj-1)*VoxelsDim(2);
end

for kk=1:1:Voxels(3)
    z(kk) = VoxelsPos(3) + (kk-1)*VoxelsDim(3);
end
```

```
for ii=1:1:Voxels(1)
    for jj=1:1:Voxels(2)
        for kk=1:1:Voxels(3)
            MatOut(ii + (jj-1)*Voxels(1) + (kk-
1)*Voxels(1)*Voxels(2),1) = ii;
            MatOut(ii + (jj-1)*Voxels(1) + (kk-
1)*Voxels(1)*Voxels(2),3) = x(ii) + VoxelsDim(1)/2;
            MatOut(ii + (jj-1)*Voxels(1) + (kk-
1)*Voxels(1)*Voxels(2),2) = x(ii);

            MatOut(ii + (jj-1)*Voxels(1) + (kk-
1)*Voxels(1)*Voxels(2),4) = jj;
            MatOut(ii + (jj-1)*Voxels(1) + (kk-
1)*Voxels(1)*Voxels(2),6) = y(jj) + VoxelsDim(2)/2;
            MatOut(ii + (jj-1)*Voxels(1) + (kk-
1)*Voxels(1)*Voxels(2),5) = y(jj);

            MatOut(ii + (jj-1)*Voxels(1) + (kk-
1)*Voxels(1)*Voxels(2),7) = kk;
            MatOut(ii + (jj-1)*Voxels(1) + (kk-
1)*Voxels(1)*Voxels(2),9) = z(kk) + VoxelsDim(3)/2;
            MatOut(ii + (jj-1)*Voxels(1) + (kk-
1)*Voxels(1)*Voxels(2),8) = z(kk);

            MatOut(ii + (jj-1)*Voxels(1) + (kk-
1)*Voxels(1)*Voxels(2),10) = MatIn(ii + (jj-1)*Voxels(1) + (kk-
1)*Voxels(1)*Voxels(2), 1);
            MatOut(ii + (jj-1)*Voxels(1) + (kk-
1)*Voxels(1)*Voxels(2),11) = MatIn(ii + (jj-1)*Voxels(1) + (kk-
1)*Voxels(1)*Voxels(2), 2);
        end
    end
end

metadata = load(inputmetadata);

switch filter
    case 'x'
        MatSelect = MatOut(double(MatOut(:,3))==double(selection), :);
        Voxels2D = [1, Voxels(2), Voxels(3)];
        metadata.metadata.Rows = Voxels(2);
        metadata.metadata.Columns = Voxels(3);
        PixSpac = [VoxelsDim(1) VoxelsDim(2)];
        metadata.metadata.Width = Voxels(2);
        metadata.metadata.Height = Voxels(3);
    case 'xVoxIndex'
        MatSelect = MatOut(MatOut(:,1)==selection, :);
        Voxels2D = [1, Voxels(2), Voxels(3)];
        metadata.metadata.Rows = Voxels(2);
        metadata.metadata.Columns = Voxels(3);
        PixSpac = [VoxelsDim(1) VoxelsDim(2)];
        metadata.metadata.Width = Voxels(2);
        metadata.metadata.Height = Voxels(3);
    case 'y'
        MatSelect = MatOut(double(MatOut(:,6))==double(selection), :);
        Voxels2D = [Voxels(1), 1, Voxels(3)];
        metadata.metadata.Rows = Voxels(1);
        metadata.metadata.Columns = Voxels(3);
        PixSpac = [VoxelsDim(3) VoxelsDim(1)];
```

```
            metadata.metadata.Width = Voxels(1);
            metadata.metadata.Height = Voxels(3);
        case 'yVoxIndex'
            MatSelect = MatOut(MatOut(:,4)==selection, :);
            Voxels2D = [Voxels(1), 1, Voxels(3)];
            metadata.metadata.Rows = Voxels(1);
            metadata.metadata.Columns = Voxels(3);
            PixSpac = [VoxelsDim(3) VoxelsDim(1)];
            metadata.metadata.Width = Voxels(1);
            metadata.metadata.Height = Voxels(3);
        case 'z'
            MatSelect = MatOut(double(MatOut(:,9))==double(selection), :);
            Voxels2D = [Voxels(1), Voxels(2), 1];
            metadata.metadata.Rows = Voxels(1);
            metadata.metadata.Columns = Voxels(2);
            PixSpac = [VoxelsDim(2) VoxelsDim(1)];
            metadata.metadata.Width = Voxels(1);
            metadata.metadata.Height = Voxels(2);
        case 'zVoxIndex'
            MatSelect = MatOut(MatOut(:,7)==selection, :);
            Voxels2D = [Voxels(1), Voxels(2), 1];
            metadata.metadata.Rows = Voxels(1);
            metadata.metadata.Columns = Voxels(2);
            PixSpac = [VoxelsDim(2) VoxelsDim(1)];
            metadata.metadata.Width = Voxels(1);
            metadata.metadata.Height = Voxels(2);
        otherwise
            error('invalid selection')
    end

    metadata.metadata.Filename = inputAddress;

    size(MatSelect)

    MatSelect = reshape(MatSelect(:,10), Voxels2D);
    dicomwrite(imrotate(MatSelect, -90), saveAddress, metadata,
    'CreateMode', 'Copy', 'PixelSpacing', 10*PixSpac, 'SOPClassUID',
    '1.2.840.10008.5.1.4.1.1.2', 'MultiframeSingleFile', true);
```